Title

The Combinational Effects of Gamma Secretase Inhibition and Radiation on the Cancer Stem Cell Population in Glioblastoma

Author

Alhiyari, Yazeed

Publication Date

2014

Peer reviewed|Thesis/dissertation

UNIVERSITY OF CALIFORNIA

Los Angeles

The Combinational Effects of Gamma Secretase Inhibition and Radiation on the Cancer Stem Cell Population in Glioblastoma

A dissertation submitted in partial satisfaction of the requirement for the degree Doctor of Philosophy in Biomedical Physics

By

Yazeed M Alhiyari

2014

ABSTRACT OF THE DISSERATION *(doctorate):*

The Combinational Effects of Gamma Secretase Inhibition

and Radiation on the Cancer Stem Cell Population

in Glioblastoma

by

Yazeed M Alhiyari

Doctor of Philosophy in Biomedical Physics

University of California, Los Angeles, 2014

Professor Frank Pajonk, Chair

Gamma secretase (GS) is an intramembraneous protease that cleaves over 91 different membrane substrates. GS is responsible for the final S3 cleavage of the notch receptor, thereby releasing the notch intracellular domain (NICD) into the cytoplasm. Upon translocation into the nucleus NICD activates the transcription of notch effector proteins that maintain cell stemness. Due to GS activity on the notch pathway, it has become an attractive target for cancer stem cells. The cancer stem cell (CSC) hypothesis states that cancers are generated and maintained by a group of cells that share similarities with normal adult stem cells. CSCs have been shown to be resistant to most current anti-cancer treatment approaches, including radiation therapy, thus contributing to tumor

repopulation after therapy. A combinational therapy that targets both cancer cells and inhibits cancer stem cell growth is highly desirable. Unfortunately, there is inconsistent data determining the combinational effects of GS inhibitors (GSI) with radiation. *In this study, the efficacy of GSI treatment with radiation therapy in reducing the cancer stem cell population in glioblastoma multiforme (GBM) was evaluated*. Utilizing a panel of GBM cell lines varying in PTEN, p53, and EGFR status, we evaluated the effects of GSI plus radiation treatment on the cancer stem cell population, using sphere-forming capacity assays, cell cycle analysis, and γH2AX and Hoechst/PY staining. Our data demonstrates that PTEN status plays a role in the sensitivity to GSI treatment in combination with radiation treatment. In addition, we observed that treating PTEN-wt cell lines with GSI improved survival among the stem cell population while PTEN-mutant lines showed a reduced survival. We believe this glioma stem cell protection is mediated through FOXO, or the Forkhead class O transcription factors, which is positively regulated by functioning PTEN. In conclusion, this study demonstrates that the effectiveness of combinational treatment of GSI and radiation on glioma stem cells depends on the genetic background of the tumor. Specifically, PTENwt neurosphere cell lines are radioprotected under GSI treatment while PTEN-null neurosphere cell lines become more radiosensitive.

This dissertation Yazeed M. Alhiyari is approved.

Nicholas A Cacalano

Keiwuke Steven Iwamoto

Anahid Jewett

Frank Pajonk , Committee Chair

University of California, Los Angeles
2014

VITA

2006-2007	Undergraduate Researcher Department of Biology Texas Tech University, TX
2006-2007	Undergraduate Researcher High Performance Computing Center Texas Tech University, TX
2007	B.S. Cell Molecular Biology Texas Tech University, TX
2007	B.S. Mathematics Texas Tech University, TX
2008	Internship Molecular Genetics Mayo Clinic, MN
2009	M.S. Molecular Pathology Texas Tech University Health Science Center, TX
2010-2014	Graduate Student Researcher Department of Cell/Molecular Oncology University of California, Los Angeles, CA
2014	Best Oral Presentation Award Biomedical Physics Program, Annual Colloquium University of California, Los Angeles, CA
2014	SIT Travel Award Radiation Research Society Annual Conference
2014	Part time Faculty Health Science Dept. University of California, Northridge, CA

PUBLICATIONS AND PRESENTATIONS

Erina Vlashi, Chann Lagadec, Laurent Vergnes, Karen Reue, Patricia Frohnen, Mabel Chan, **Yazeed Alhiyari**, Milana Bochkur Dratver and Frank Pajonk, Metabolic differences in breast cancer stem cells and differentiated progeny, Breast Cancer Research and Treatment, 2014

Lagadec C, Vlashi E. **Alhiyari Y**, Phillips TM, Bochkur Dratver M, Pajonk F. *Radiation*

Induced Notch Signaling in Breast Cancer Stem Cells Int J Radiat Oncol Biol Phys. 2013;87(3):609-18. PMCID: 3788036.

Lagadec C, Vlashi E, Frohnen P, **Alhiyari Y**, Chan M, Pajonk F. *The RNA-binding protein Musashi-1 regulates proteasome subunit expression in breast cancer- and glioma-initiating cells*. Stem Cells. 2013.

Acknowledgements:

This dissertation could not have been completed without the help of many individuals that have provided professional and educational guidance, moral support, and friendship.

First, I would like to thank Dr. Frank Pajonk for allowing me to work and grow under his supervision. Frank embodies hard work, perseverance, dedication, and a true passion for research and cancer biology. He has been demonstrated what it takes to be a successful academic and I have benefited immensely from his example. Along with Frank, Dr. Erina Vlashi has also been a source of knowledge and information for me in the lab. Erina was always kind and consistently helped me think of new ideas or different ways to think about my project.

It would've been extremely difficult to finish my Ph.D. without the help of Patricia Frohnen. Patricia was always supportive and made sure I had the necessary supplies for all of my experiments. Patricia has served not only as laboratory manager, but as a true friend as well.

Terry Moore and Reth Im have assisted me with every issue administratively that I ever needed help with and were a resource for any questions I may have had. Both were easy to talk to and took care of any issue I needed. Their help allowed me to focus my efforts on my research and not on administrative issues.

Dr. McNitty Gray is not only a great professor, but he was an outstanding individual to have as director of the Biomedical Physics program. I was able to interact with Dr. Grey both professionally and socially and in each circumstance he carried himself with intelligence, compassion, and understanding. He is one of the first people I met ~4 long years ago when I came to interview for the program and I thank him immensely for accepting me to complete my Ph.D. here at UCLA.

Lastly, I would like to thank the three people who have been with me on this journey from the very, very beginning: my Mom, my Dad, and my sister. My family has not only encouraged me from day one, but they have also accepted me when I struggled and celebrated me when I succeeded. My path would've been entirely different without their guidance and I am truly thankful to have had them to share this experience with.

Table of Contents

Glossary of Terms

Term:	Abbreviation	Definition
Adult stem cell	(ASC)	Normal Adult stem cells
Cancer stem cell	(CSC)	Cancer cells with stem properties
Glioma stem cell	(GSC)	Cancer stem cell of the in brain tumor
Gamma Secretase	(GS)	Membrane Protease
Gamma Secretase Inhibitor	(GSI)	Stops gamma secretase cleavage
Glioblastoma	(GB)	Aggressive brain astrocytoma
Glioblastoma Multiforme	(GBM)	Old terminology for glioblastomas
Ionizing Radiation	(IR)	EM energy with >400nm wavelengths
O-6-methylguanine-DNA methyltransferase	(MGMT)	Repairs alkylating DNA damage
Neural Stem cell	(NSC)	Brain stem cell
Notch-intracellular domain	(NICD)	Propagates Notch down signaling
Nuclear Export Sequence	(NES)	Involved in FOXO localization
Nuclear Localization Sequence	(NLS)	Involve in FOXO nuclear localization
Reactive Oxygen Species	(ROS)	Generated through metabolized or IR
Temozolomide	(TMZ)	DNA alkylating agent

CHAPTER I: Introduction

Cancers are one of the leading causes of death claiming approximately 8.2 million lives world-wide (www.who.int). One of the complications of aggressive cancers is that they frequently recur after treatment. Many mechanisms have been proposed to explain cancer treatment resistance and recurrence, but a new concept explaining cancer organization and growth, the cancer stem cell hypothesis, has become an accepted model to explain cancer treatment failure. The cancer stem cell hypothesis identifies a rare "special cancer cell", a cancer stem cell, that drives and maintains tumor growth, development, and resistance to treatment. Targeting cancer stem cells may provide a more positive outcome on patient survival. In this study, we test the efficacy of targeting a stem cell pathway to limit cancer stem cell development, and thus tumor growth in brain cancers.

Cancer stem cells

Cancer stem cell hypothesis

The idea of cancer stem cells (CSCs) has been around for a long time and was first proposed by Dr. Julius Cohnheim, a German pathologist who lived from 1839-1884. Dr. Cohnheim significantly contributed to our understanding of neoplastic disease, and was the first to distinguish between epithelial and mesenchyme tumors, as well as develop a theory of tumor proliferation and metastasis. The idea of cancer stem cells gained interest again

in 2003 when methods to prospectively identify CSCs were demonstrated (Al-Hajj, Wicha et al. 2003). Since then, the cancer stem cell field has been pushed by many other groups including Peter Derks, Harley Kornblum, Frank Pajonk, Inder Verma, and Jeremy Rich to name a few. These collective publications have contributed to our understanding of cancer stem cell response to treatment, tumor growth, and development in many different tumor tissue types. The identification of CSCs has led to the cancer stem cell hypothesis to describe tumor growth and organization. The cancer stem cell hypothesis states that tumors are organized hierarchically and there exists a unique and rare population of stem cells, which maintain the bulk tumor population through the generation of progenitor cells. Progenitor cells may further generate differentiated cells that constitute the bulk tumor population. In this model, tumorigenic potential is solely confined to cells that have gained stem cell like properties, the cancer stem cells. CSCs are a functionally distinct group of cells with stem like characteristics and tumorigenicity, while the remaining population of cells have no tumorigenic potential (Clarke, Dick et al. 2006, Kennedy, Barabe et al. 2007).

It is unknown whether CSCs arise from mutations in Adult Stem Cells (ASC) or mutations in progenitor/differentiated cells, which then gain stem-like features. A cancer cell must possess the capacity for both self-renewal and tumor formation in order to be classified as a cancer stem cell (Clarke, Dick et al. 2006). Self-renewal describes the ability of a stem cell to replicate itself by dividing into the same non-specialized cell type for long periods of time. Self-renewal is not synonymous with cellular proliferation, in which the resulting daughter cells are more differentiated and are capable of a limited number of subsequent cellular divisions. There exist a variety of cellular markers for CSCs (CD133, CD44, CD24 in brain) (Sahlberg, Spiegelberg et al. 2014). These markers are cancer tissue

type specific and in most cases still fail to capture the true cancer stem cell population. Evaluating the functional properties of cancer cells, self-renewal via neurosphere formation assays, and tumorgenicity through limiting dilution *in vivo* assays, has become the gold standard to identify CSCs. Just like normal tissues maintain a certain number of stem cells to replace dying cells or tissue damage, tumors may vary greatly in the number of CSCs they contain depending on tumor and tissue type (Kelly, Dakic et al. 2007, Eaves 2008). Although normal embryonic stem cells and ASCs have been associated with specific markers, it has been more difficult and complicated to identify a specific marker for CSCs (Lottaz, Beier et al. 2010). CSCs have become an important field of study because of their increased resistance to therapies. Since CSCs are the only cells capable of tumor initiation and formation, the CSCs hypothesis therefore implies that CSCs are responsible for tumor relapse after treatment (Rahman, Deleyrolle et al. 2011). There are many publications that demonstrate that CSCs are more resistant to therapy (Bao, Wu et al. 2006, Salmaggi, Boiardi et al. 2006, Ghods, Irvin et al. 2007, Shafee, Smith et al. 2008, Frame and Maitland 2011, Chen, Huang et al. 2013) and in some cases the recurring tumor is more aggressive after treatment (Lagadec and Pajonk 2012).

Gliomas

In the United States, approximately 24,000 new brain cancers are diagnosed and another 15,000 deaths are attributed to brain cancer each year (www.cancer.gov). Any tumor that arises from the glial or supportive tissues of the brain is classified as a glioma. Gliomas constitute approximately 30% of all brain and central nervous system tumors and 80% of all malignant brain tumors (www.abta.org). Gliomas are further stratified into

subgroups: astrocytoma, brainstem glioma, ependymoma, mixed glioma, oligodendroglioma, and optical nerve glioma, depending on the cell type they arise from. Astrocytomas are further categorized by their abnormality and malignancy, grades 1-4. The most malignant astrocytoma, Glioblastoma, GB, or previously known as glioblastoma multiforme, GB is the focus of this study.

Glioma Treatment

Surgical debulking is currently the most common initial therapeutic approach for glioma (Stupp, Tonn et al. 2010). Surgery provides the greatest benefit for low-grade gliomas adding 40 months to the average survival. In high-grade gliomas tumor debulking increases survival by only 4 months (Stupp, Tonn et al. 2010). Surgery is generally followed by radiotherapy. Radiotherapy for glioblastoma is usually applied in 30-33 daily fractions of 1.8 or 2Gy for a total dose of 59.4 or 60Gy respectively. Hypo-fractionated radiotherapy treatment schemes (40Gy in 15 fractions) are commonly used for elderly patients or individuals with other health complications (Buatti, Ryken et al. 2008). The current standard of care combines radiotherapy with chemotherapy. Temozolomide (TMZ), an alkylating agent for DNA, is usually the main chemotherapeutic agent utilized for brain cancers. Many brain tumors have been found to have poor repair of alkylating DNA damage as a result of inactive MGMT; a gene involved in alkylating DNA damage repair. Although it is unknown why TMZ treatment still provides a therapeutic benefit in MGMT positive patients, most clinicians don't even consider MGMT status when deciding to use TMZ as part of treatment (Holdhoff, Ye et al. 2012). Other chemotherapeutics such as, iomustine and procabazine hydrochloride, which are alkylating agents, and vincristine

sulfate, which is a mitotic inhibitor, have been shown in a clinical trial (NCT00003375) to provide a survival benefit for low-grade gliomas, but have yet to be used regularly in a clinical setting because the clinical trial is still ongoing (http://www.clinicaltrials.gov/). Classical chemotherapeutic strategies and treatments that significantly improve the survival of high-grade gliomas have remained elusive, as standard therapy fails to improve the two-year survival of high-grade gliomas over 30%.

Glioma Recurrence and Resistance

Despite advances in glioma treatment with radiotherapy and chemotherapy, and the increased knowledge of glioma biology, long-term survival after treatment remains poor, with a median five-year survival of only 10%when treated with surgical debulking, radiation and TMZ (Stupp, Mason et al. 2005). Furthermore, glioma patients quickly succumb to very aggressive recurrent tumors, with an average median progression-free survival of 7 months for GB (Stupp, Mason et al. 2005). The tumors that relapse have been found to have mutations in genes for mismatch repair including, MSH6, MSH2, MLH1, and PSM2 (Hunter, Smith et al. 2006, Cahill, Levine et al. 2007, Yip, Miao et al. 2009), leading to TMZ resistance. Another mechanism that contributes to TMZ resistance is the change in promoter methylation status of MGMT after radiation treatment. Brandes et al demonstrated that 62% of recurrent brain tumors had changed MGMT methylation status after surgical debulking, radiation and TMZ treatment when compared to samples taken at first surgery (Brandes et al., 2010). The frequent recurrence found in GB has led some groups to suggest CSCs or in brain, GSCs, to be the cause of recurrence. GSCs have been found to be more radioresistant and chemoresistant than the rest of the bulk tumor

population. Furthermore, GSCs also possess the properties of normal neural stem cells (NSCs), with the ability of self-renewal, the ability to produce differentiated progeny, and repopulate the tumor (Clarke, Dick et al. 2006).. Self-renewal and asymmetric division allows GSCs to maintain the cancer stem cell pool and produce a differentiated progeny. Many groups have demonstrated gliomas ability to form in a hierarchical organization (Altaner 2008, Venere, Fine et al. 2011, Yan, Wu et al. 2014), with a rare "special cell" with stem like properties supporting the bulk tumor mass.

In patients, these cells, which escape therapy, can stay dormant for long periods of time after treatment (Allan, Vantyghem et al. 2006). Upon reentry into the cell cycle these cells that have evaded therapy contribute to local tumor recurrence. Current glioma treatment focuses on treating the bulk tumor population, and since tumor recurrence is attributed to therapy resistant GSCs, treatments targeting glioma stem cells may lead to longer survival. However, it has been proposed that in some gliomas, the differentiated tumor cell population can revert back into glioma stem-like cells upon glioma stem cell depletion, thus maintaining a GSC population (Gupta, Chaffer et al. 2009, Chen, Nishimura et al. 2010). This would eventually result in tumor regrowth.

Therapeutic Resistance

GSCs contribute to therapy resistance through a variety of mechanisms. These include, but may not be limited to: quiescent phenotype, enhanced DNA repair in GSCs, expression of drug efflux pumps, and anti-apoptotic proteins. Many groups have reported that proliferating GSCs can assume a quiescent state and later repopulate the tumor after DNA repair (Mellor, Ferguson et al. 2005, Scopelliti, Cammareri et al. 2009). Also as demonstrated in our own lab (Lagadec and Pajonk 2012) and recently confirmed by (Wang,

Li et al. 2014) radiation can cause radiation induced CSCs (iCSCs) formation from differentiated cancer cells. Furthermore, these iCSC are more aggressive than the original cancer phenotype (Lagadec and Pajonk 2012). Chemotherapeutics such as TMZ or BCNU have been shown to cause CSC cell cycle arrest, and reduce neurosphere formation. However, upon the formation of secondary sphere cultures, they aggressively recover (Mihaliak, Gilbert et al. 2010). Other labs have published data supporting chemoresistance of GSCs, comparing the GSC marker CD133+ vs CD133-, CD133+ being more chemoresistant to a variety of chemotherapeutics (Carboplatin, Taxol, TMZ, VP16) (Liu, Yuan et al. 2006). In some cases the remaining population of cancer cells after chemotherapeutic treatments are enriched in CSCs (Kang and Kang 2007). GSCs also exhibit increased radioresistance in which IR enriches the CD133+ population (Bao, Wu et al. 2006). CD133+ cells are more radioresistant in colony formation assays, and CD133+ cells only moderately decrease in cell growth following IR treatment (Wang, Wakeman et al. 2010). Tamura et al. also demonstrated that glioma patients who undergo radiotherapy have increased levels of CD133+ expression suggesting that CD133+ cells may be more radioresistant or that radiation promotes the formation of cells with CD133+ expression in a clinical setting, thus leading to tumor relapse. However, a number of laboratories have shown that using chemotherapeutics can reduce the CD133+ population (Beier, Rohrl et al. 2008). These inconsistencies can be explained through a variety of mechanisms. But more importantly, CD133 expression varies greatly within human gliomas independent of cell stemness, and therefore may not be a good stem cell marker for gliomas. These results emphasize the need for functional assays such as neurosphere formation or *in vivo* serial

dilution assays to evaluate stemness. Nonetheless, the general consensus supports the theory that GSCs are more resistant to glioma therapy.

After cancer treatment, GSCs express many pro-survival and anti-apoptotic proteins. Pro-survival and anti-apoptotic expression may be mediated in part by hyperactive pAKT (Strozyk and Kulms 2013), and Notch signaling to maintain GSC formation. Increased pAKT expression is found in many GBs that have mutated or loss of PTEN expression. PTEN is mutated or lost in 44% of GBs (Wang, Puc et al. 1997). PTEN acts as a tumor suppressor by reversing PI3K activity thus negatively regulating pAKT expression and restricting growth. GBs with loss of PTEN function are more aggressive than PTENwt GBs.

Signaling Pathways

Notch pathway

Notch signaling plays a key role in proliferation, differentiation and survival in many tissue types under a variety of cellular contexts. Deregulation of the Notch signaling pathway has been implicated in many cancers (Allenspach, Maillard et al. 2002). In the brain, Notch signaling has roles in the regulation of migration, morphology, synaptic plasticity, and survival of immature and mature neurons (Ables, Breunig et al. 2011) as well as maintaining stemness in NSCs (Hitoshi, Alexson et al. 2002, Johnson, Ables et al. 2009, Ables, Decarolis et al. 2010).

The Notch signaling pathway is an evolutionarily conserved pathway which was first discovered and characterized in Drosophila where a mutated copy of the gene generated flies with visibly “notched” wings (Radtke and Raj 2003). From there, the

various homologs were identified in humans. There are four mammalian Notch receptors; Notch 1 to 4, which are associated with five membrane-bound ligands of the DSL Deta, Serrate/Jagged, and Lag or (DSL) family. The Notch protein is a single-pass transmembrane protein that contains up to 36 tandem EGF-like repeats in their extracellular domain (Fortini 2009). The binding between a DSL family member and notch occurs via direct cell to cell contact thus leading to a structural change exposing the S2 site for cleavage on the Notch receptor. The ADAM metalloprotease, a member of alpha secretases, cleaves the Notch receptor at the S2 site in a process called ectodomain shedding. The left over product of Notch or the Notch Extracellular Truncation (NEXT) can then become a substrate for gamma secretase proteolytic cleavage at the S3/S4 site (Stockhausen, Kristoffersen et al. 2010) releasing the Notch Intracellular Domain or NICD (Fortini 2009, Pannuti, Foreman et al. 2010). In contrast, when the DSL ligand and Notch receptor interact on the same cell, Notch signaling is inhibited (Jacobsen, Brennan et al. 1998). In canonical Notch signaling, the NICD forms a complex with CBF1/Suppressor of Hairless/Lag1, also known as RBP-J. CBF1 is a transcriptional repressor that recognizes a 7 base pair DNA sequence (GTGGGAA) (Tun, Hamaguchi et al. 1994). The complex of NICD and CBF1 recruits transcription factors facilitating in the transcription of downstream Notch targets, hes/hey family or transcriptional repressors (Iso, Kedes et al. 2003), cyclin D (Das, Lanner et al. 2010), c-myc (Palomero, Lim et al. 2006), p21 (Niimi, Pardali et al. 2007), and NFkB (Ang and Tergaonkar 2007). Notch signaling can also occur through the non-canonical pathway, independent of the NICD/CBF1 complex (Andersen, Uosaki et al. 2012). The non-canonical Notch-signaling pathway is a less understood and less well-

studied characteristic of Notch signaling. Canonical Notch signaling is depicting in **Figure A**.

Abnormal Notch signaling has been attributed to many cancer types, and was first identified as an oncogene in T-cell acute lymphoblastic leukemia (T-ALL). Upregulation of the Notch pathway has also been observed in other cancer types such as glioma (Kanamori, Kawaguchi et al. 2007, Stockhausen, Kristoffersen et al. 2010), breast (Reedijk 2012), lung (Dang, Gazdar et al. 2000, Westhoff, Colaluca et al. 2009), and cervical cancers (Zagouras, Stifani et al. 1995). Aberrant Notch activation in solid tumors is due to hyperactivation of notch ligands or of upregulation of upstream targets of Notch. Notch is an attractive target for therapy because of its many roles in development, survival, and stemness. Notch can be inhibited at different steps within its pathway (Rizzo, Osipo et al. 2008), but the most common laboratory approach to block Notch is through the use of small molecule inhibitors of gamma secretase. Some gamma secretase inhibitors, R04929097, have been utilized in Phase 1 and Phase 2 clinical trials. Gamma secretase inhibitors are thought to block the S3 cleavage step for all four Notch receptors, leading to the NICD to remain bound thus stopping NICD translocation into the nucleus and further Notch signaling. In *in vivo* models, excessive use of gamma secretase inhibition induces goblet cell metaplasia in the small intestines and leads to gastrointestinal tract cytotoxicity (Barten, Meredith et al. 2006).

Figure A: Cononcial Notch Signaling Pathway

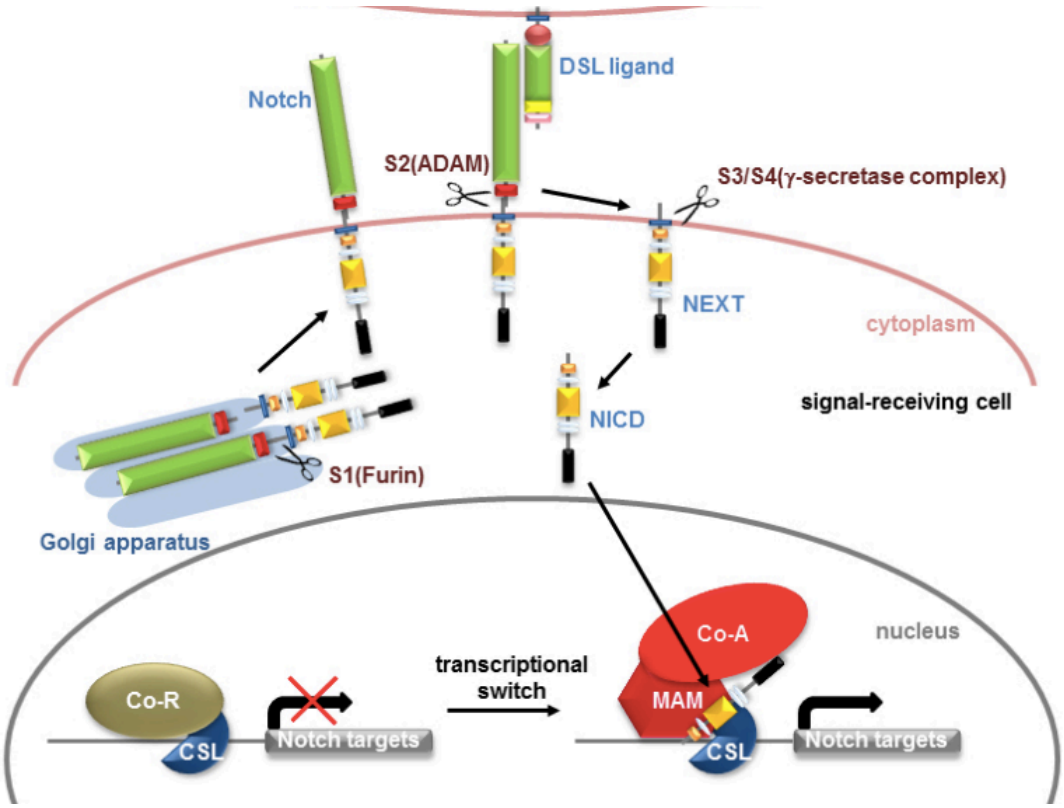

Figure A: Notch activation leads to NICD formation and downstream notch signaling. Image reference from http://med.fsu.edu/userFiles/image/katofigure1.jpg

Notch signaling in glioma

The Notch signaling pathway maintains Neural and glioma stem cells. The effects of high Notch expression results in a quiescent stem cell phenotype in brain and fibroblast tissues. In quiescent fibroblast cells, the Notch target gene *Hes1* is upregulated and upon Notch inhibition with DAPT (a gamma secretase inhibitor) or dominant negative form of *Hes1* expression shifts the quiescent cells into a permanent arrested cell cycle state (Sang, Coller et al. 2008). These permanently arrested cells also express increased b-galactosidase, a feature of senescence. Finally, re-expression of wt*Hes1* inhibited the cells from entering senescence, demonstrating that Notch expression effects the cell cycle and cell fate.

Notch activity in glioma has been correlated with glioma severity (Wang, Wakeman et al. 2010). In general, Notch receptors, ligands, and downstream targets are overexpressed in glioma tissues and cell lines (Kanamori, Kawaguchi et al. 2007, Chen, Kesari et al. 2010, Jiang, Wu et al. 2011). Notch1 expression and protein levels increase with glioma grade 1 to 4, and high Notch1 expression is associated with a poorer prognostic outcome (Jiang, Wu et al. 2011). Another research group demonstrated that Notch1 and Notch2, but not Notch3 or 4, are important for regulating GB cell cycle growth with Notch2 having a more dominate role (Chen, Kesari et al. 2010). Inhibiting the Notch pathways with siRNA or gamma secretase inhibitors (GSI), decreases the ability of adherent glioma cultures to form colonies while increasing differentiation in treated cells (Kanamori, Kawaguchi et al. 2007). Conversely, increasing Notch downstream signaling targets enhances glioma survival.

Notch's role in maintaining GSCs makes it a potentially specific target for inhibiting GSCs. Notch receptors and downstream targets, *hes* and *hey* are upregulated in CD133+ cell populations (Ulasov, Nandi et al. 2011). Glioma neurosphere cultures with higher Notch signaling have higher growth rates than those with lower Notch signaling (Zhang, Zheng et al. 2008). Overexpression of constitutively active NICD in neurosphere cultures further increases cell growth and neurosphere formation (Zhang, Zheng et al. 2008). Notch signaling directly activates the transcription of the stem cell marker Nestin (Shih and Holland 2006), while knocking down Notch with siRNA or GSI decreases both Nestin and CD133+ markers in neurosphere cultures (Jeon, Jin et al. 2008, Lin, Zhang et al. 2010).

Notch expression causes radioresistance in glioma (Wang, Wakeman et al. 2010) and treatment with GSI or shRNA, sensitizes neurosphere cultures to radiotherapy (Lin, Zhang et al. 2010, Wang, Wakeman et al. 2010). However, Notch signaling is not the only stemness pathway in glioma. Other pathways such as Sonic Hedgehog (SHH) which also confer radioresistance, GSC renewal, and tumor growth (Clement, Sanchez et al. 2007) in GB are insensitive to gamma secretase inhibition (Hatton, Villavicencio et al. 2010). Furthermore, GBs with high Notch expression are susceptible to Notch inhibition via gamma secrtease while GBs with low/no Notch expression do not respond to treatment (Saito, Fu et al. 2014). Therefore, although targeting Notch signaling may be effective for a vast majority of GB tumors there are subsets of GB that do not respond.

Gamma secretase

Gamma-secretase is an aspartyl protease made up of four membrane proteins, presenilin (PS), nicastrin, PEN2, and Aph-1 (Edbauer, Winkler et al. 2003, Kimberly, LaVoie

et al. 2003, Fraering, Ye et al. 2004). Together these four membrane proteins function to identify and cleave type 1 membrane proteins such as Notch and APP in Alzheimers. PS is a nine-pass transmembrane protein that contains the catalytic activity of the core protease (Esler, Kimberly et al. 2000, Li, Xu et al. 2000, Laudon, Hansson et al. 2005). Nicastrin functions in assisting with substrate selection (Shah, Lee et al. 2005). Aph-1 promotes the assembly, stabilization, and trafficking of the complex (Niimura, Isoo et al. 2005), and PEN2 triggers PS endoproteolysis (Thinakaran, Borchelt et al. 1996, Luo, Wang et al. 2003). To add to the complexity, PS comes in two isoforms, PS1 and PS2, PS1 being the more dominant form, but PS selection has been found to vary between tissues. More importantly however, PS1 and PS2 have strong phenotypic differences between the two PS systems, and each isoform exhibits differential susceptibility to certain gamma-secretase inhibitors (Beel and Sanders 2008). Furthermore, Aph-1 has been identified to have three isoforms, Aph-1a (which has two splicing variants, Aph-1aS and Aph-1aL) and, Aph-1b. Similar to PS, Aph-1 has tissue specific expression patterns (Hebert, Serneels et al. 2004) and evidence suggests that each isoform may associate with functionally distinct versions of gamma-secretease complexes (Serneels, Dejaegere et al. 2005). The various associations with the four different core isoforms allows gamma-secrtease to cleave over 91 different membrane substrates (Haapasalo and Kovacs 2011). Understanding the functional significance and regulation of gamma-secretase mediated cleavage requires further study. Currently, the functions of some of GS cleaved products like NICD are known, can regulate gene transcription. It is also thought that the generation of some ICDs may operate as a means to terminate or antagonize protein signaling, such as in cell adhesion or neurite outgrowth,

but currently it is not known if all ICDs generated by gamma-secretase even have a function (Haapasalo and Kovacs 2011).

Of the 91 different substrates gamma-secretase processes, there are many substrates that can effect the regulation of cell fate, the regulation of cell death, and the regulation of angiogenesis and tumorigenesis. Cell fate regulation via gamma-secretase is mediated through Notch and ErbB4 (Srinivasan, Gillett et al. 2000, Fiuza and Arias 2007). In both cases, the release of the cleaved ICD maintains stemness in brain cancers (Sardi, Murtie et al. 2006). Gamma-secretase regulates cell death by processing LRP1 (Polavarapu, An et al. 2008), and p75 (Majdan, Lachance et al. 1997). Cleavage of both LRP1 and p75 leads to apoptosis in neurons, while inhibiting gamma-secretase activity prolongs survival (Podlesniy, Kichev et al. 2006, Polavarapu, An et al. 2008). Although gamma-secretase may process many different substrates, loss of Notch signaling through gamma-secretase inhibition has a greater impact on cell fate then the other membrane substrates.

FOXO family of transcription factors

FOXO has more recently, been implicated in the maintenance of stemness in neural stem cells, but the signaling involved in FOXO mediated stemness is less understood. FOXO, or forkhead box transcription factors, consists of FOXO1, FOXO3, FOXO4, and a more distantly related FOXO6. Together, the FOXO class of transcription factors control apoptosis, stress resistance, longevity, metabolism and cellular development (Calnan and Brunet 2008). The FOXO family, once activated by phosphorylation of conserved serine/threonine sites, recognizes the same core consensus motifs TTGTTTAC, TT(G/A)TTTTC, (C/A)(A/C)AAA(C/T)AA (Furuyama, Nakazawa et al. 2000, Xuan and

Zhang 2005, Obsil and Obsilova 2011), and therefore serves to integrate many cellular signals and stimuli. FOXO proteins function as transcriptional activators, but bioinformatics analysis suggests FOXO may also act as transcriptional repressors (Ramaswamy, Nakamura et al. 2002). Currently, the role of FOXO action on tissues has been determined via conditional knockout mice. Knocking out all three FOXO factors (FOXO1, FOXO3, and FOXO4) cause a myriad of abnormalities. Specifically, in stem cells knockout of FOXO3 depletes the stem cell pools of hematopoietic (Miyamoto, Araki et al. 2007) and brain stem cell compartments (Ro, Liu et al. 2013). In differentiated cells FOXO1 has been established in metabolic function and insulin resistance (Martinez, Cras-Meneur et al. 2006). In differentiated tissues many studies have also identified the FOXO3 mediated apoptotic activity after oxidative stress, via BH-3 proteins (Sunters, Fernandez de Mattos et al. 2003), but it hasn't until recently been observed that FOXO3 also participates DNA damage repair by interacting with ATM to promote DNA foci formation for repair (Tsai, Chung et al. 2008). Lastly, FOXO4 null mice do not show any distinct phenotype (Hosaka, Biggs et al. 2004), and therefore FOXO4 hasn't been studied as extensively as FOXO1 and FOXO3. FOXO6 expression is found exclusively in the brain, specifically the hippocampus region and is thought to function in memory consolidation (Jacobs, van der Heide et al. 2003).

The structure of all FOXOs consists of a Forkhead domain, or DNA recognition binding domain, a nuclear localization signal (NLS), a nuclear export sequence (NES), and varying numbers of serine and tyrosine phosphorylation sites (Greer and Brunet 2005). Furthermore, FOXO proteins can undergo various post-translational modifications or acetylation events altering its DNA binding affinity, and recognition. FOXO proteins are

constantly shuttling between the cytoplasm and nucleus however, in all cases, FOXO activation requires nuclear localization to interact with DNA (Brownawell, Kops et al. 2001). FOXO export from the nucleus abrogates any downstream FOXO signaling, by inhibiting FOXO binding to DNA. The FOXO pathway is regulated by PTEN/PI3K/AKT signaling (depicted in **Figure B**). pAKT, the active form of AKT, negatively regulates FOXO activity by phosphorylation on threonine-32, serine-253, and serine-315, thus masking the nuclear localization sequence (NLS) preventing FOXO nuclear localization and promoting FOXO degradation. This causes FOXO to be exported from the nucleus leading to its degradation (Biggs, Meisenhelder et al. 1999, Brunet, Sweeney et al. 2004). PTEN antagonizes PI3K/AKT by reversing the action of PI3K. This action positively regulates FOXO, allowing sustained FOXO expression (Luo, Yang et al. 2013). The multiple phosphorylation sites on FOXO proteins integrate many signaling pathways allowing for a differential response to stimuli. The different environmental context and cell type determine FOXOs phosphorylation patterns and hence response to stimuli (Calnan and Brunet 2008). In the presence of growth factors FOXO1 is phosphorylated at S249, S322, and S325 leading to its export from the nucleus by 14-3-3 (Brownawell, Kops et al. 2001), while under a stress response Ser90, Ser284, Ser294, Ser300, Ser413, Ser425, Thr427, and Ser574 are just a few phosphorylation sites that may be utilized for nuclear localization (Greer and Brunet 2005). As stated earlier, FOXO3 mediates apoptotic activity after oxidative stress through BH-3 proteins such as BIM (Sunters, Fernandez de Mattos et al. 2003). Alternatively, FOXO3 phosphorylation by c-JUN and MST1 then subsequently are deacetylated by sirtuin-1 (SIRT1) in the forkhead domain, leads to the inhibition of FOXO-

induced expression of pro-apoptotic genes and enhanced expression of genes involved in cell cycle regulation, DNA-repair, and stress resistance (Brunet, Sweeney et al. 2004).

The dynamics of how FOXO proteins are regulated, and the combination of phosphorylation and acetylation events are poorly understood. It is clear however, that FOXOs carry out differential functions that depend on the tissue type, environmental stimuli, and cells phase or stemness (Asserlechner 2012).

Figure B: FOXO regulation

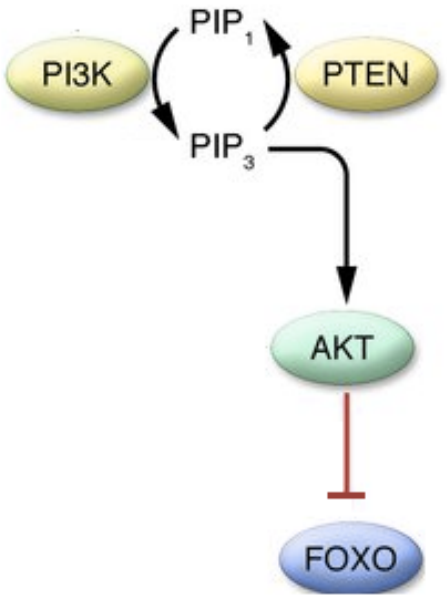

Figure B: The FOXO/PTEN/Akt pathway

FOXOs in neural stem cells

Throughout the development of the nervous system, FOXO members are likely to play many seemingly contradictory roles. However, in stem cells FOXO3 has established itself as a key regulator of stem cell quiescence in the hematopoietic system, adult muscle stem cells, and now neural stem cells (Miyamoto, Araki et al. 2007, Renault, Rafalski et al. 2009, Gopinath, Webb et al. 2014). FOXO3's regulation of stemness is linked to the expression of genes involved in maintaining quiescence, preventing premature differentiation, and regulation of oxygen metabolism (Renault, Rafalski et al. 2009). FOXO3 knockout mice share a similar phenotype to PTEN knockout mice in that the brains of these mice are larger due to rapidly proliferating stem cells. However, PTEN functions as a negative blockade on quiescence stem cell cycle entry (Groszer, Erickson et al. 2006), while FOXO3 promotes genes required for quiescence and stemness (Gopinath, Webb et al. 2014). The difference is observable in *in vivo* mouse models between PTEN null mice and FOXO null mice. Both PTEN knockout and FOXO3 knockout mice show a depleted neural stem cell pools, but FOXO3 null mice suffer because the resulting neural stem cells have a severely limited proliferating capacity (Renault, Rafalski et al. 2009). One mechanism by which FOXO3 blocks premature differentiation is by inhibiting ASCL1 dependent neurogenesis (Webb, Pollina et al. 2013). Through a CHiP analysis, Webb et al. found that FOXO3 shares many targets of ASCL1, and also suggested some other targets of FOXO expression may be Notch target genes like Hes1. Lastly, although not established in neural cells, FOXO1 in muscle tissue has been shown to interact with the CSL or (CBF1) to promote corepressor clearance of the Notch signaling pathway. In doing so, FOXO1 inhibits myoblast differentiation through the expression of Notch target genes (Kitamura, Kitamura

et al. 2007). Furthermore, FOXO3 has been shown to regulate the expression of both Notch1 and Notch3 (Gopinath, Webb et al. 2014). Although the mechanism of how FOXO regulates Notch receptors and notch activity is not fully understood, it does provide an interesting alternative mechanism for Notch activation.

Research objectives:

In the interest of improving current glioma treatment outcomes, we evaluated the efficacy of combinational treatment of GSI plus radiation to reduce glioma recurrence. In this study, we focus on evaluating the effects of GSI and radiation on GSCs with different genetic backgrounds. The basis for this research is that current radiation and chemotherapeutic treatment do not provide curative means for patients. Here, we investigate how PTEN radio-protects GSI treated GSCs, and we propose this mechanism is through FOXO3 mediated control of quiescent stem cells.

CHAPTER 2: Materials and Methods

Considerations when growing GSCs

Traditionally, glioma cell cultures are grown as adherent cultures supplemented with serum. However, the gene expression profiles of adherent cultures can vary drastically from the original tumor (Lee, Kotliarova et al. 2006) and when these cultures are transplanted into intracranial xenograph animal models they fail to grow in a diffuse phenotype as observed in glioma patients. Adherent or serum grown cells also have relatively low CSCs within the population, the majority of the cells being differentiated cells. Currently, there are two methods to propagate CSCs: the neurosphere method, which is the most popular, and the laminin-coated plate method. Gliomas grown in neurosphere cultures, are in a defined serum-free media supplemented with growth factors (EGF, FGF). Glioma neurospheres form non-adherent spheres with a greatly enhanced population of CSCs that closely resemble the original tumor genetically and morphologically in intracranial xenographs. The neurosphere model is a good *in vitro* model because it more closely maintains the characteristics of the tumor from which it was derived (Lee, Kotliarova et al. 2006, Ernst, Hofmann et al. 2009). However, neurospheres that grow to large tend to have more cell death as a result of lack of nutrients to diffusion to the interior of the sphere (Woolard and Fine 2009). In the Laminin-coated method, cells are grown adherently on plates coated with laminin in serum-free media (Pollard, Yoshikawa et al. 2009). Laminin coated cultures have the added benefit that of less cell death than neurospheres grown cultures. However, because cells grown in laminin plates are more homogeneous, the cultures do not exhibit hierarchical growth, which is one defining characteristic of a CSC (Venere, Fine et al. 2011).

Because the neurosphere methods more closely represents *in vivo* tumors genetically and produces progenitor cells we chose the neurosphere method to enrich for GSCs for our experiments. To solve the lack of diffusion of nutrients to the interior of the neurospheres, neurospheres where dissociated weekly. To ensure drug treatment diffused to all neurosphere cells, neurospheres were dissociated one day before drug treatment occurred.

Cell Culture

U87 and U87 PTEN cell lines were a kind gift from Dr. Paul Mischel (Department of Pathology, UCSD). Cell lines 146, 189, 2345, ES were a kind gift from Dr. Harley Kornblum. ZsGreen-cODC positive fluorescence correlates with current stem cells markers as well as functional assays. In all GBM lines (146, 189, 2345, ES, U87, and U87 PTEN), cells were cultured in the log-growth phase in Dulbecco's modified Eagle Medium (DMEM) (Invitrogen Carlsbad, CA) supplemented with 10% fetal bovine serum (Sigma-Aldrich, St. Louis, MO), penicillin (100 units/ml) and streptomycin (100 µg/ml) (both Invitrogen). All cells were grown in a humidified incubator at 37C with 5% CO2.

To convert adherent cell lines to neurosphere cultures were trypsinized and immediately plated defined serum-free media consisting of DMEM/F12 1:1 (Life Technologies 11320-033) B27 (Invitrogen) HEPES (Life Technologies 15630-130) 1% pen-strep (Life Technologies 15140-122) 20ng/mL epidermal growth factor (Sigma Aldrich), 20ng/mL basic fibroblast growth factor 2 (Sigma-Aldrich), 5ug/mL bovine insulin (Sigma-Aldrich), 4ug/mL heparin (Sigma-Aldrich) in ultra low-adhesion suspension culture plates. Neurospheres were dissociated, and reseeded in plates after one a week or when the media

needed to be changed as indicated by phenol red color change (phenol red is a pH indicator, and turns yellow with the pH become increasing more acidic).

Drug Treatment

Gamma-Secretase Inhibitior WPE-III-31C also known as InSolution gamma-Secretase Inhibitor XVII, was purchased from Millipore. GSI concentration was determined on the inhibitory concentration 50%, or IC50. It was determined that 5uM of WPE-III-31C would provide 100% inhibition for 1 day. LY294002 concentration was determined based off of previous literature (Takeuchi, Kondo et al. 2005) in which 5nM of LY294002 demonstrated inhibition of pAkt with limited cell death. Adherently grown cells were treated with corresponding drugs when they reached 80% confluence, while neurosphere or suspension grown cultures were dissociated, reseeded and treated the next day with the corresponding drug. Dissociating the neurosphere allows the drug to penetrate all the cells in culture. Large spheres limit drug diffusion for cells residing in the interior of the neurosphere. After GSI or LY treatment, if cells were going to also receive radiation, then cells were allowed to incubate for 4 hours with GSI/LY before irradiation.

RNA isolation

RNA was harvested from the cells grown adherently or in suspension in 10cm dishes using 1mL Trizol reagent (Invitrogen) according to the manufacturer's protocol. RNA concentration was measured using a Nanodrop and 1ug of RNA was converted to cDNA using Super Script III First-Strand Synthesis (Invitrogen) for future use in

Quantitative-PCR (q-PCR). q-PCR was performed using the BioRad iQ5 Real-Time PCR machine. SYBR Green was used as the reporter system in the q-PCR master mix (BioRad).

RT-PCR and qRT-PCR

Quantitative PCR was performed in the MY iQ thermal cycler (Bio-Rad, Hercules, CA, www.bio-rad.com/) using the 2x iQ SYBR Green Supermix (Bio-rad). C_t was determined for each gene and $\Delta\Delta C_t$ was calculated relative to the designated reference sample (RPLP0). Gene expression values were then set equal to $2^{-\Delta\Delta Ct}$ as described by the manufacturer of the kit (Applied Biosystems). An annealing temperature of 54 °C was used and ran for 50 cycles for the following primers: PCR primers were synthesized by Invitrogen and designed for the human sequence of FOXO1 (Forward: 5'-GACAGCCCTGGATCACAGTTT-3' and Reverse 5'-CGGTCATAATGGGTGAGAGTCT-3'), FOXO3 (Forward: 5'-CGGACAAACGGCTCACTCT-3' and Reverse: 5'-GGACCCGCATGAATCGACTAT-3'), FOXO4 (Forward: 5'-TCTGGGGGAAAAGGTACACAC-3' and Reverse: 5'-CTCCCTTCCGAGGACCTGTTA-3'), Grx1 (Forward: 5'-TGCAACCAGTTTGGGCATCA-3' Reverse: 5'-ACCGTTCACCTCGCACTTC-3'), and RPLP0 (5'-GGCGACCTGGAAGTCCAACT-3' Reverse: 5'-CCATCAGCACCACAGCCTTC-3'). Hes1 (Forward: 5'-AGTGAAGCACCTCCGGAAC-3', Reverse 5'-TCACCTCGTTCATGCACTC-3'), Hey1 (Forward: 5'-GCTGGTACCCAGTGCTTTTGAG-3', Reverse: 5'-TGCAGGATCTCGGCTTTTTCT-3'), HeyL (Forward: 5'-GCCCGGGGTTCTATGATATT-3', Reverse: 5'-GAGTTCGGCCTTCACAAAAG-3') Notch1 (Forward: 5'-CAGGCAATCCGAGGACTATG-3', Reverse: 5'-CAGGCGTGTTGTTCTCACAG-3'), Notch2 (Forward 5'-CACTGGGTCGATGATGAAGG-3', Reverse 5'-ATCTGGAAGACACCTTGGGC-3'), Notch3 (Forward 5'-

TCTTGCTGCTGGTCATTCTC-3', Reverse 5'-TGCCTCATCCTCTTCAGTTG-3') and Notch4 (Forward 5'-CACTGAGCCAAGGCATAGAC-3', Reverse 5'-ATCTCCACCTCACACCACTG-3') . The ΔΔCt method was used and gene expression recorded relative to U87. Normalization was performed utilizing RPLP0 as a housekeeping gene.

Western Blotting

Cells were lysed on ice using RIPA buffer. The lysates were centrifuged at 12,000 rpm for 15 mins at 4 C, and the protein concentration in the supernatant was determined using the microBCA protocol (Pierce, Rockford, IL). The protein lysate was separated using an SDS-PAGE gel and then transferred to a Polyvinylidene difluoride (PVDF) membrane (BioRad). Membranes were blocked in 4% BSA/Tris Buffered Saline (TBS)-0.01% Tween20 and then blotted overnight for the various proteins: rabbit anti-PTEN primary antibodies (Abcam Y184, Cambridege, MA, 1:2000, www.abcam.com), anti-EGFR (Nanomarkers MS-400-P0), anti-pAkt (Cell Signaling S473), and anti-Akt (Cell Signaling #9272S). Antibodies used for the loading controls were: GAPDH (abcam ab9484) or alpha-tubulin (Calbiochem Cat#: CP06). After washing, the blots were incubated with anti-rabbit horseradish peroxidase-conjugated secondary antibody (1:50,000 GE Healthcare Bio-Sciences, Pittsburgh, PA, www.gelifesciences.com/webapp/wcs/stores/servlet/Home/en/GELifeSciences-US/) and visualized by ECL plus Membrane Blotting Detection System (Pierce, ECL 2 Western Blotting Substrate #80196, Rockford, IL) using a laser scanner (Typhoon 9410, GE Healthcare).

Radiation Treatment

Both cells grown in adherent and suspension conditions were irradiated at room temperature using an experimental X-ray irradiator (Gulmary Medical Inc. Altlanta, GA) at a dose rate of 1.43Gy/min for the time required to apply the prescribed dose of 2, 4, 6, or 8Gy.

ROS measurements

ROS measurement were carried out using the dichlorofluorescein assay (DCF) as described in previous literature (Hafer, Iwamoto et al. 2008). Cultured cells were trypsinized then washed with 5mL of 1x PBS. Cells were counted and 1 million cells were resuspended in 1mL of PBS. DCF was added to corresponding tubes at a concentration of 50uM and the mixture of DCF and cells were incubated in the dark at 37C for 30 minutes. After 30 minutes, cells were placed on ice and maintained in the dark while transporting them to and from the X-ray machine. Cells were either sham irradiated or irradiated with 8Gy and immediately analyzed via FACs in the green fluorescent channel.

Clonogenic Survival Assay

1 million cells were plated in 10 cm dishes one day prior to radiation and/or drug treatment. The next day, cell plates were treated with the appropriate drug or control and incubated for 4 hours. After a 4-hour incubation, plates were trypsinized and cells are harvested, washed with 1x PBS and counted. Cells for both treated and untreated conditions were resuspended in eppendorf tubes such that there were 512 cells per 100uL

for 0Gy, 1024 cells per 100uL for 2 Gy, 2048 cells per 100uL for 4 Gy, 4096 cells per 100uL for 6 Gy and, 8192 cells per 100uL for 8Gy. eppendorf tubes were then irradiated with the corresponding dose. Each radiation dose was plated in triplicate with 100uL of cells from the corresponding eppendorf tubes such that 0Gy received 512 cells per plate, 2Gy received 1024 cells per plates, ending at 8Gy receiving 8192 cells per plate. Plates were incubated for 3 weeks. Media was removed and 70% ethanol fixed the cells for 5 minutes. 70% ethanol was removed and a 5% crystal violet stain was applied to the dishes and allowed to stain for 5-10 minutes. The 5% crystal violet solution was poured off and the remaining stain was gently washed off in warm water. Plates were allowed to dry over night and scanned the next day. Colonies were counted from scanned images using the free open-source software ImageJ. Colonies containing a density of ≥50 cells were counted, and the number of colonies formed per plate is expressed as a percentage of the initial number of cells plated.

Neurosphere-forming capacity assay

Similar to the clonogenic assay, dissociated neurosphere cells were resuspended in eppendorf tubes at concentrations of 512, 1024, 2048, 4096, and 8192 cells per 100ul for each corresponding radiation dose of 0, 2, 4, 6, and 8Gy. Neurosphere cells were then plated in serum free media, in ultra-low adhesion 96-well plates in 200ul DMEM/F-12 supplemented with 0.4% bovine serum albumin (BSA) (Sigma-Aldrich), 10mL/500mL of B27 (Invitrogen), 5ug/mL bovine insulin (Sigma-Aldrich), 20ng/mL of basic fibroblast growth factor 2 (Sigma-Aldrich) and 20ng/mL of epidermal growth factor (Sigma-Aldrich). 96-well plates were serially diluted and after 15 days in culture, neurospheres with

diameters larger than 100um were counted. The numbers of neurospheres were expressed as a percentage between the numbers of cells plated verses the number of spheres counted.

gH2Ax Formation Assay

Cells were plated at 100,000 cells per 10 cm dish, allowed to grow for 2 days, and then treated with GSI or DMSO control 4 hours prior to 0 or 8Gy irradiation. Cells were then harvested and fixed in 70% ice-cold ethanol over night at -20C either 30 minutes or 24 hours after IR exposure. Samples where then washed to remove the 70% ethanol and incubated with anti-gH2Ax (Millipore H2A.X Ser139 FITC 16-202A) at 1:200 dilution for 4 hours at room temperature before analysis via FACS in the green fluorescent channel.

Cell Cycle Analysis

Cells grown under adherent conditions were trypsinized and then washed with 1x PBS three times. Afterwards, cells were fixed in 70% ice-cold ethanol over night at -20C. Cells grown in neurosphere suspension conditions were collected in media, spun down, and then washed with 1x PBS two times. Neurospheres were then allowed to incubate in 200uL TrypLE for 10 minutes at 37C. Neurosphere were then passed though a fire polished glass pipette for dissociation. Afterwards, dissociated neurospheres were replated and allowed to recover for two days before harvesting. After two days, (dissociated neurospheres haven't started to clump but are still single cells) dissociated neurospheres were harvested, washed two times with 1x PBS and fixed in 70% ethanol

over night at -20C. Both neurosphere grown and adherently grown glioma cells were incubated in Hoechst dye (5ug/mL) for 45 minutes in the dark at room temperature. PY staining (10ug/mL) was added immediately after the 45 minutes incubation of Hoechst, and incubated an additional 10 minutes in the dark at room temperature. Cells were spun down and washed with PBS once, and then resuspended in 100uL of 1x PBS for FACs analysis.

Statistics

Statistics were done in Graphpad Prism. Comparisons between groups were done using students t-test, and significance was taken at $p < .05\%$. Survival curves were fitted using the linear quadratic model.

CHAPTER 3

Results: GBs sensitivity to Gamma-secretase inhibition and radiation depends on PTEN status.

Currently, the combination of surgery, IR, and chemotherapy provide the best treatment for gliomas. However, even with the advancement in our understanding of glioma, better dose delivery treatment modalities for radiation, and more potent chemotherapeutic drugs for glioma tissues, the 5-year median survival after treatment remains low. The development of drugs or techniques that target the factors that cause glioma recurrence, i.e. GSCs are promising for future treatments. Taking into consideration that many glioma subtypes rely on notch signaling, and Notch is critical in glioma stem cell maintenance, we were interested in evaluating the efficacy of combinational treatment by blocking Notch with GSIs and radiation. Interestingly, previous studies have demonstrated that there is a group of glioma stem cells that respond to GSI mediated Notch inhibition and a subgroup of non-responders to GSI treatment. (Saito, Fu et al. 2014). Saito et al. did not evaluate how this translates with radiation therapy. However, Debeb et al. reported that treatment with GSI radio-protected breast cancer stem cells. Radioprotecting a CSC population would be a counterproductive measure to curative therapy. Hence, we first generated survival curves for neurospheres, and adherently grown cultures for a variety of patient derived GB cell lines (146, 189, 2345, ES, U87MG, U87MG PTEN restored). Utilizing

escalating doses of radiation, 0, 2, 4, 6, and 8Gy, with or without combined treatment GSI, 5uM WPE-III-31C, we were able to establish the initial effects of GSI and radiation on the survival of GSCs. Utilizing primary, secondary, and tertiary sphere forming capacity, we were able to determine the effects of GSI, IR alone, or GSI and IR in combination, to the long-term proliferative potential of glioma stem cells. Next, we established some of the genetic differences between our GB lines that are known to effect tumorigenicity via western blotting. Lastly, to determine if changes in DNA damage response produced the differences we observed in neurosphere survival curves, we performed gH2Ax staining. gH2Ax served as a surrogate marker to measure DNA double strand breaks. We further investigated the differences between PTENwt cell lines and PTEN mutant cell lines that could account for the differences we observed in GSC survival, and we propose a mechanism to describe our observations.

Results

Establishing glioma neurosphere cultures

As a first step in understanding how glioma stem cells respond to treatment with radiation and GSI individually we first converted adherent glioma cell lines to serum-free neurosphere media establishing primary neurosphere cultures. Neuroosphere morphology between the cell lines (U87, 189, 146, 2345, ES, U87PTEN resotred) all had moderately dense spheres with 146 and 189 being harder to dissociate during sphere passages. 2345 and ES represented a much slower growing neurosphere population while U87MG and U87MG PTEN restored had the fastest growing spheres. The percent of

spheres capable of forming neurospheres, neurosphere-initiating cells, varied between the cell lines, with U87MG/U87MG PTEN restored having the highest percent of sphere formation at 2.12% ± .57 (**Figure 1a**).

Neurosphere cultures are a convenient method to study glioma stem cells, however, analysis of neurospheres should not be used to make direct comparisons to *in vivo* tumor formation or growth. The *in vitro* setting lacks much of the biological niche that regulates the balance between growth and death, and *in vitro* methods are designed to improve growth conditions for cells compared to an *in vivo* setting. The neurosphere culture lines, 146, 189, 2345, ES, U87MG, U87MG PTEN restored have not all been established on their ability to form tumors in nude mice. Furthermore, the PTEN and EGFR status was established via western blotting, while p53 and MGMT status was already determined by the labs who derived the cell lines. PTEN, EGFR, p53 and MGMT status have all been implicated in glioma resistance to therapy, and therefore it is important to determine if they also play a role in the effectiveness of GSI treatment. 2345 is the only cell line with mutant p53 status; all cell lines have some level of active MGMT. 146, 189 and U87MG PTEN restored have normal PTEN expression, while 2345, ES and U87MG have no PTEN expression. Only ES and 146 have low EGFR expression while the rest of the cell lines have normal EGFR expression. The status of each cell line is summarized in **Table 1**. Treatment with GSI shows no significant difference in sphere formation between untreated cell lines except for cell lines 2345, and ES, (both PTEN null) where treatment with GSI increased the percent number of spheres (**Figure 1b**).

Figure 1A: Neurosphere Initiating Potential

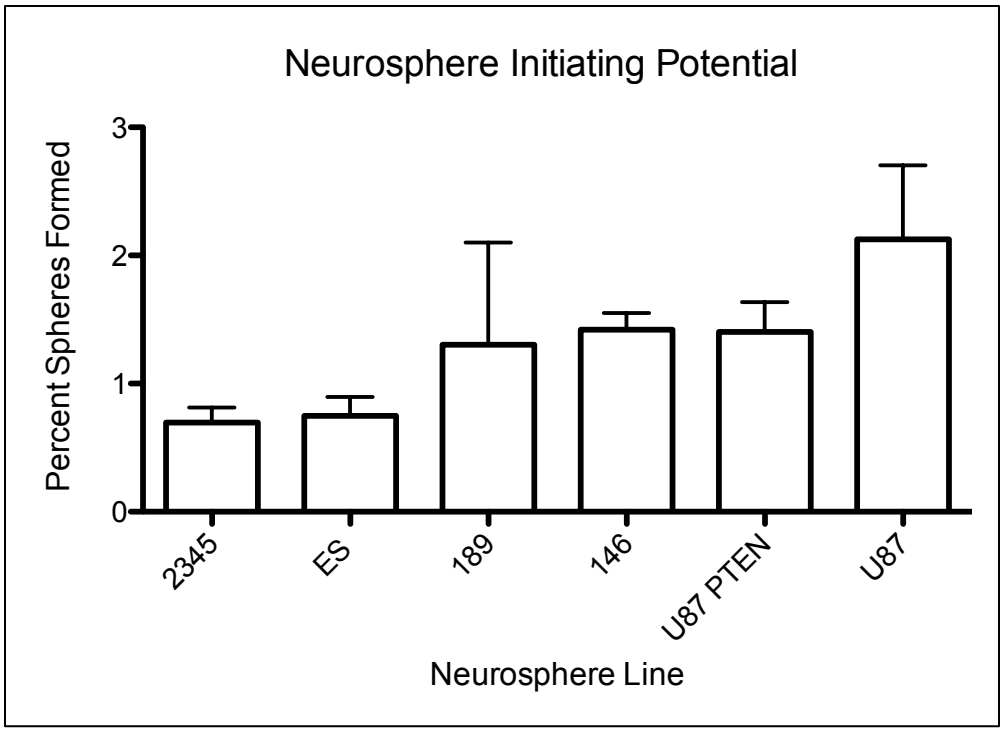

2345	ES	189	146	U87PTEN	U87MG
.69% ± .11	.75% ± .33	1.3% ± .79	1.4% ± .13	1.4% ± .23	2.12% ± .57

Figure 1a: Neurosphere plated at low density represent the population of cells with tumor initiating potential or neurosphere initiating potential. Here we show the neurosphere initiating potential of our human derived GB cell lines. Replicates were averaged and error bars displayed as standard error of the mean.

Table 1: Cell Lines

	ES	2345	146	189	U87MG	U87MG PTEN
PTEN	-	-	+	+	-	+
EGFR	Low	Normal	Low	Normal	Normal	Normal
MGMT	High	High	Low	Low	Low	Unknown
p53	Normal	Mutant	Normal	Normal	Normal	Normal

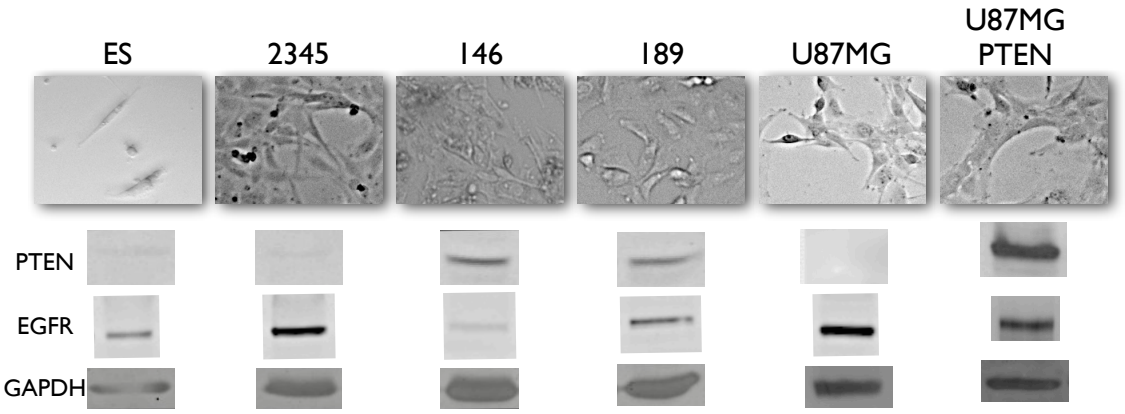

Table 1: Shows the different cell lines and their status in relation to PTEN, EGFR, MGMT and p53.

Figure 1B: DMSO vs GSI treatment on Neurosphere formation

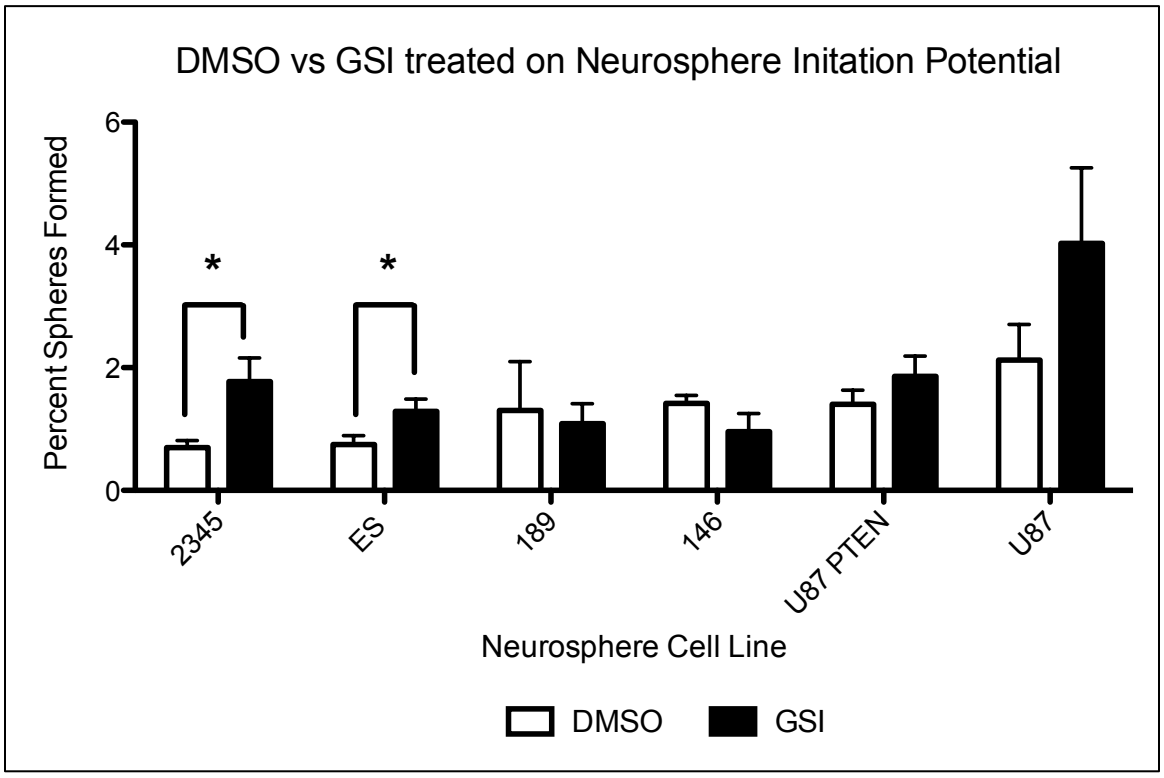

	2345	ES	189	146	U87PTEN	U87MG
DMSO	.69% ± .11	.75% ± .33	1.3% ± .79	1.4% ± .13	1.4% ± .23	2.12% ± .57
GSI	1.7% ± .37	1.2% ± .19	1.08%±.32	.95% ± .29	1.8% ± .33	4.0% ± 1.23
Significance	p = .023	p = .04	N/A	N/A	N/A	N/A

Figure 1b: Here we compare neurosphere initiation potential when treated with GSI verses DMSO control treatment. Only 2345 and ES showed a significant increase in sphere formation while GSI does not affect neurosphere formation for the rest of the cell lines. Replicates were averaged and error bars are displayed as standard error of the mean.

Irradiating our cell lines with 0, 2, 4, 6, or 8Gy and plating them for neurosphere formation assays and classical clonogenic assay allowed us to generate survival curves **Figure 2a** and **Figure 2b**. Consistent with current literature, our PTEN null glioma neurospheres lines (2345, ES) were more radio-resistant than the PTEN-wt neurospheres (146, 186) (**Figure 4a, Figure 5**) (Hambardzumyan, Becher et al. 2008). However, U87MG (PTEN-null) neurospheres were more radiosensitive then U87MG PTEN restored (Figure 4b, Figure 5). In a classical clonogenic assay comparing adherent grown cultures, U87MG was more radioresistant than U87MG PTEN restored. Comparing adherent grown survival curves between all cells lines showed no correlation to radiosensitivity between PTEN-null and PTEN-wt glioma cell lines (**Figure 3**).

To evaluate the effects of combined treatment of GSI and radiation we performed neurosphere formation assays and clonagenics treated with GSI with the varying doses of IR, 0, 2, 4, 6, 8Gy. When comparing control treated neurosphere survival curves to the GSI treated neurosphere survival curves, we observed that for the PTEN-wt lines, GSI showed a radio-protective effect. In the PTEN-null glioma cell lines, GSI enhanced radiation sensitivity (**Figure 6**). In survival curves generated from adherently grown cultures, no correlation could be found between radiation sensitivity and PTEN status (**Figure 7**). Since PTEN plays a role in the combined response of GSI and IR, we decided to use U87MG (PTEN-null) and U87MG PTEN restored as our model system for further investigation on the effects of GSI with radiation.

Figure 2 : Clonogenic Survival Assay

Figure 2A

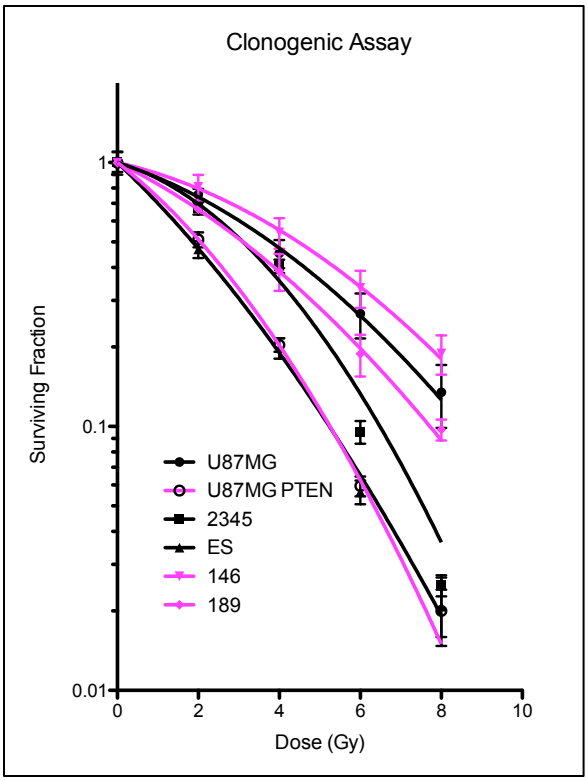

Figure 2B

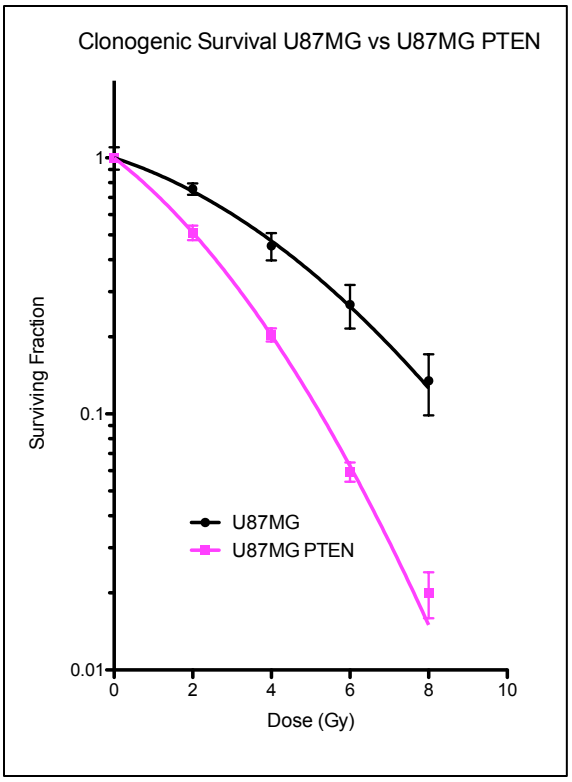

Figure 2: A) Represents survival curves generated from adherently grown cultures. Cell lines colored in pink are PTEN-wt cells lines while cell lines in black are PTEN-null. **B)** Represents the difference between our syngeneic model U87MG and U87MG PTEN restored. Curves were generated using GraphPad Prism and fitted using the Linear-Quadratic Model for radiation survival. Error bars represent the standard error of the mean.

Figure 3: 10% Survival

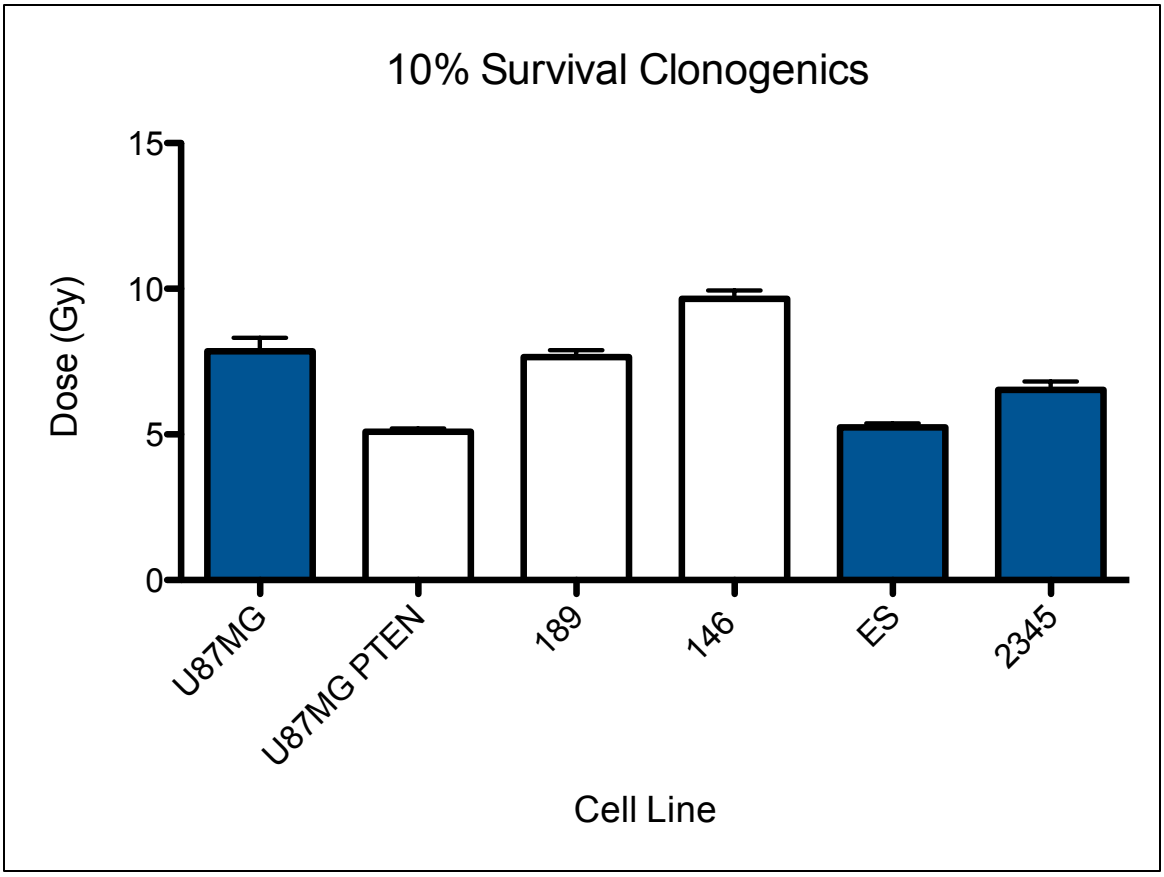

Clonogenics	*U87MG*	*U87MG PTEN*	*189*	*146*	*ES*	*2345*
α	.114 ± .049	.27 ± .028	.172 ±.031	.080 ± .042	.336 ± .04	.102 ± .05
β	.018 ± .01	.031 ±.008	.016 ±.006	.016 ± .008	.019 ± .013	.038 ± .01
10% Survival	8.57Gy	5.28Gy	7.77Gy	9.75Gy	5.27Gy	6.55Gy

Figure 3: Illustrates the 10% survival dose between the adherently grown glioma cell lines. PTEN-null glioma lines are depicted in blue, while PTENwt lines are depicted in white. The 10% survival dose has no correlation to PTEN status. 10% survival dose was calculated using the α and β ratio generated by fitting the survival curves to a Linear-Quadratic Model.

Figure 4: Neurosphere Survival Assay

Figure 4a

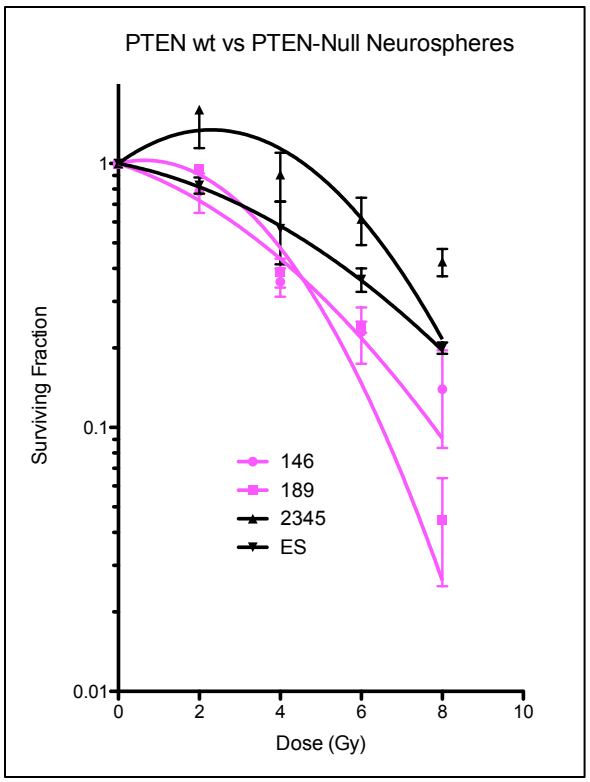

Figure 4b

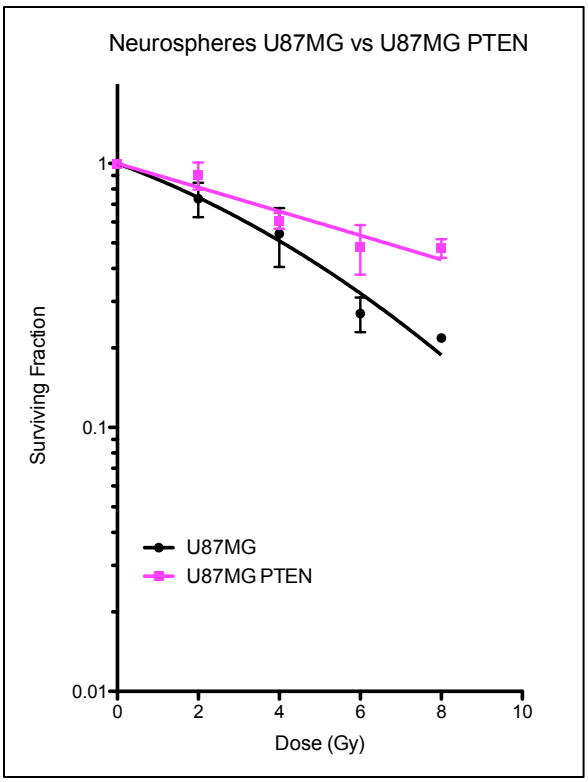

Figure 4: A) Represents survival curves generated from neurosphere grown cultures. Cell lines colored in pink are PTEN-wt cells lines while cell lines in black are PTEN-null. **B)** Represents the difference between our syngeneic model U87MG and U87MG PTEN restored. Curves were generated using GraphPad Prism and fitted using the Linear-Quadratic Model for radiation survival. Error bars represent the standard error of the mean.

Figure 5: 10% Neurosphere survival

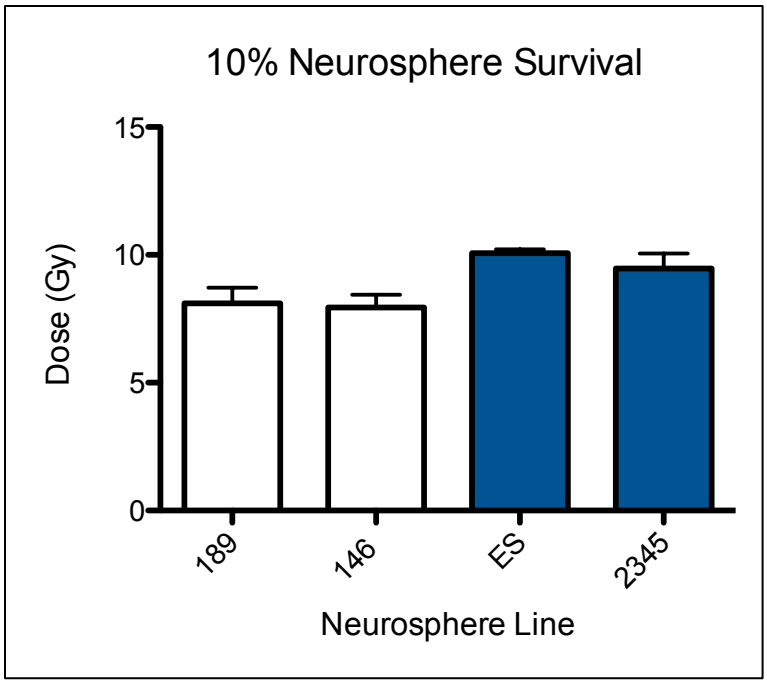

Neurospheres	*U87MG*	*U87MG PTEN*	*189*	*146*	*ES*	*2345*
α	.128 ± .05	.103 ± .04	-.086 ± .04	.115 ± .066	.068 ± .048	-.256 ± .1
β	.01 ± .01	.0001 ± .0006	.067 ± .01	.022 ± .014	.01 ± .008	.056 ± .021
10% Survival	10.06	21.8Gy	8.4Gy	7.95Gy	10.05Gy	9.2Gy

Figure 5: Illustrates the 10% survival dose between the neurosphere grown glioma cell lines. PTEN-null glioma lines are represented in blue, while PTENwt lines are represented in white. The 10% survival dose has no correlation to PTEN status. 10% survival dose was calculated using the α and β ratio generated by fitting the survival curves to a Linear-Quadratic Model.

Figure 6: Neurosphere Survival Treated with GSI

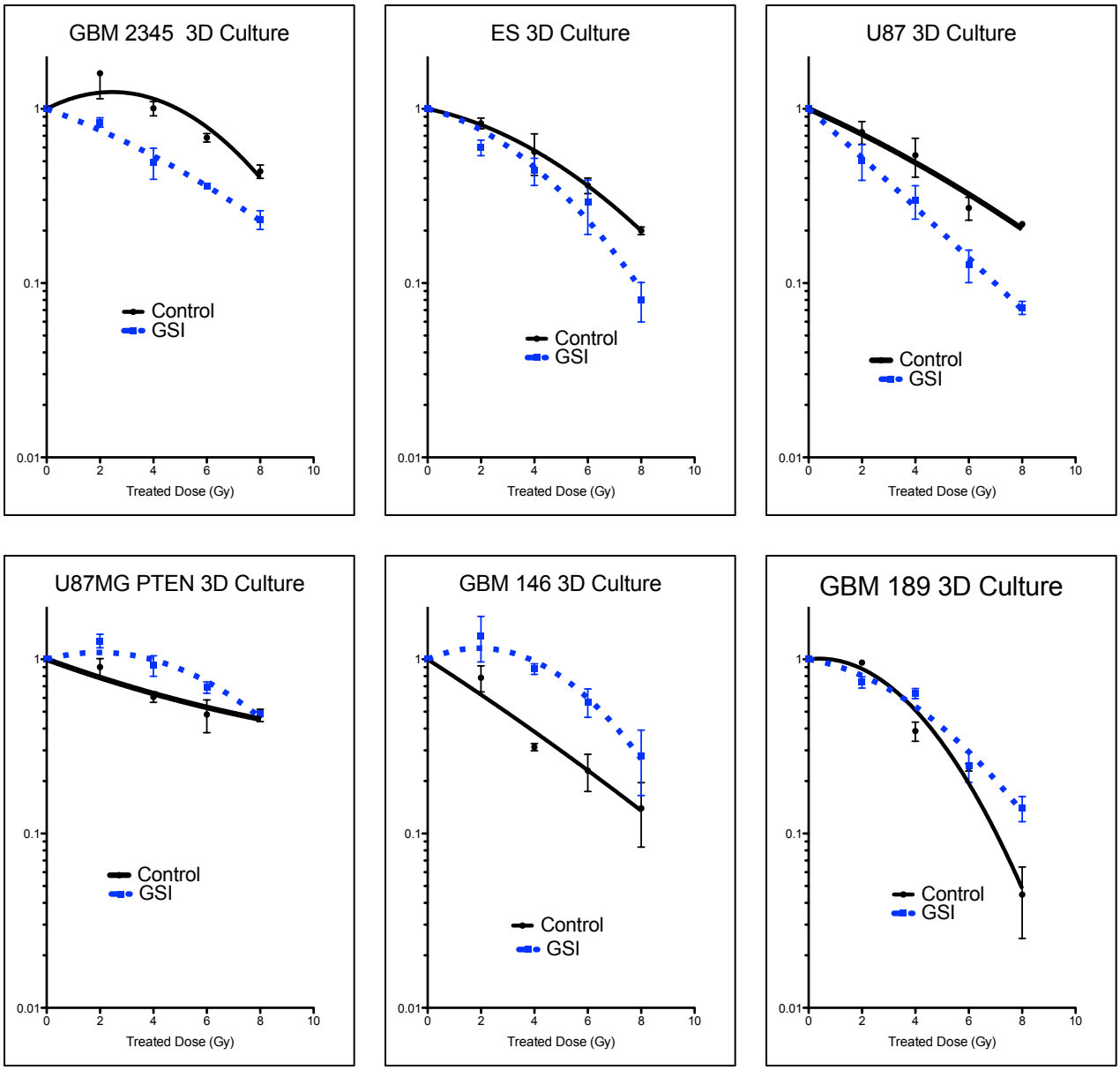

Figure 6: Shows the neurosphere survival curves for untreated (black) and treaded with GSI (BLUE dotted) lines. The PTEN-null neurosphere lines, top three graphs (U87MG, ES, 2345), are radiosensitized to GSI treatment while the PTENwt neurosphere lines bottom, 3 graphs (U87MG PTENwt, 146, 189) are radioprotected.

Figure 7: Clonogenic Surivival Assay treated with GSI

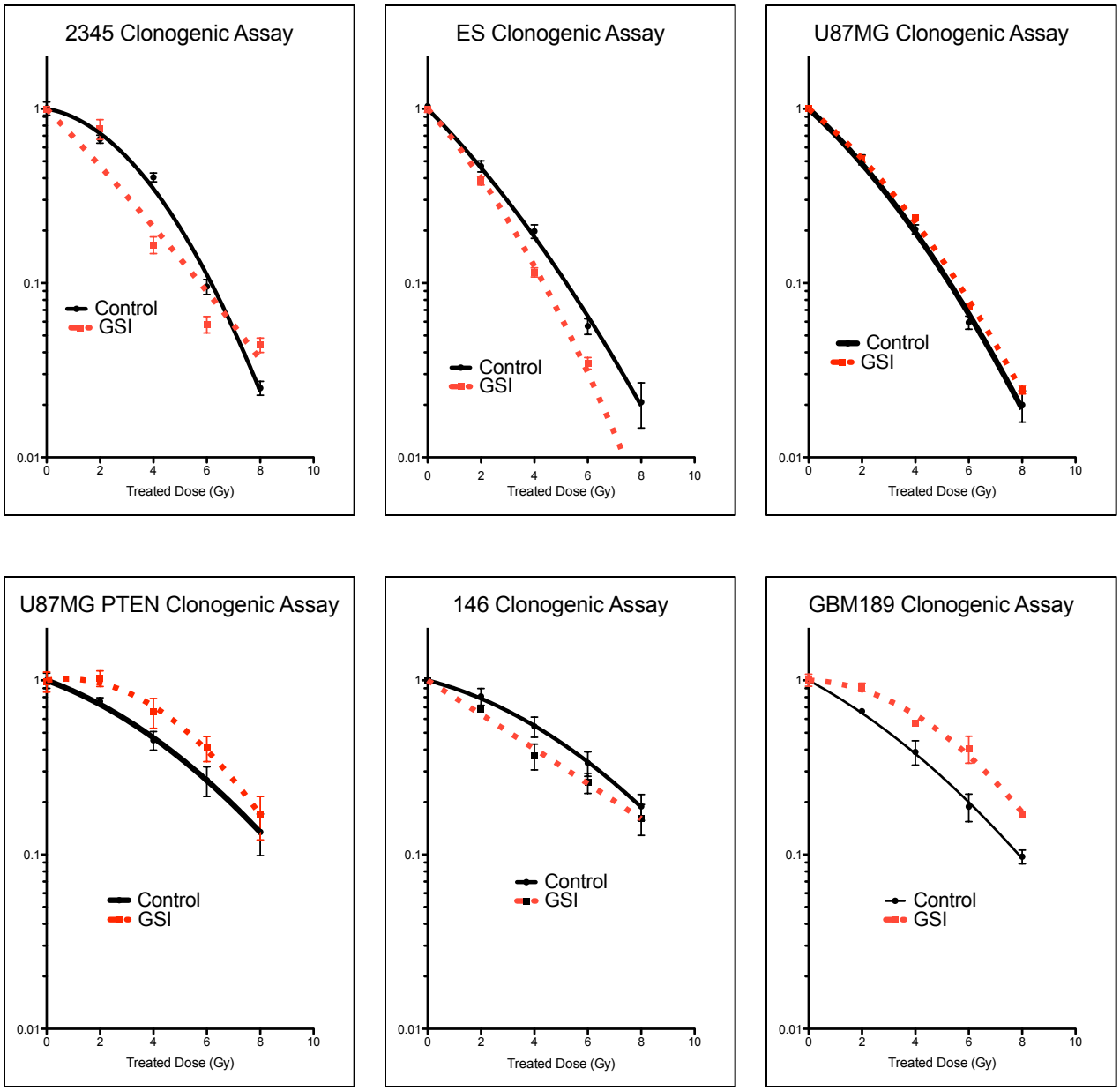

Figure 7: Shows the adherently grown survival curves untreated (black) and treated with GSI (red dotted) lines. There is no consistent correlation between PTEN-null adherently grown lines top three graphs (U87MG, ES, 2345), verses the PTENwt adherently grown lines, bottom 3 graphs (U87MG PTENwt, 146, 189).

Glioma neurospheres express Notch receptors and downstream targets

To confirm that our neurosphere cell glioma lines express Notch receptors, Notch downstream targets, and that GSI reduces downstream Notch target genes, we preformed RT-PCR on Notch receptors 1-4 and notch target genes *Hes1, Hey1* and *HeyL* treated with and without GSI. Neurosphere lines U87MG and U87MG PTENwt, both express high levels of transcripts for Notch receptors 1-4, and the downstream products of Notch, *Hes1, Hey1, HeyL*. The major difference between these cell lines is that U87MG PTENwt has a much lower expression of Notch1 transcripts while a much higher expression of Notch4 compared to U87MG. Notch 2 Expression has been implicated in protecting glioma stem cells from radiation (Wang, Wakeman et al. 2010), and in both cell lines, U87MG, U87MG PTENwt, we observe a dramatic increase in Notch 2 transcripts after 8Gy of IR with U87MG increasing 6345 fold while U87MG PTEN increased 17 fold (**Figure 8a, Figure 8b**). U87MG also had a significant reduction in Notch1, 45 fold, and Notch3, 49 fold, expression (**Figure 8**). Comparing the notch receptor expression of U87 to U87PTEN at 0Gy we find that U87MG has an 8.8 fold higher expression of Notch1 while U87MG PTENwt has a 954 fold higher expression of Notch2. However, these values are considered to be not quite significant with p values of .6 and .602 respectively (**Figure 8c**). After radiation however Notch receptors 1, 2, and 3 in U87MG PTENwt increases 5.7 fold, 5.5 fold, and 1194 fold respectively. Only Notch2 receptor expression was considered significant with a, p value of .018, while Notch1 and Notch3 expression were not quite statistically significant with p values of .062 and .06 respectively (**Figure 8d**). Notch4 receptor expression does not change significantly between 0 or 8Gy and did not vary between U87MG and U87MG PTENwt neurosphere lines. Evaluating the combination of GSI and radiation treatment

(**Figure 8e**) we observe that U87MG PTEN increase Notch receptor expression 1-3 while U87MG only increase Notch receptor 2. Comparing the downstream products of Notch activation we find that the initial level of transcription of *Hes1, Hey1,* and *HeyL* between U87MG and U87MG PTENwt are comparable with *Hes1, Hey1* and *HeyL* expression being 2280 ± 1247, 14905 ± 1948, and 26907 ± 8417 respectively for U87MG and 2733 ± 83, 6436 ± 3476, and 30321 ± 8174 respectively for U87MG PTEN (**Figure 9a**). However, *Hes1* failed to increase upon radiation in U87MG PTEN compared to U87MG neurospheres (**Figure 9b**). Treatment with GSI reduced *Hes1, Hey1* but not *HeyL* transcripts in U87MG after 8Gy radiation (Figure 9c), while U87MG PTEN restored shows no significant change in *Hes1 Hey1, and HeyL* after GSI treatment after 8Gy radiation (**Figure 9d**). These results demonstrate that the presence of an active Notch pathway, and that GSI at least in PTEN-null neruosphere cell lines, consistently reduces downstream notch factors.

Figure 8A: Base Levels of Notch receptor expression in U87MG after 0Gy and 8Gy

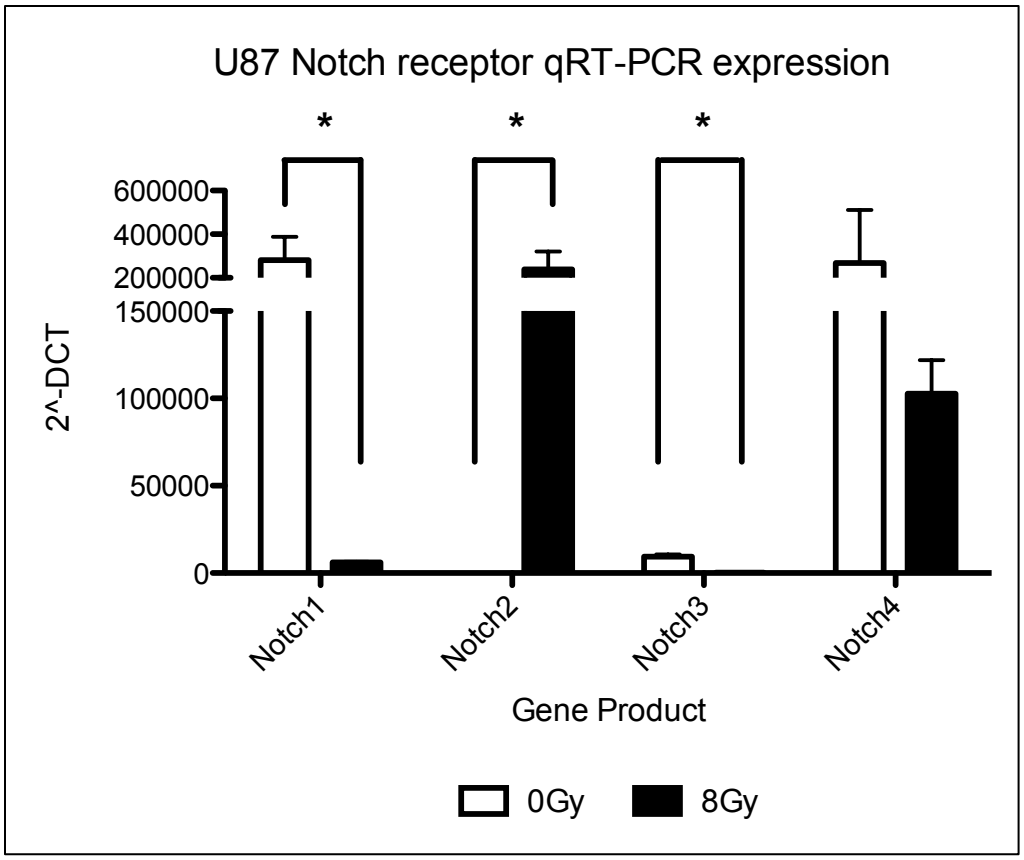

Figure 8a: U87MG Notch receptor expression at baseline (0Gy) and after 8Gy of radiation treatment. Expression values represent ΔCt and are normalized to RPLP0. Changes in Notch1 expression are significant with p value = .043, Notch1 at 0Gy 280775 ± 10709, at 8Gy 6165 ± 269. Changes in Notch2 are significant with a p value = .039, Notch2 at 0Gy 37.6 ± 37.6, at 8Gy 238600 ± 81989. Changes in Notch3 expression are significant with a p value = .0124, Notch3 at 0Gy 9368 ± 1312, at 8Gy 190 ± 55.

Figure 8B: Base Levels of Notch receptor expression in U87MG PTEN after 0Gy and 8Gy

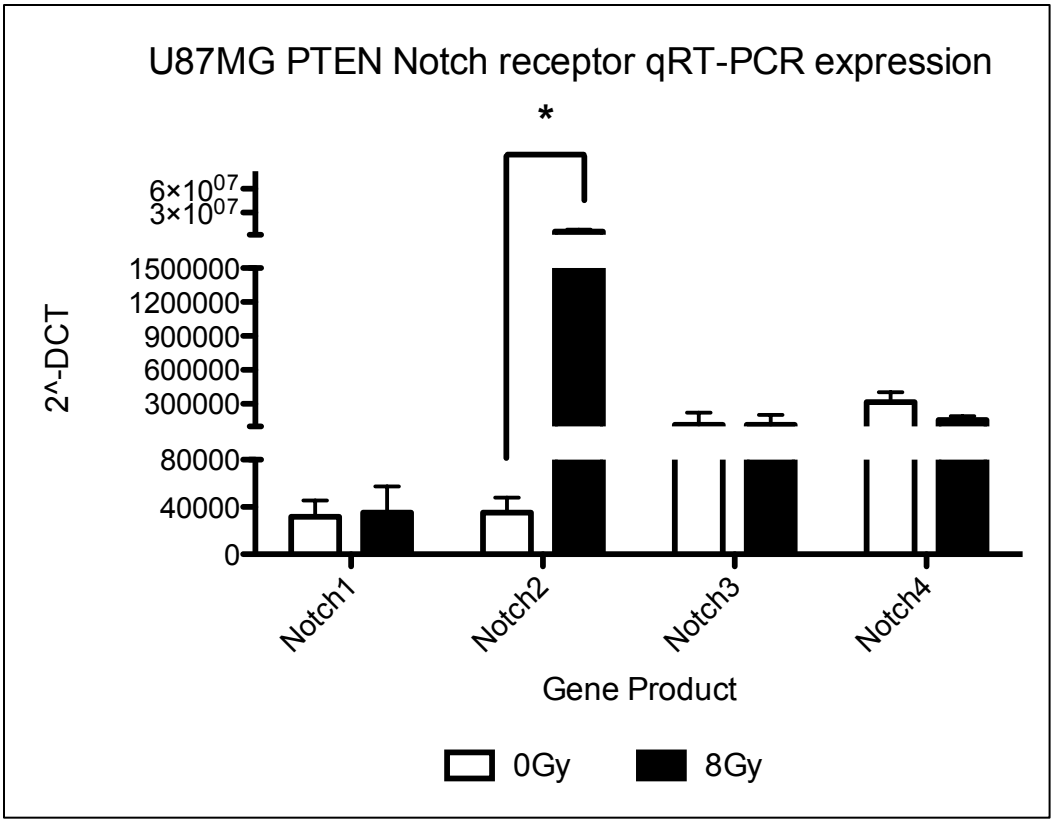

Figure 8b: U87MG PTENwt Notch receptor expression at baseline (0Gy) and after 8Gy of radiation treatment. Expression values represent ΔCt and are normalized to RPLP0. Changes in Notch2 expression are significant with p value = .0486, Notch2 at 0Gy 35327 ± 12775, at 8Gy 625217 ± 238761

Figure 8C: Notch receptor expression U87MG verses U87MG PTEN at 0Gy

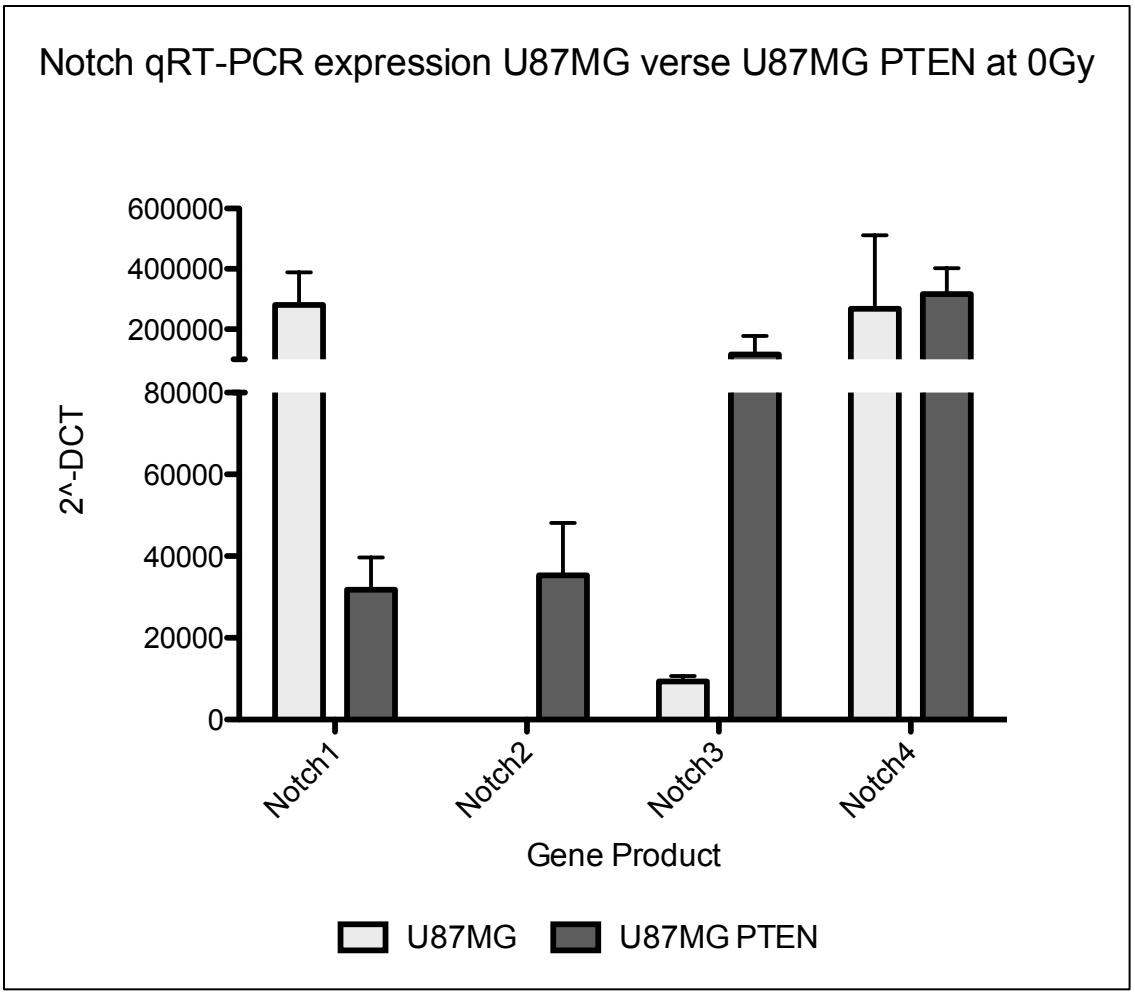

Figure 8c: U87MG Notch receptor expression compared to U87MG PTENwt do not differ significantly. Mean and SEM are as follows: Notch1 U87MG 280775 ± 107690 and 31791 ± 15797 for U87MG PTEN p value = .06, Notch2 U87MG 37.67 ± 37.67 for U87MG PTEN 35327.0 ± 12775, Notch3 U87MG 9368 ± 1312 for U87MG PTEN 115996 ± 61364 p values = .20, Notch4 U87MG 268375 ± 243692 for U87MG PTEN 316787 ± 85332

Figure 8D: Notch receptor expression U87MG verses U87MG PTEN at 8Gy

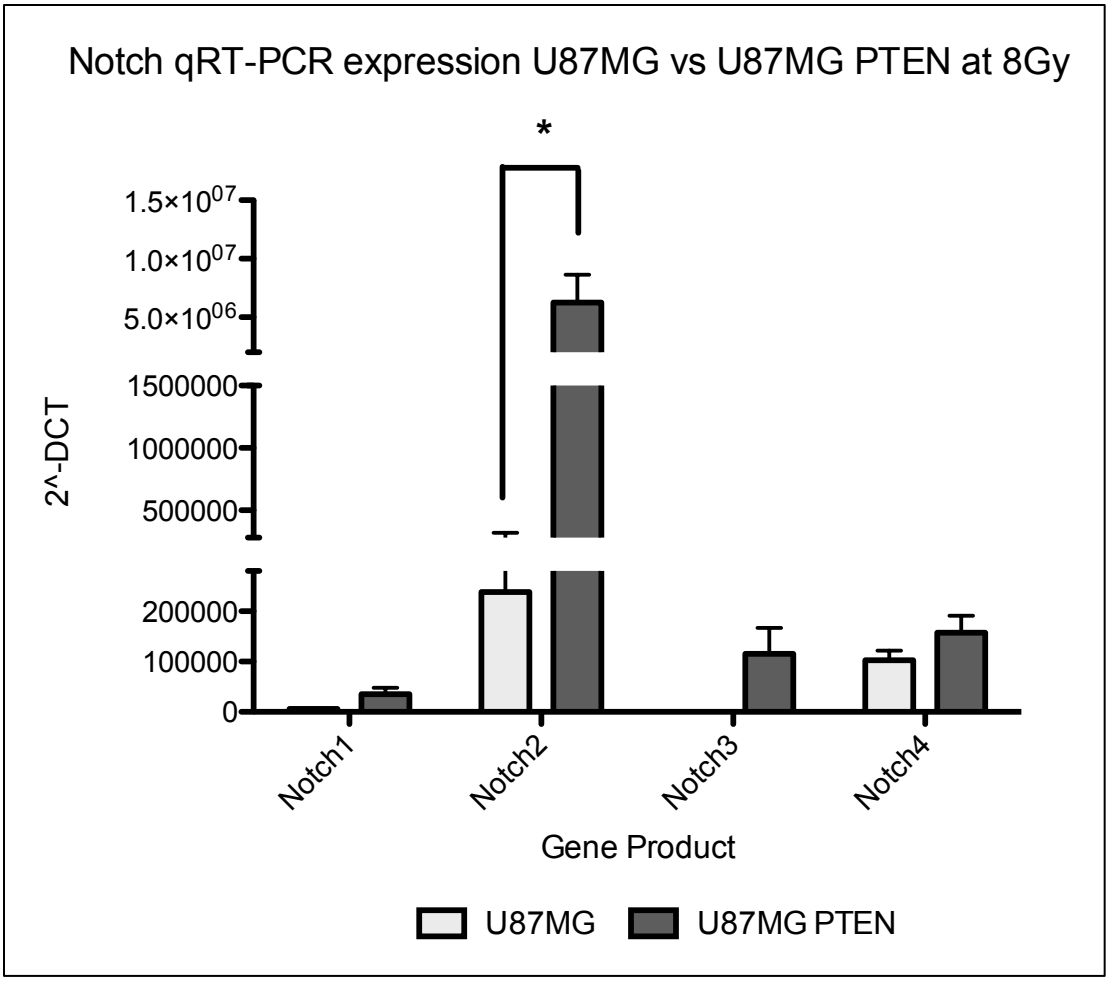

Figure 8d: Comparing U87MG verses U87MG PTENwt notch receptor induction after radiation we find that U87PTENwt has a significant increase in Notch2 expression, p value = .018, with a mean and SEM of 285936 ± 94073 for U87MG and for U87MG PTENwt 1577757 ± 311187. Notch1 increases U87MG PTEN but is not quite significant with a p value of .062 and mean and SEM for U87MG 6165 ± 269 and U87MG PTEN 35327 ± 12775. Notch3 expression is also not quite significant with a p value of .06, and mean and SEM for U87MG 487 ± 55 and U87MG PTEN 227049 ± 51141. Notch 4 is not significant with a corresponding mean of 102697 ± 19151 for U87MG and 157803 ± 33716 for U87MG PTEN.

Figure 8E: Notch receptor expression after GSI plus radation treatment

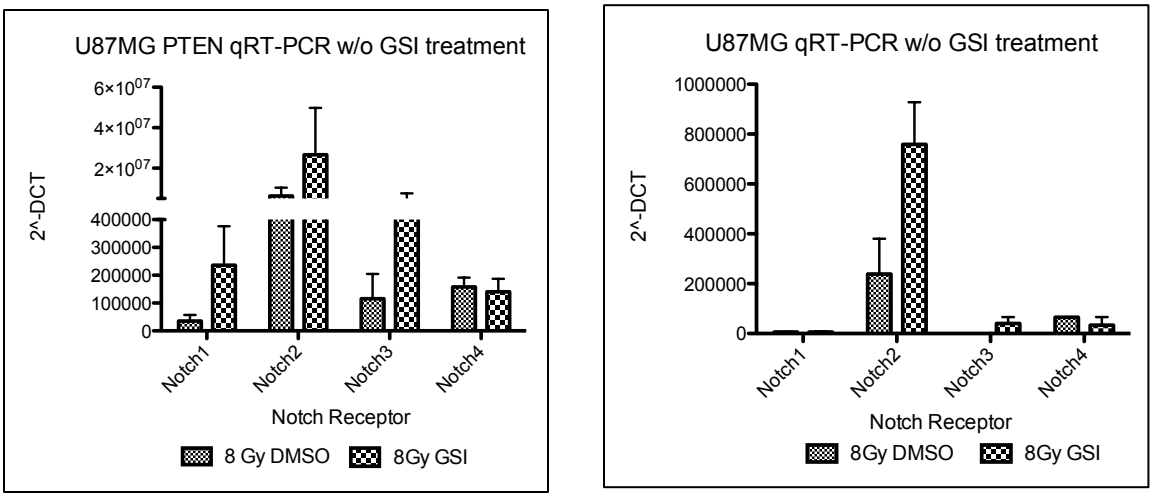

Figure 8e: Notch receptor expression comparing GSI plus radiation treatment verses DMSO and radiation. U87MG PTEN has an increase in Notch receptors 1 - 3 while U87MG only increases in Notch receptor 2.

Figure 9: Downstream Notch target gene expression treated with 0Gy or 8Gy

Figure 9a

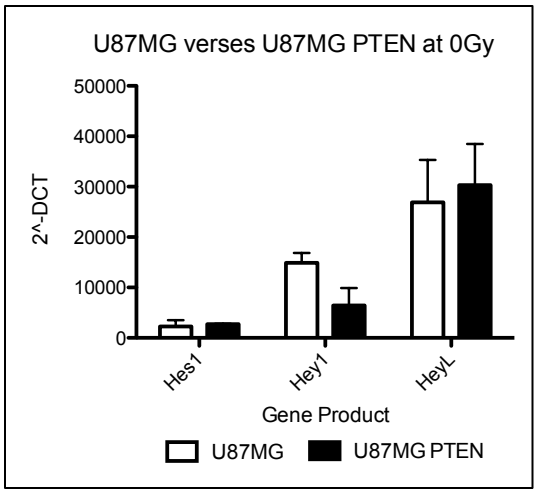

Figure 9b

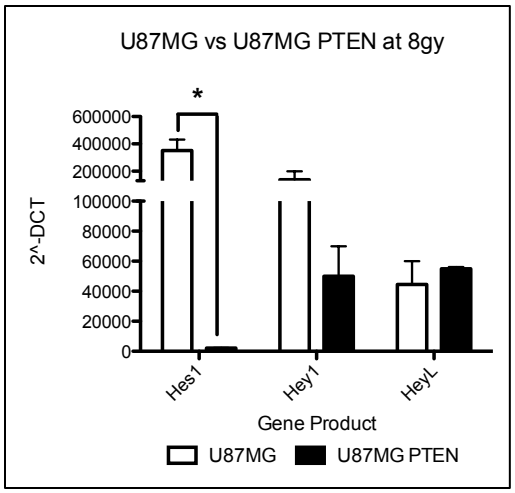

Figure 9: A) Establishes the baseline levels of the downstream Notch signaling factors *Hes1, Heyl* and *HeyL* comparing U87MG verses U87MG PTEN. We observe no significant differences in initial levels of downstream Notch factors. *Hey1* expression in U87MG is 2280 ± 1247 and in U87MG PTEN 2733 ± 83. *Hey1* expression in U87MG is 14905 ± 1948 while in U87MG PTEN it is 6436 ± 3476. *HeyL* expression in U87MG is 26907 ± 8417 while in U87MG PTEN 30321 ± 8174 **B)** Depicts the downstream Notch signaling factors *Hes1, Heyl* and *HeyL* after 8Gy. *Hes1* expression is significantly more in U87MG than in U87MG PTEN neurosphere lines. *Hes1* expression for U87MG is 352108 ± 78963 while U87MG PTEN is 2180 ± 53 with a p value of .004. *Hey1* expression in U87MG is 82436 ± 54161 while in U87MG PTEN it is 49950 ± 20025. *HeyL* expression in U87MG is 44543 ± 15543 while in U87MG PTEN it is 55019 ± 1091.

Figure 9C: U87MG Downstream Notch target gene expression after GSI plus 8Gy

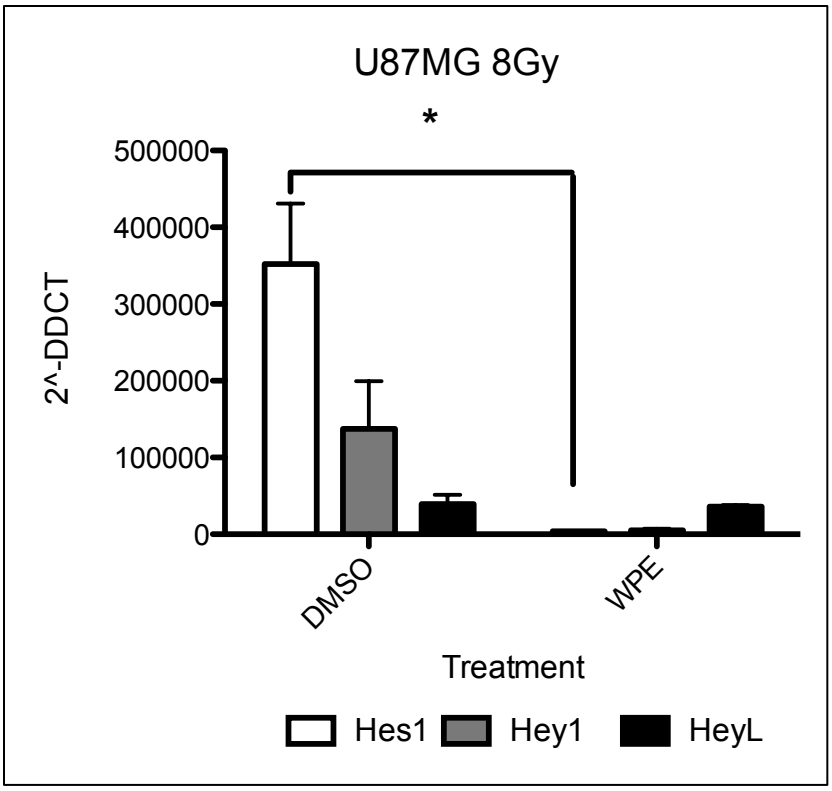

Figure 9a: The effect of GSI treatment and radiation on the downstream products of the Notch pathway in U87MG. The mean and SEM for Hes1 DMSO 352083 ± 75977 verses GSI 3983 ± 150 with a p value .0045. Hey1 expression DMSO 137436 ± 62053 and GSI treated 5271 ± 2178 with a p value of .07. HeyL expression DMSO treated 39288 ± 12007 and GSI treated 35870 ± 2292, which is not significant.

Figure 9D: U87MG PTEN Downstream Notch target gene expression after GSI plus 8Gy

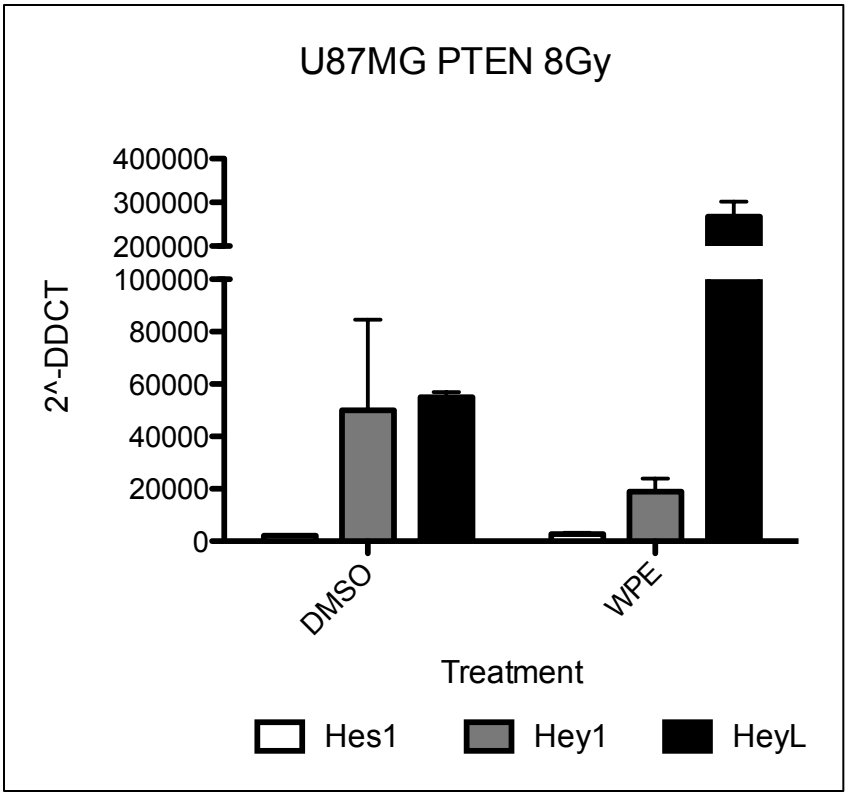

Figure 9b: The effect of GSI treatment and radiation on the downstream products of the Notch pathway in U87MG. The mean and SEM for Hes1 DMSO 2180 ± 92 verses GSI 2745 ± 487 with a p value = .37. Hey1 expression DMSO 49950 ± 34684 and GSI treated 18915 ± 5066 with a p value of .46. HeyL expression DMSO treated 55019 ± 1890 and GSI treated 267170 ± 34376, which is not significant.

GSI plus Radiation enriches self-renewal of PTEN-wt neurospheres

Measuring neurosphere propagation in the form of generating primary, secondary, and tertiary neurospheres helps to determine the self-renewing capacity after a treatment. After dissociating the neurospheres and re-plating the cells at low density, we can determine if the treatment with GSI has a long-term effects on GSCs proliferative potential. Both glioma neurosphere cultures, U87MG PTEN and U87MG, experience a reduction in neurosphere formation by second passage. However, by tertiary neurosphere formation both neurosphere lines recover. U87MG PTENwt treated with GSI plus radiation not only recovers but increases in neurosphere formation compared to radiation treatment alone.

GSI treatment does not affect the DNA damage response

Survival curves describe the relationship between radiation dose and the fraction of cells that survive that given dose. There are models to explain the shape of a survival curve, namely the linear quadratic model or multi-target model, but these do not describe the biophysical processes that occur during ionizing radiation exposure. In mammalian tissues, dose survival curves exhibit a linear region, which equates to cell killing that is proportional to dose, while the shoulder region of the curve represents cell killing that is proportional to dose squared. The biological explanation is based on DNA double strand breaks being the sole important lesion determining cell death. Therefore, the initial slope of the curve represents a single hit by IR to DNA that causes cell death while, the final slope after the curve represents the two independent ionizing events the lead to a lethal DNA double

Figure 10: Primary, Secondary, and Tertiary neurosphere formation

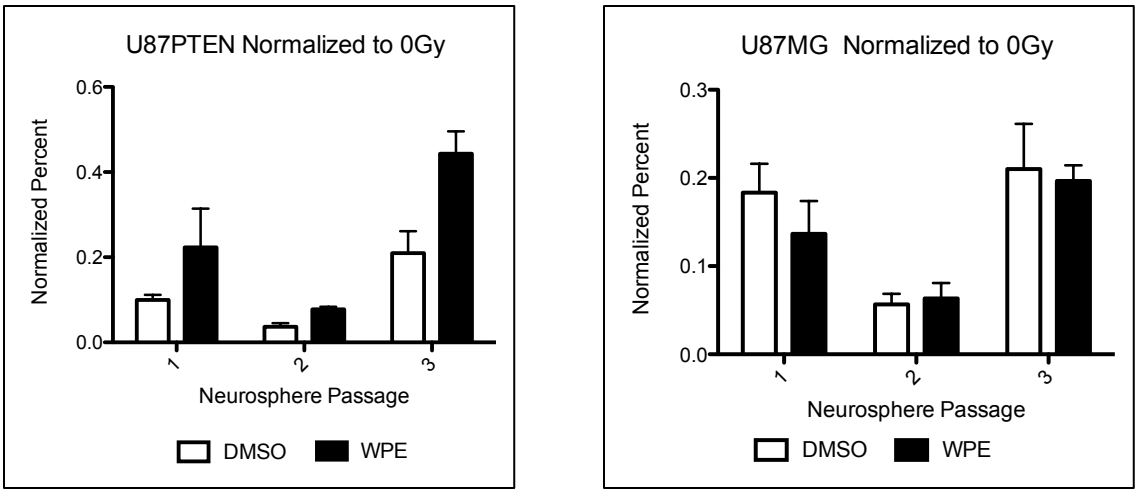

Figure 10: Shows the effect of GSI treatment and radiation over the course of 3 neurosphere dissociations. U87MG PTEN and U87MG experience a reduction in neurosphere formation by second passage. However, both neurosphere lines recover. U87MG PTEN treated with GSI has a larger increase in neurosphere formation by tertiary formation.

strand break. Measuring DNA double strand breaks thus becomes the important factor in determining sensitivity to ionizing radiation. Biologically, however, DNA damage from IR can occur in two ways, direct action, and indirect action. Direct action involves IR imparting energy directly on the DNA causing a lesion, while indirect action involves the creation of unstable free radical intermediaries with then go on to cause DNA lesions. In both cases, we can ultimately measure DNA double strand breaks via gH2Ax, a nucleosome protein bound to DNA that is phosphorylated upon DNA double strand breaks. We measured DNA double strand breaks using a fluorescent anti-gH2Ax antibody. We measured the induction of gH2Ax 30 minutes after radiation to assess DNA damage from IR, and 24 hours after IR to observe if there was reduced DNA repair efficiency. In both cases, 30 minutes after or 24 hours after, we observed no change in DNA damage when compared to 0Gy DMSO or GSI treated, or when comparing 8Gy DMSO to 8Gy GSI treated in both cell lines. Furthermore, there is no difference in DNA damage received between U87MG and U87MG PTENwt. This affirms that GSI doesn't affect the DNA damage response (**Figure 11**).

Forkhead Box 3 (FOXO3) expression in PTEN-wt neurospheres is changed by GSI

The FOXO class of proteins has been found to mediate the response to oxidative stress. Oxidative stress is one of the mechanisms IR causes damage to DNA. FOXOs can effect the survival and fate decision of cells upon oxidative stress. Since FOXO is part of the PTEN/PI3K/AKT pathways, we wanted to evaluate if GSI affects the FOXO pathways by affecting cell survival after treatment and radiation. Utilizing the DCF assay, which

measures reactive species with a chemical that fluoresces green upon oxidation. The more free radical activity, the more green fluorescence can be measured via FACs. We observed that U87MG PTENwt had lower initial oxidative (1459 ± 17) stress over U87MG (3243 ± 207). Furthermore, upon radiation exposure U87MG PTEN marginally increases in oxidative stress to 2011 ± 67 while U87MG significantly increases from 0 to 8Gy (5196 ± 18). The difference between oxidative stress U87MG PTEN and U87MG at 8Gy is also significant (**Figure 12**). Since the oxidative impact between the U87MG and U87MG PTEN were different, we then measured the expression levels between the different FOXO factors, FOXO1, FOXO3 and FOXO4 using qRT-PCR at 0Gy and 8Gy treated and untreated with GSI. We found that U87MG PTEN neurospheres were enriched in FOX3 over adherently grown U87MG PTEN, and U87MG didn't differ in FOXO3 levels (**Figure 13h**). Furthermore, FOXO3 expression was significantly higher in U87MG PTEN over U87MG (**Figure 13f**) in all conditions, 0Gy and 8Gy treated and untreated with GSI. Lastly, in U87MG PTEN, we observed a decrease in FOXO3 expression upon radiation that was rescued by GSI treatment in the 8Gy GSI treated (**Figure 13f**). However, the difference between the decrease of FOXO3 and the rescue of FOXO3 expression in the 8Gy GSI treated was considered to be not quite significant ($p = .12$). FOXO1 and FOXO4 levels did not change significantly between the two neurosphere cell lines (**Figure 13**).

Figure 11: gH2Ax Foci formation

Figure 11a

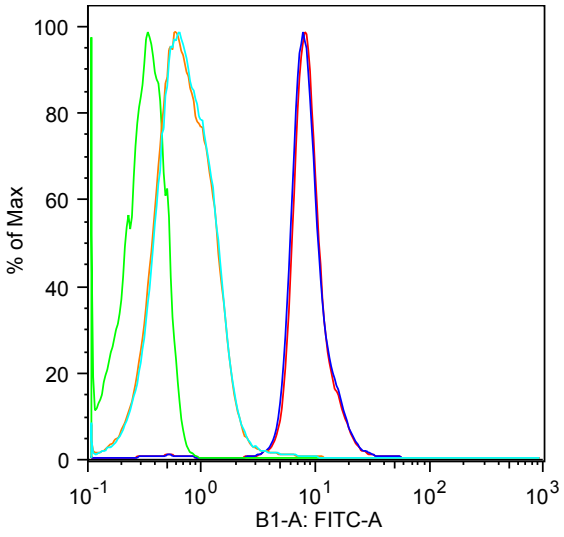

Sample	%
PTEN 0Gy WPE.018.fcs	63.3
PTEN 0Gy DMSO.017.fcs	64.2
no flow.016.fcs	68.1
PTEN 8Gy WPE.020.fcs	63.5
PTEN 8Gy DMSO.019.fcs	58.7

Figure 11b

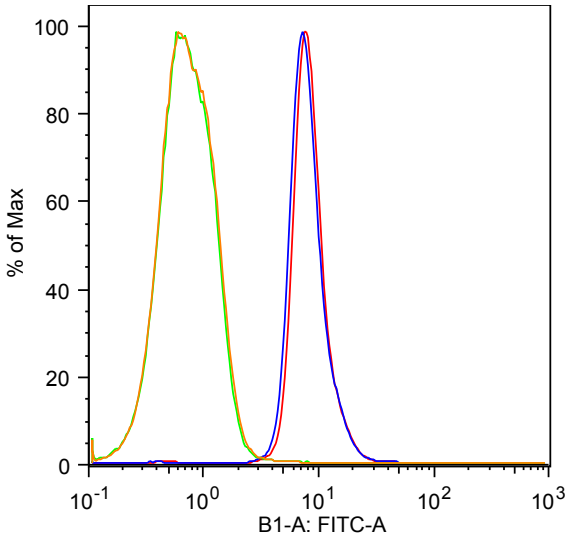

Sample	%
U87 0Gy WPE.022.fcs	70.7
U87 0Gy DMSO.021.fcs	72.8
U87 8Gy WPE.024.fcs	69.4
U87 8Gy DMSO.023.fcs	70.5

Figure 11: A) U87MG PTEN neurospheres FACs analaysis after gH2Ax staining. Peaks represent from left to right, no fluorescent antibody control, 0Gy DMSO (orange), 0Gy GSI treated (cyan), 8Gy DMSO (red) and 8Gy GSI treated (blue). No shifts in the peaks are observed from GSI treatment. **B)** Shows the evaluation of U87MG neurospheres, in this chart from left to right 0Gy DMSO (orange), 0Gy GSI treated (green), 8Gy DMSO (red) and 8Gy GSI treated (blue). Again there are no shifts in the peaks in the GSI treated samples, when compared to their corresponding radiation dose received.

Figure 12: Oxidative Stress (DCF Assay)

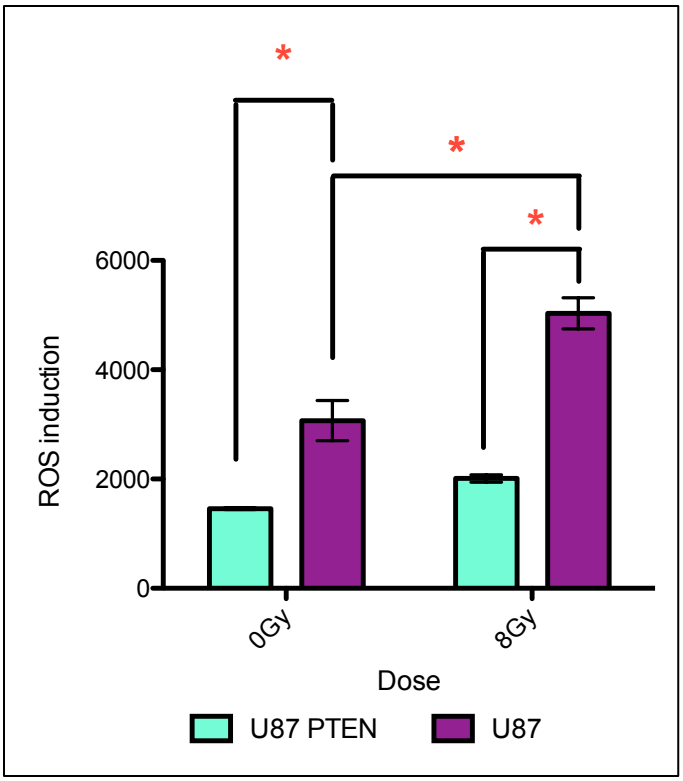

Figure 12: Measurement of oxidative stress through free radical action on DCF. Here we find that initial levels (0Gy) of oxidative stress are lower in U87MG PTEN (1459 ± 17) over U87MG (3243 ± 207) with a p value of .04. After radiation U87MG increases significantly from 3243 ± 207 to 5196 ± 18 (p = .045). U87MG PTEN after radiation increased to 2011 ± 67.

Figure 13: FOXO expression in Adherent and neuroshere cultures

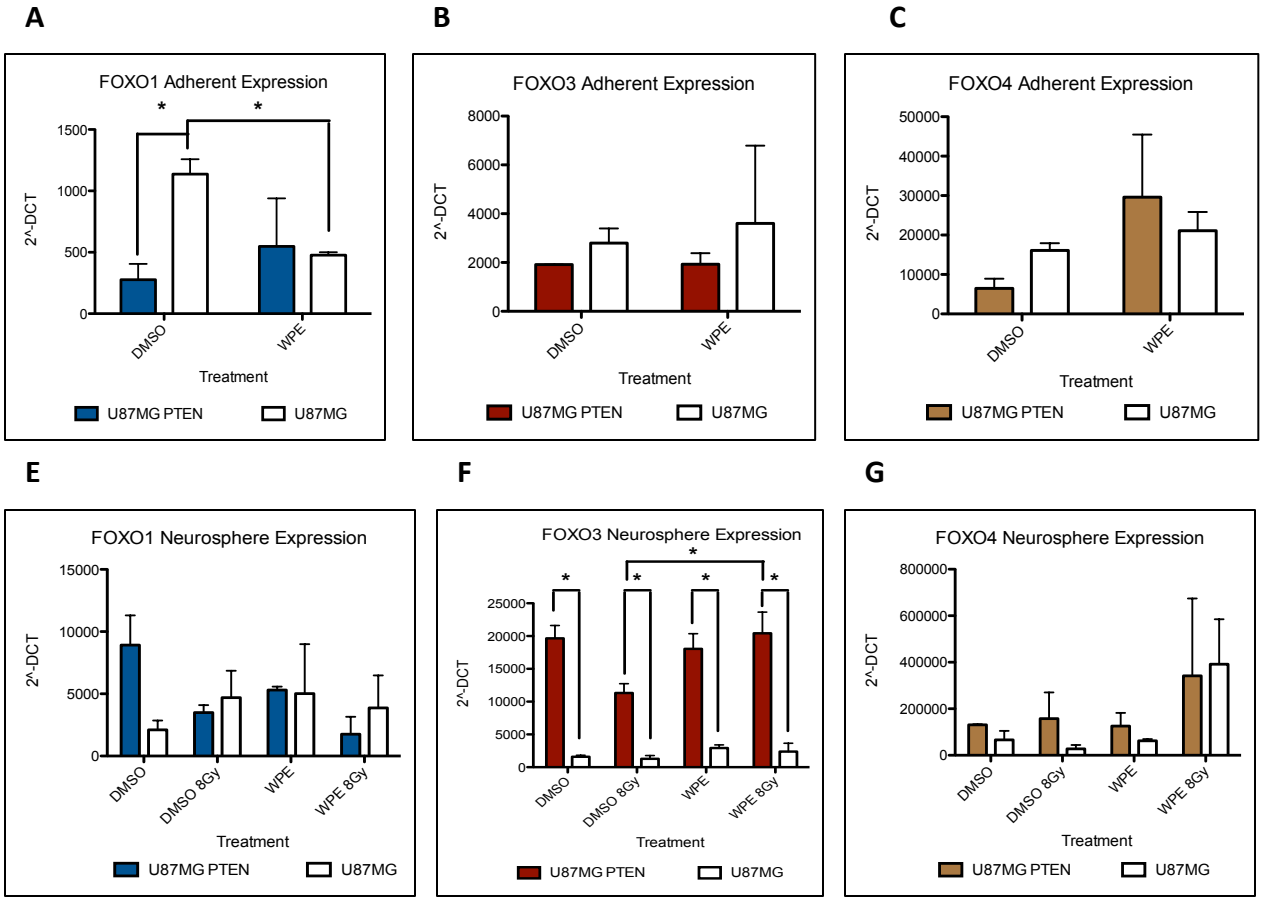

Figure 13: **A, B, C**) Show the expression levels of FOXO1, FOXO3 and FOXO4 in adherently grown conditions. GSI treatment only reduces FOXO1 expression in U87MG. The FOXO expressions are comparable between U87MG PTEN and U87MG in adherent conditions except FOXO1 expression is increased in U87MG (1137 ± 121) verse U87MG PTEN (276 ± 126) **E,F,G**) Show the expression levels of FOXO1, FOXO3 and FOXO4 in neurosphere conditions. The FOXO levels between U87MG and U87MG PTEN are not significantly different except for FOXO3. FOXO3 expression in U87MG PTEN was increased over U87MG in all conditions, 0Gy, 8Gy, 0Gy GSI, and 8Gy GSI with a mean and SEM of (DMSO U87MG PTEN19650 ± 1583, U87MG 1954 ± 230, with a p value of .012, GSI treated U87MG PTEN 18058 ± 2308 verses U87MG 2935 ± 472 with a p value of .0037, 8Gy treated U87MG PTEN 11321 ± 1423 verses U87MG 1277 ± 495 with a p value of .0039, and 8Gy GSI treated U87MG PTEN 20422 ± 3239 verses 2392 ± 1268 with a p value of .0085.) Lastly, radiation reduces FOXO3 expression in U87MG PTEN, which is restored in GSI plus radiation, but is not considered to be significant p values of .12.

Figure 13H: FOXO3 expression in Adherent vs Neurosphere comparison

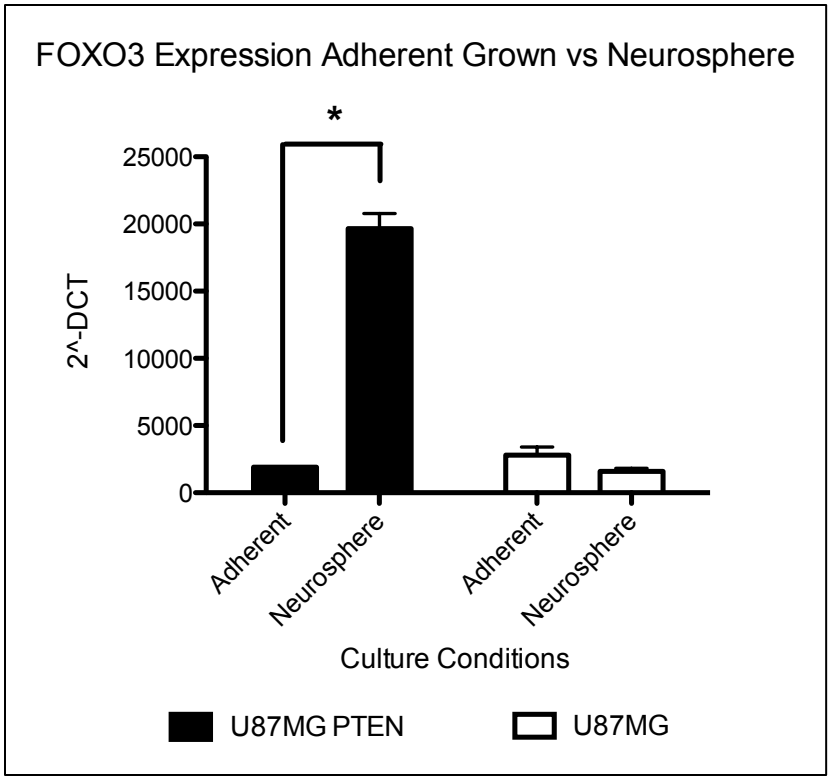

Figure 13: H) We demonstrate that FOXO3 expression is enriched in U87MG PTEN when compared to U87MG and to adherently grown conditions. FOXO3 expression in U87MG PTEN adherent is 1914 ± .58 while U87MG PTEN neurospheres had 19650 ± 1128 with a p value of .0001

GSI treatment alters the quiescent population of neurosphere cells.

To assess how GS inhibition affects the cell cycle we evaluated the cell cycle profile of adherently grown and neurosphere cultures using Hoechst staining one day after treatment with or without GSI, radiation, or combinational radiation and GSI. Hoechst staining will stratify cells based on DNA content. Cells occupying the G1 phase of the cell cycle have the lowest amount of DNA compared to S/G2 phase cells where DNA is being duplicated already. A cell cycle histogram contains a G1, S, and G2/M peak, and depending on gating parameters, one can also view a sub-G1 peak. The sub-G1 peak describes apoptotic cells. We used sub-G1 peak analysis to evaluate GSI on cell viability. Furthermore, we evaluated the quiescent population of cells using a combination of Hoechst and pyronin y (PY) staining to compare DNA verses RNA content. Graphing DNA verses RNA or (Hoechst verses PY) generates a plot with four quadrants. Quiescent cells by definition exhibit little to no RNA content and hence occupy the lower left quadrant where the least amount of staining was taken up due to low DNA and RNA content. By comparison, cells occupying the G1 phase have high RNA but the same amount of DNA content as quiescent cells and therefore occupy the upper left quadrant. Lastly, the cells occupying either S/M/G2 are shifted along the Hoechst axis because they contain the most DNA content but equivalent RNA content to G1 cells. Example figures on how a cell cycle profile, sub-g1 peak and Hoechst/PY quiescent staining looks like are in displayed in **Figure 14** and **Figure 16** respectively.

In neurosphere grown cultures, cell cycle analysis between each cell line revealed that PTENwt neurosphere lines with GSI treatment changed the cell cycle profile when combined with IR, by increasing the percent of cells occupying the G1 phase of the cell

cycle. This cell cycle change in G1 was significant for 189 and not quite significant for U87MG PTENwt, with an average of 13.5% ($p = .012$) increase for 189 treated with GSI and 8Gy and of 13.4% ($p = .16$) increase for U87MG PTEN. PTEN-null U87 and ES exhibited no change in cell cycle distribution. Adherently grown U87MG and U87MG PTENwt lines displayed the similar cell cycle distributions to their neurosphere grown counterparts. Lastly, all cell cycle distributions exhibited radiation induced G2 arrest causing an increase in cells occupying the G2 phase after radiation (**Figure 15**).

Evaluating the quiescent population in the neurosphere lines displayed two effects. First, radiation causes a depletion of quiescent stem cells. Second, the rate at which the quiescent population changes is more significant for PTEN-null lines. Adding GSI and IR causes PTEN-null neurosphere lines to retain their quiescent population. The effect was reversed for PTENwt neurosphere lines. PTENwt neurospheres had a reduction in their quiescent population when treated with the combination of GSI plus IR (**Figures 18a, 18b**). No changes in the quiescent population were observed in adherently grown U87MG or U87MG PTEN (**Figure 17**).

To evaluate cell death after treatment we analyzed the sub-G1 peak that forms representing an apoptotic group of cells. We found that in PTEN-null neurosphere lines, the percent of cells occupying the sub-G1 peak doesn't change under any condition. However, in the PTENwt neurosphere lines, we observed an increase

Figure 14: Cell Cycle Analysis and Sub-G1 peak

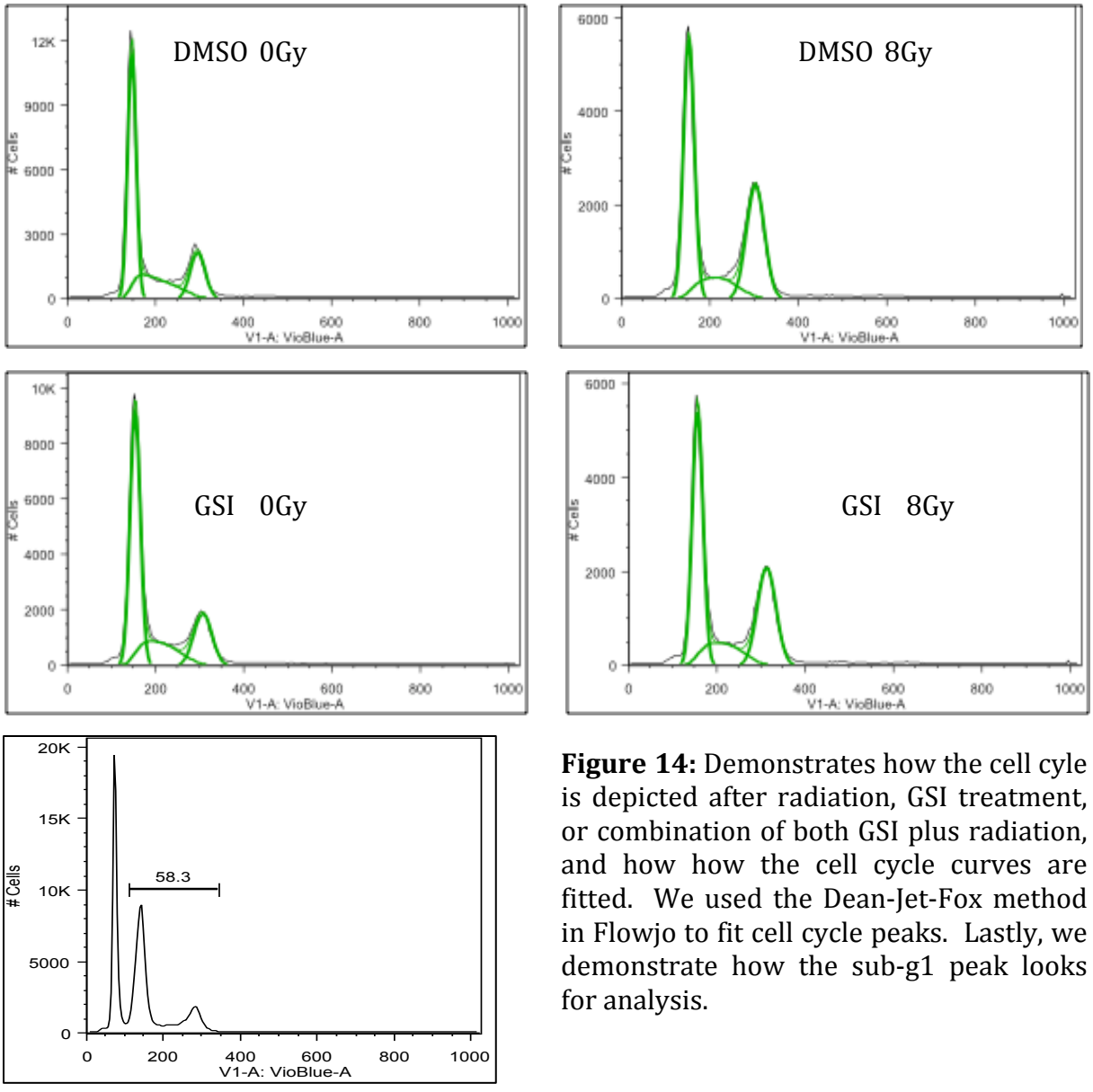

Figure 14: Demonstrates how the cell cyle is depicted after radiation, GSI treatment, or combination of both GSI plus radiation, and how how the cell cycle curves are fitted. We used the Dean-Jet-Fox method in Flowjo to fit cell cycle peaks. Lastly, we demonstrate how the sub-g1 peak looks for analysis.

Figure 15: Neurosphere /Adherent Cell cycle Data

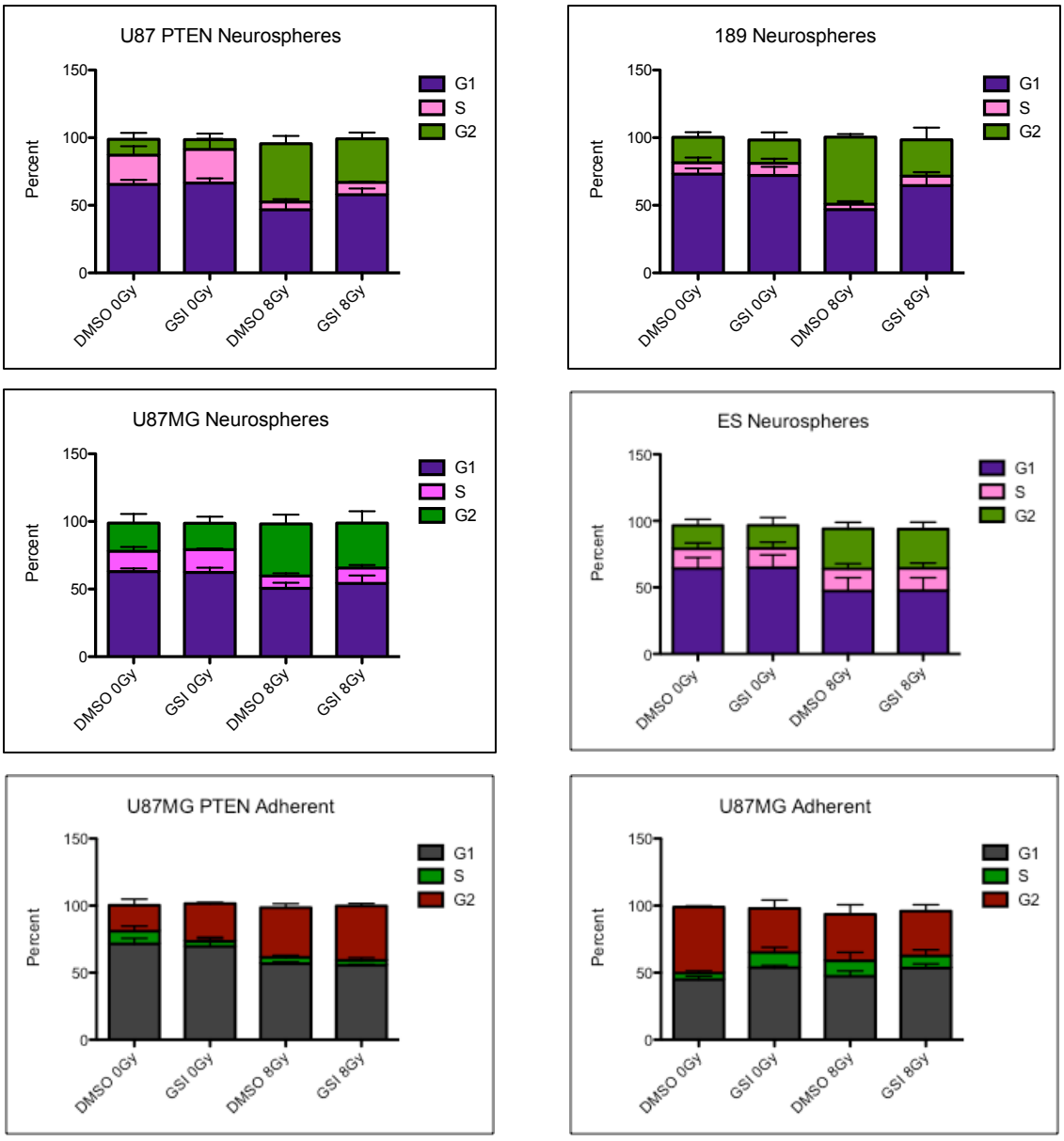

Figure 15: In the PTENwt neurosphere lines 189 and U87MG PTENwt, we observed that without radiation, GSI does not change the cell cycle distribution. Radiation individually causes cell cycle arrest while, GSI plus IR increases the G1 phase of the cell cycle. However, in the U87MG and ES, PTEN-null neurosphere lines we observed no difference in cell cycle when compared to the corresponding radiation treatment. Lastly, the cell cycle changes both U87MG and U87MG PTEN grown adherently respond similarly to their neurosphere grown counterparts. U87MG PTEN G1 phase averaged at 8Gy 46.6% ± 6.3 while 60.7% ± 5.13 with a p = .16 when treated with 8Gy and GSI. 189 averages 50% ± 5.01 at 8Gy while 8Gy with GSI averaged 74.26% ± 2.4 with a p = .012.

Figure 16: Heochet/PY FACS Analysis

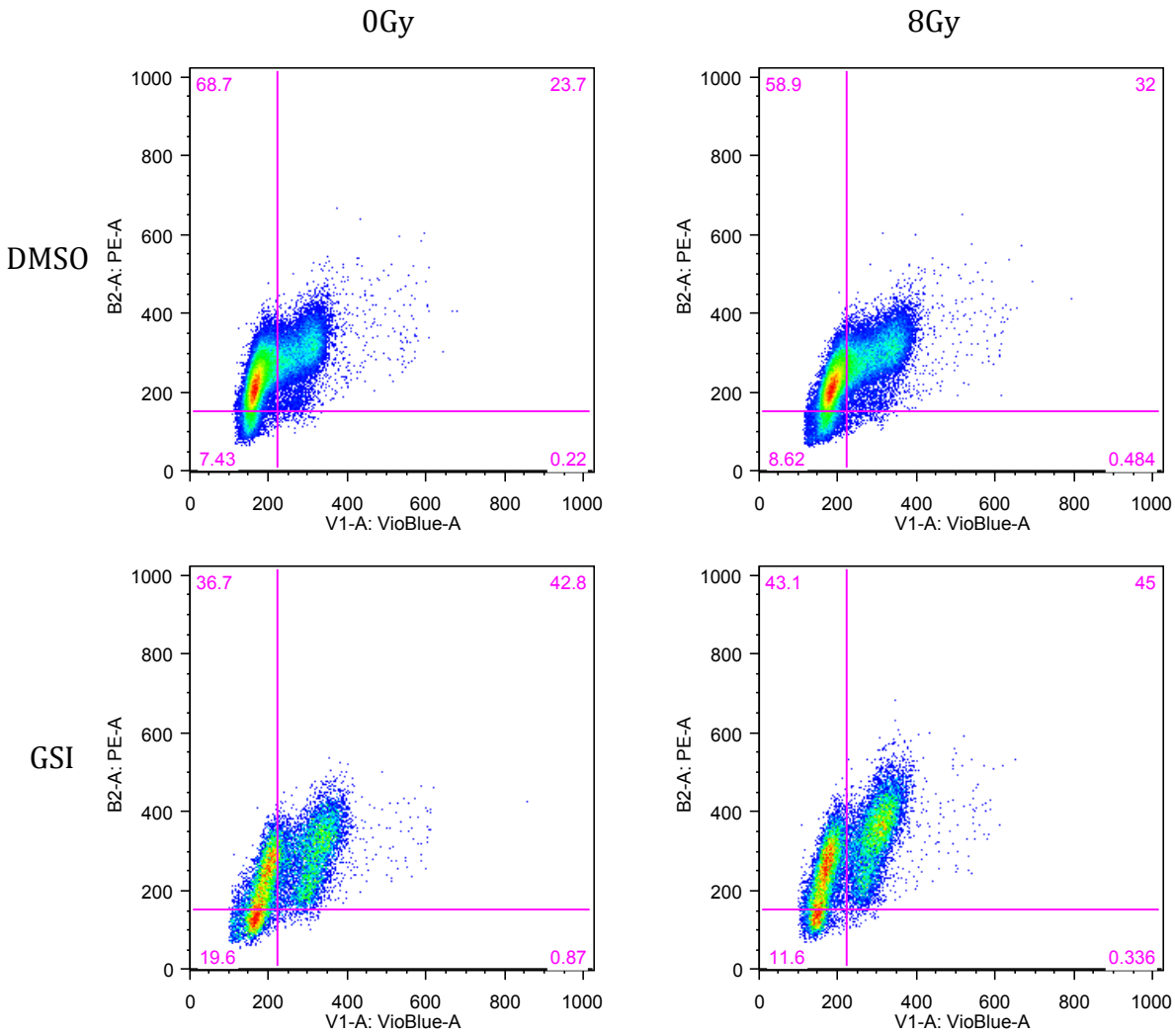

Figure 16: Demonstrates how the quiescent gating is depicted in graphical format. Dual staining with Hoechst/PY results in four quadrants. The upper left quadrant represents the G1 phase of the cell cycle, the lower left quadrant represents the quiescent population, and the upper right represents the G2/M phase of the cell cycle.

Figure 17: G0, Quiescent Neurosphere population in U87MG and U87MG PTEN treated and untreated with GSI/radation

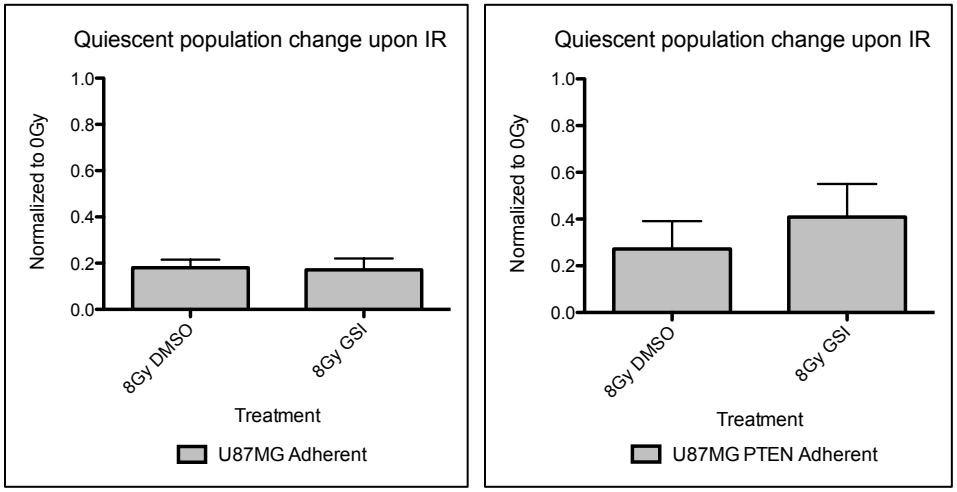

Figure 17: Quiescent population after radiation normalized to 0Gy in U87MG PTEN and U87MG adherently grown. Treatment with GSI does not significantly change the number of cell occupying the quiescent state.

Figure 18A: G0, Quiescent Neurosphere population change after Radition in PTEN-null cell lines

Figure 18 a

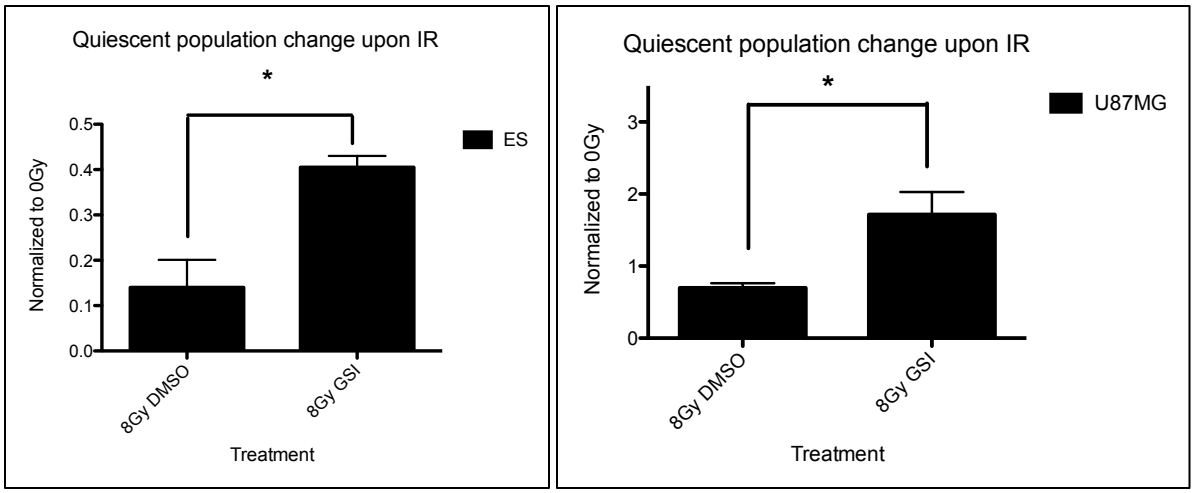

Figure 18a: Represents the change in the quiescent population normalized to 0Gy. Anything less than 1 means the quiescent cells entered the cell cycle. At 8Gy we see the quiescent neurosphere population enter the cell cycle in both PTEN-null cell lines. Upon treatment with GSI less quiescent cells enter the cell cycle. The value or ES at 8Gy was .14 ± .06 while radiated and treated with GSI was .405 ± .02 with p = .04. U87MG at 8Gy was .7 ± .069 while at 8Gy with GSI was 1.716 ± 1.31 and a p = .03.

Figure 18B: G0, Quiescent Neurosphere population change after Radiation in PTEN-wt cell lines

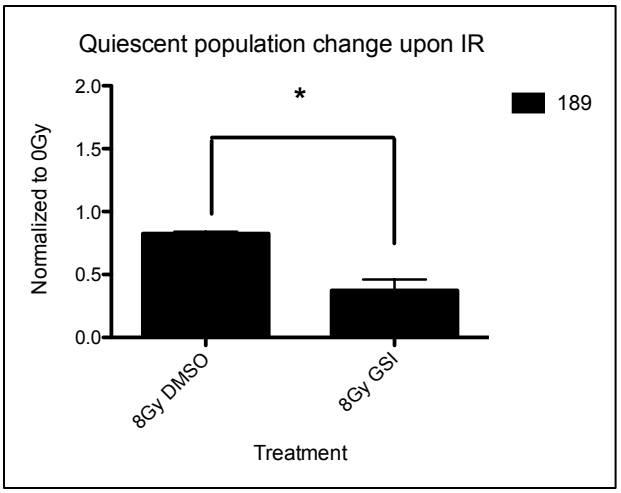

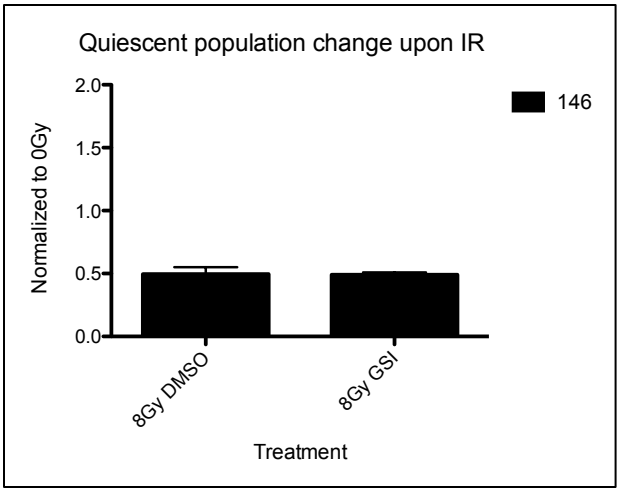

Figure 18b: Represents the change in the quiescent population normalized to 0Gy for PTENwt neurosphere lines. In U87MG PTEN and 189, we observe that at 8Gy there is minimum change in quiescent, while when treated with GSI the quiescent population reduces and enters the cell cycle. U87PTEN at 8Gy was 1.05 ± .045 and at 8Gy with GSI treatment .726 ± .053 with a p = .008. 189 at 8Gy was .826 ± .014 while at 8Gy treated with GSI was .375 ± .086 p = .0068. 146 showed no change between treated and untreated with 8Gy the average being .45 ± .01 and 8Gy treated with GSI .53 ± .02.

Figure 19: Sub-G1 peak Analysis

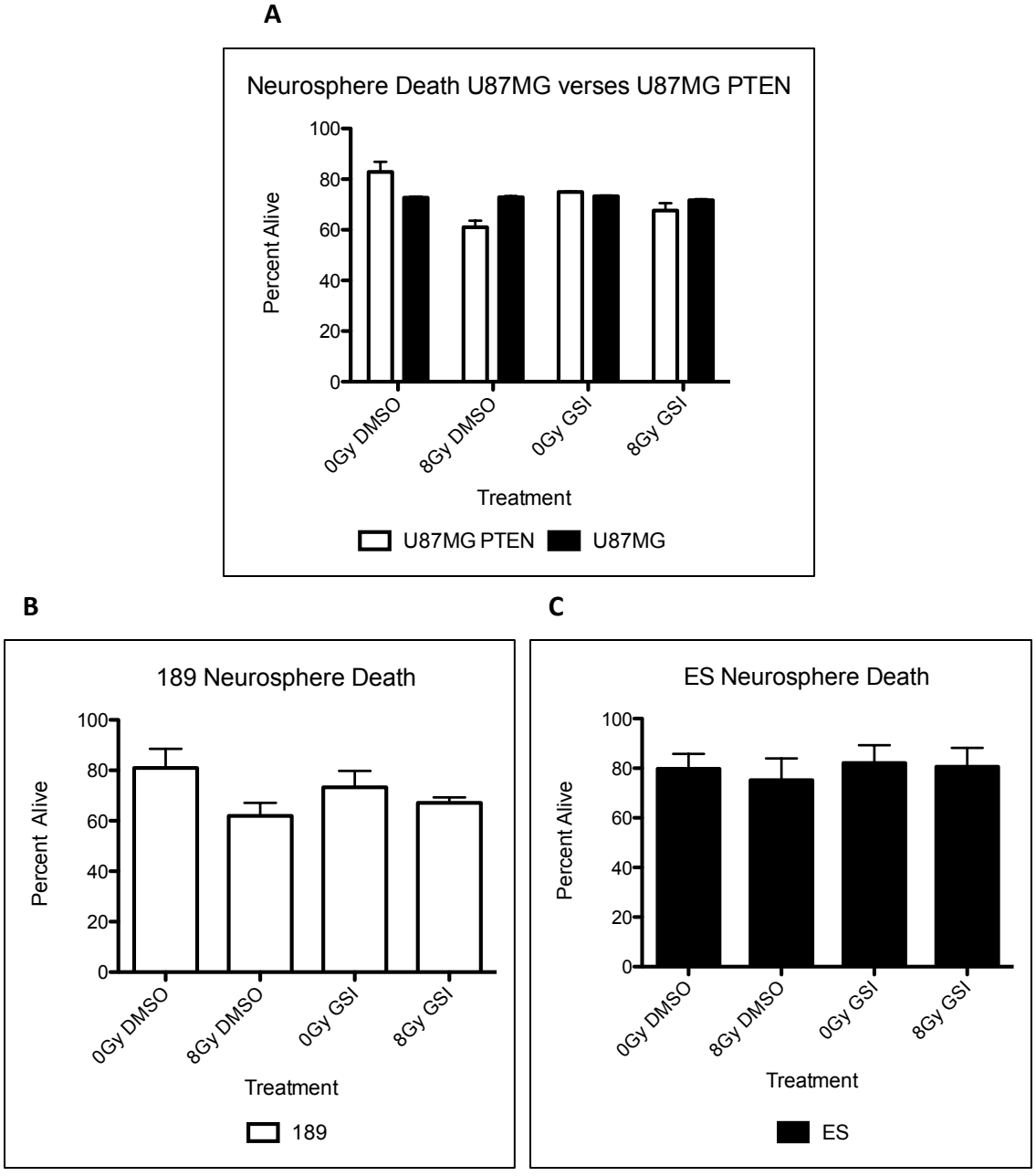

Figure 19: A) Depicts U87MG verses U87MG PTENwt 100-sub-G1 peak values, and represent viable cells. U87MG PTENwt has a minium increase in viable cells when treated with GSI plus radiation compared to radiation alone. U87MG does not change. **B)** Depicts another PTENwt neurosphere line. 189 displays a drop in viable cells after radiation. Combinational treatment of GSI plus radiation, show a minimum increase in viable cells over radiation alone. **C)** Depicts a PTEN null neurosphere line which follows the same pattern as U87MG. No changes in viability observed in any of the conditions.

in the sub-G1 peak after radiation treatment. When GSI is added in combination with radiation treatment we observe a decrease in the sub-G1 peak indicating a larger viable cell population (**Figure 19**).

PI3K inhibition plus a combination of GSI and radiation improves survival of PTEN-null neurospheres

To phenotypically mimic U87MG PTEN, with functioning PTEN in U87MG we utilized a PI3K inhibitor, LY294002. LY inhibits the action of PI3K therefore copying PTEN by negatively regulating AKT, and reducing pAKT. We utilized the neurosphere assay and treated U87MG neurospheres with 0Gy, or 8Gy, then with 0Gy or 8Gy with the addition of PI3K inhibitor, and lastly 0Gy or 8Gy with GSI plus PI3K inhibitor. This would allow us to test if we could rescue the response we see in U87MG PTEN when treating U87MG with LY/GSI and radiation. Interestingly, the combinational treatment of LY/GSI plus radiation improved survival of U87MG when compared to GSI plus irradiation alone or LY alone. The PI3K inhibitor when administered alone radiosensitizes U87MG by reducing neurosphere formation at both 0Gy and at 8Gy. GSI treatment alone slightly enriched for neurospheres at 0Gy but in combination with radiation, radiosensitized. Lastly, we observed that U87MG radiation enriches for neurospheres when compared to 0Gy (**Figure 20**).

Figure 20: Neurosphere formation in U87MG treated with PI3K inhibitor

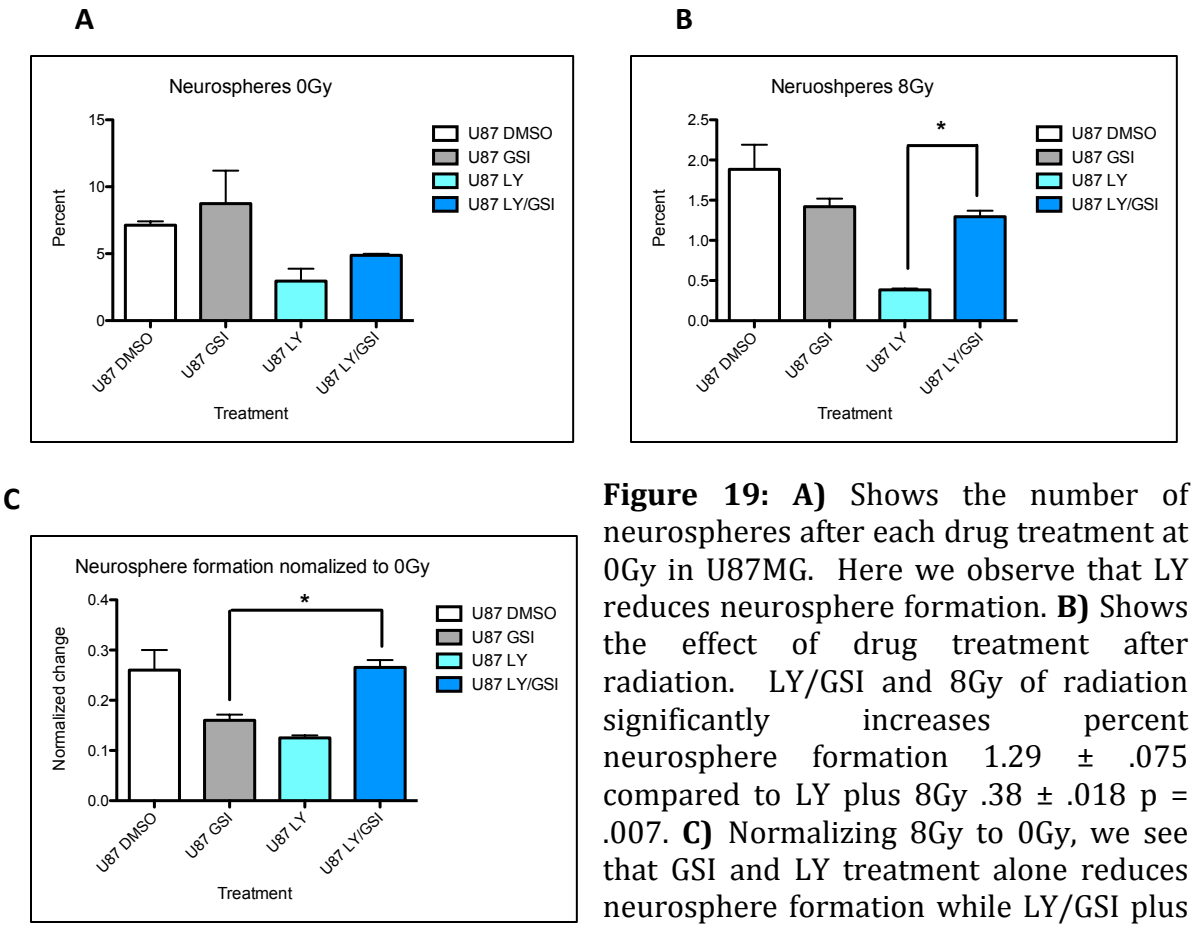

Figure 19: A) Shows the number of neurospheres after each drug treatment at 0Gy in U87MG. Here we observe that LY reduces neurosphere formation. **B)** Shows the effect of drug treatment after radiation. LY/GSI and 8Gy of radiation significantly increases percent neurosphere formation 1.29 ± .075 compared to LY plus 8Gy .38 ± .018 p = .007. **C)** Normalizing 8Gy to 0Gy, we see that GSI and LY treatment alone reduces neurosphere formation while LY/GSI plus 8Gy increases neurosphere formation in U87MG. Effect of GSI plus 8Gy .16 ± .01, effect of GSI/LY plus 8Gy .26 ± .015

Chapter 4

The proposed model for Notch inhibited glioma stem cell maintenance

Discussion

The relative radioresistance of glioma cell lines in culture do not differ from other curable cancers. Even though GBs share similar radiosensitivities to other curable cancers, current treatments for patients do not provide the same survival benefit. This may suggests that the brain microenvironment enhances the survival of GSCs after treatment. The GSCs that survive radiation or chemotherapeutic treatment can repopulate the tumor (Sakariassen, Immervoll et al. 2007, Mihaliak, Gilbert et al. 2010).

Previous research utilizes CD133+ or CD44+ cell surface markers to identify GSCs. Current GSC markers, CD133+ and CD44+, do not capture the entire GSC population(Brescia, Richichi et al. 2012). In order to capture the full GSC population we utilized neurosphere cultures, which enriches for GSCs. Neurosphere culturing methods have the added benefit that they more closely represent *in vivo* tumors genetically and phenotypically, compared to adherently grown culturing methods. To evaluate our human derived glioma cell lines we first characterized them by looking at the common mutations found in GB (MGMT, PTEN, p53 and EGFR). Mutations in MGMT, PTEN, p53 or EGFR play a role in the changes in radiosensitivity and/or drug treatment. Knowing the status of MGMT, PTEN, p53 and EGFR in our cell lines will help us determine if one of the particular mutations affects the treatment sensitivity with GSI, and GSI plus radiation. Since PTEN

activity demonstrated a consistent radioprotective effect in combination with GSI treatment. This lead us to utilize the syngeneic model, U87MG (naturally PTEN-null) and U87MG with PTENwt restored (call U87MG PTENwt) through retroviral vector infection, to carry out further experiments. PTEN is part of the PI3K/AKT/PTEN/FOXO pathway; therefore we evaluated pAKT and PTEN activity via western blotting while FOXO signaling was assessed via qRT-PCR. pAKT expression was inhibited by inhibiting of PI3K in PTEN-null cell lines. Given the results of our data we determined that FOXO3 plays a role in GSC maintenance upon Notch inhibition via gamma secretase.

Glioma cell lines and current literature

Upon radiation treatment, PTENwt gliomas have been identified to be more radiosensitive (Li, Kim et al. 2009). This is consistent within our GB lines as well; ES and 2345 (PTEN-null) neurosphere cultures have a higher survival over 189 and 146 (PTENwt) neurospheres. Interestingly, our syngeneic model was consistent with literature in that U87MG PTEN-null was more radioresistant, but only in adherently grown cultures. In neurosphere grown cultures, U87MG PTENwt has superior survival over U87MG. However, the increased survival in U87MG PTEN neurospheres was limited to primary neuropsheres only, and upon passaging into secondary neurosphere formation the radioprotection was lost. U87MG PTENwt neurosphere grow slower than the U87MG PTEN-null counterparts. We attributed the delayed cell cycle death upon radiation in U87MG PTENwt neurospheres to mitotic catastrophe (Vakifahmetoglu, Olsson et al. 2008). In a situation of mitotic catastrophe a tumor cell that has suffered DNA damage may divide a few times eventually dying during a mitotic event. Dissociation of neurospheres and

replating as single cells into secondary cultures allows us to identify which cells still have the capacity to replicate, by evaluating new sphere formation. The reduced number of spheres after radiation in U87MG PTENwt suggests that the initial radioprotective effect observed after radiation may just be a delayed cell death response.

The radioresistence found in PTEN-null glioma cell lines is attributed to overactive pAKT (Li, Kim et al. 2009). PTEN reverses PI3K activity, thus negatively regulating pAKT (Carnero, Blanco-Aparicio et al. 2008). pAKT is responsible for activating mTOR for cell growth and MDM2 for inhibition of cell cycle arrest, while also inhibiting BAD and FKHR to stop apoptosis (Vivanco and Sawyers 2002). Therefore, high pAKT activity leads to reduced apoptosis and rapid growth found in many cancers with non-functioning PTEN. The hyperactivation of AKT (pAKT) has been attributed to radioresistance (Li, Kim et al. 2009) and glioma aggressiveness (Chautard, Ouedraogo et al. 2014). We also confirmed in our syngeneic model, (U87MG, U87MG PTENwt), that lack of PTEN expression does lead to hyperactivation of pAKT via western blotting, while constituently active PTEN completely inhibits pAKT. The effects of overexpression of pAKT are visible in primary, secondary and tertiary sphere forming cultures. When U87MG and U87MG PTENwt neurospheres are dissociated and passaged into secondary and tertiary sphere forming capacity, we observe a higher sphere forming potential in PTEN-null U87MG compared to U87MG PTENwt, demonstrating that PTEN-null GBs have more aggressive GSC growth. Upon radiation, the number of neurospheres increases dramatically in U87MG verses U87MG PTENwt. The increase in neurosphere aggressiveness and proliferative potential seen in our own data for PTEN-null lines is consistent with literature suggesting that hyperactive pAKT leads to more radioresistent and aggressive tumors (Chautard, Ouedraogo et al. 2014).

Notch expression is a regulator of neural stem cell renewal and glioma aggressiveness (Zhang, Zheng et al. 2008, Stockhausen, Kristoffersen et al. 2010, Wang, Wakeman et al. 2010). GBs that do not depend on Notch signaling are insensitive to GSI treatment (Saito, Fu et al. 2014). We wanted to confirm that our glioma cell lines would be affected by Notch inhibition by establishing if our gliomas have increased Notch receptor and downstream Notch target expression. We analyzed Notch expression through qRT-PCR in our syngeneic. Our data showed that regardless of PTEN status both neurosphere lines have increased Notch receptors and downstream Notch signaling. We confirmed that both U87MG and U87MG PTENwt had expression of Notch receptors 1 – 4. After radiation Notch receptor expression increased in both neurosphere lines.

Targeting Notch through gamma secretase inhibition

There are many caveats to consider when inhibiting gamma-secretase to block notch activity. First, the various assembly of the four gamma-secretase proteins (PS, Aph-1, pen-2, and nicastrin) and their isoforms leads to tissue specific membrane protein processing, as well as GSI effectiveness. Second, the vast number of membrane proteins processed, may lead to unknown physiological effects upon gamma-secretase inhibition depending on the genetic background of the tissue and the environmental stimulus occurring at the time of gamma secretase inhibition. Although it has been described that GBs rely on Notch signaling (Chen, Kesari et al. 2010), it has recently been identified that there is a subset of glioma that are insensitive to GSI (Saito, Fu et al. 2014). It is important to note that the glioma cell lines that did not respond to GSI treatment were enriched for CD44, a stem cell marker, which is also processed by gamma secretase cleavage. The

distinct function of CD44-ICD is not known but it is thought to play a role in the expression of enzymes for aerobic glycolosis (Miletti-Gonzalez, Murphy et al. 2012). On the other hand glioma cell lines sensitive to GSI treatment share a proneural phenotype and have high notch activity (Saito, Fu et al. 2014). We tested the expression of Notch downstream targets after GSI inhibition (*Hes1, Heyl,* and *Hey1*) and found a significant reduction in Notch target gene expression. This suggested to us that the gamma secretase inhibitor, WPE-III-31C, is affective at reducing Notch expression in our human derived gliomas. To be sure that the effects we see are indeed due solely to Notch inhibition would require the use of siRNA targeting the four Notch receptors. Other publications have already compared GSI and siRNA against Notch and found that Notch inhibition through GSI is phenotypically similar to siRNA Notch inhibition (Alqudah, Agarwal et al. 2013).

PTEN confers Radioprotection to GBs treated with GSI

Active pAKT promotes growth and survival proteins. Interestingly however, the PTEN-null neurosphere lines, the initially more aggressive neurospheres, were sensitive to GSI treatment in combination with radiation while PTENwt neurospheres were radioprotected. Radioprotection of the cancer stem cell population upon GSI treatment has also been demonstrated within inflammatory breast cancer (Debeb, Cohen et al. 2012). Although no mechanistic explanation was provided for this observed phenomenon, it does suggest that inhibition of Notch through gamma-secretase cannot be applied as a blanket treatment to target cancer stem cell populations for all tumor types. The work by Debeb et al. in breast cancer and our data with glioma suggests that radioprotection of cancer stem cell populations upon GSI treatment is not unique to one-tumor type but likely a

phenomenon in other tumors depending on their genetic background. In neural stem cells PTEN functions to limit cell cycle entry of quiescent stem cells (Hill and Wu 2009). Loss of PTEN leads to brain enlargement, increased proliferation and decreased cell death (Groszer, Erickson et al. 2001). In our data we observe both increased proliferative potential and reduced cell death after radiation in PTEN-null U87MG compared to U87MG PTENwt. Neurosphere formation assay demonstrated the increased proliferative potential in U87MG, while sub-G1 peak analysis showed less apoptosis after radiation in 8Gy treated U87MG verses U87MG PTEN. U87MG PTENwt neurosphere treated with GSI prior to radiation showed reduced apoptosis, increased radioprotection, and sustained increase in neurosphere generation in primary, secondary and tertiary neurosphere formation. Comparatively, PTEN-null U87MG showed reduced neurosphere survival, and reduced neuroshpere formation in primary, secondary, and tertiary neurospheres. No changes in apoptosis were detectable in sub-g1 peak analysis for U87MG. We attributed the lack of detection due to the fact that PTEN-null cell lines favor senescence after radiation treatment while PTENwt lines favor apoptosis (Lee, Kim et al. 2011). Sub-g1 peak analysis cannot detect senescent cells, and therefore no changes in apoptosis would be observed. To confirm increased senescence is mediating cell death in GSI plus radiation treated U87MG; measuring β-galactosidase expression would be the appropriate experiment.

Recently, FOXO3 expression has been identified as a key factor for the maintenance of neuronal stem cells. PTEN positively regulates FOXO expression by reserving PI3K activity. Measuring FOXO expression in our syngeneic model with qRT-PCR we found that only FOXO3 expression was significantly higher in U87MG PTEN. This follows that FOXO expression is positively regulated by active PTEN. Within U87MG PTENwt, FOXO3

expression was also significantly much higher than in adherently grown conditions. Our data suggests that FOXO3 maybe protecting the stem cell phenotype in GBs treated with GSI.

Radioprotection is not mediated through DNA damage and repair

IR imparts energy displacing electrons. This can happen directly to DNA causing DNA strand breaks or to any other material in the cell. Ionization of water produces highly reactive free radicals that quickly steal back the displaced electrons from near by cellular constituents. Free-radical formation also causes DNA damage and is considered an indirect mode of DNA damage from radiation. Naturally, high metabolic activity causes the formation of radical species, and cells are equipped to deal with mild oxidative stress. Many cancers with PTEN mutations exhibit high oxidative stress as a result of overexpression of pAKT. In tumors with overactive AKT, the accumulation of reactive oxygen species (ROS) can eventually lead to cellular senescence (Finkel 2003, Collado, Blasco et al. 2007, Nogueira, Park et al. 2008). In contrast, functioning PTEN provides oxidative stress protection by inducing the expression of free radical scavengers (Sakamoto, Iwasaki et al. 2009) through FOXO signaling. FOXO3 increases the expression of the enzyme Manganese Superoxide Dismutase (MnSOD), a free radical scavenger (Sakamoto, Iwasaki et al. 2009), thus lowering oxidative stress. The differences we observed in oxidative stress between PTENwt and PTEN-null U87MG neurosphere lines led us to test if oxidative stress mediated increased DNA damage. We measured DNA damage utilizing the gH2Ax phosphorylation. gH2Ax becomes phosphorylated upon DNA double strand breaks. The number of double strand breaks increases the number of gH2Ax histones that are phosphorylated.

Evaluating gH2Ax 30 minutes after radiation measures initial DNA damage received from IR, while evaluating gH2Ax 24 hours after IR measures repair efficiency. In both cases, 30 minutes or 24 hours later, we did not observe any changes in DNA damage within the GSI treated or untreated conditions in both U87MG PTENwt and PTEN-null. Furthermore, there is no difference in DNA damage received when comparing U87MG to U87MG PTEN. These results establish first, that GSI treatment does not increase DNA damage or affect the DNA repair response, and second that radioprotection of PTENwt neurospheres treated with GSI does not depend on DNA damage and repair.

FOXO3 improves survival PTENwt neurospheres treated with GSI plus radiation

There are many established roles of FOXO signaling, which are involved in many seemingly opposing processes. FOXO1 has been identified in its function with insulin resistance (Martinez, Cras-Meneur et al. 2006), while one of the first activities described by FOXO signaling was the FOXO3 mediated apoptosis (Sunters, Fernandez de Mattos et al. 2003) and later in neurons after oxidative stress (Xie, Hao et al. 2012). But, FOXO3 expression has also been implicated in oxidative stress protection through activation MnSOD (Sakamoto, Iwasaki et al. 2009). In contrast to inducing apoptosis, FOXO3 can also mediate DNA repair and quiescence. Identifying which role FOXO plays within our cellular context can be difficult and would require identifying which sites on FOXO3 are phosphorylated/acetylated and subsequently evaluating what downstream proteins are activated. However, utilizing our syngeneic model of U87MG, which only differs in PTEN status, we can make a direct comparison in our observed experimental outcome and relate this to FOXO expression without evaluating FOXO phosphorylation status, since FOXO is

part of the PI3K/AKT/PTEN pathway. First we established through qRT-PCR that FOXO expression, specifically FOXO3 expression, is elevated in PTENwt U87MG neurospheres, but not in PTEN-null U87MG neurospheres. Comparing the qRT-PCR of adherent grown U87MG PTENwt verses the neurosphere grown culture also showed that FOXO3 expression was enriched in neurospheres but not adherently grown conditions. Given that FOXO3 expression was enriched in U87MG PTENwt neurospheres, and U87MG PTENwt neurospheres exhibited radioprotection when treated with GSI plus radiation we concluded that FOXO3 might be a key player in mediating the radioprotective response under notch inhibition. FOXO's diverse functionality can make it difficult to identify which FOXO pathway predominates. However, observing differences between FOXO mediated cell death and survival can be assessed easily. Analyzing sub-g1 peak analysis established that in U87MG PTENwt treated with GSI plus radiation had improved survival over just radiation treated neurospheres.

FOXO3 regulates Notch receptors expression

Literature has identified Notch expression to promote a quiescent stem cell phenotype in glioma (Zhang, Zheng et al. 2008). Recently, FOXO3 has also been implicated in regulation of stem cell quiescence in the hematopoietic (Miyamoto, Araki et al. 2007), muscle (Gopinath, Webb et al. 2014) and in neuronal stem cell compartments (Renault, Rafalski et al. 2009). Consistent with literature, our data for PTENwt or FOXO3 enriched neurospheres had a larger quiescent population over PTEN-null (FOXO3 low expression) neurospheres (Renault, Rafalski et al. 2009). However, PTEN knockout phenocopies FOXO3 knock out mice, with a reduced quiescent stem cell population in murine brains.

The difference being that PTEN negatively regulates quiescent stem cell entry into the cell cycle (Groszer, Erickson et al. 2006) while FOXO3 regulates genes involved in quiescent maintenance as well as genes involved in cell cycle entry (Renault, Rafalski et al. 2009). In adult muscle stem cells, FOXO3 is suggested to function by activating the Notch pathway (Gopinath, Webb et al. 2014). Although no established literature has suggested Notch activation from FOXO3 in the neural system, some of our PCR data suggests downstream Notch factors may still be active under GSI, and coincide with some of Gopinath et al. findings in muscle stem cells. For instance, Gopinath et al. finds that FOXO3 knockout reduces the levels Notch receptor 1 and 3. Furthermore, Gopinath et al. demonstrated through qRT-PCR that FOXO3 overexpression increased the levels of notch downstream targets, *Hes1, Hes2,* and *HeyL*. Consistent with Gopinath et al. results, U87MG PTEN, which has high expression of FOXO3, has higher levels of Notch receptors 1, 2 and 3 compared to U87MG. Interestingly after radiation treatment U87MG neurospheres lose expression of Notch receptors 1 and 3 but Notch receptor 2 increases, while U87MG PTENwt neurospheres maintain Notch 1 and 3 expression while Notch 2 expression is increased even higher than in U87MG (Notch1 U87MG 6165 ± 256, Notch1 U87MG PTEN 35327 ± 12775, Notch 3 U87MG 437 ± 55, Notch3 U87MG PTEN 102697 ± 19157). Radiation treatment, which produces oxidative stress on tissues, activates the nuclear translocation of FOXOs, further increased Notch receptor expression in U87MG PTENwt, but not U87MG. Furthermore, GSI plus radiation also had increased Notch receptor expression in U87MG PTENwt but not U87MG. Lastly, evaluating Notch target genes showed that in the presence of radiation GSI was ineffective at reducing the expression of *Hes1, Hey1* and *HeyL,* in U87MG PTEN neurospheres, while U87MG had a significant reduction in Notch target gene

expression. This provides evidence that FOXO3 may act as a redundant pathway to maintain the quiescent stem cell pool in the glioma. The increased expression of Notch receptors 1 and 2 are implicated in promoting tumor resistance in glioma (Wang, Wakeman et al. 2010), and the overall higher expression of Notch receptors 1, 2 and 3 after radiation and GSI treatment in U87MG PTEN neurospheres may explain U87MG PTEN's increased radioresistance compared to U87MG.

The difference observed in Notch receptor expression between PTENwt and PTEN-null neurospheres translates in neurosphere formation assay. U87MG PTENwt, neurospheres treated with radiation and GSI, have increased neurosphere formation in primary neurospheres. When these primary U87MG PTENwt neurospheres are dissociated and passage into secondary, and further on into tertiary neurospheres we observe that the radioprotective effect of GSI in PTENwt neurospheres is sustained. In contrast, U87MG shows a radiosensitizing effect in primary and secondary neurospheres. When dissociated and passage into tertiary neurospheres the GSI plus radiation treated U87MG recover. Treatment with radiation alone produces the opposite effect. U87MG generated more neurospheres over U87MG PTENwt, resulting from over active pAKT expression. The neurosphere formation assay establishes that, in PTENwt neurosphere lines, GSI protects by increasing the number of GSCs, which is visible in tertiary neurosphere formation. However in PTEN-null neurospheres, GSI reduces the GSC population. The PTEN-null GSCs that survive combinational treatment eventually recover.

GSI plus radiation stimulates cell cycle entry in PTENwt neurospheres

Literature has established in both brain and breast cancers that radiation activates CSCs to proliferate, leading to more aggressive tumors (Rich 2007, Lagadec and Pajonk

2012). Similarly, after radiation treatment we measured a decrease in the number of GSCs occupying a quiescent state in U87MG and U87MG PTEN. The reduction in GSCs occupying the quiescent state after radiation was greater in U87MG because of the lack of PTEN to negatively regulate cell cycle entry (Groszer, Erickson et al. 2006). Upon treatment with GSI, the opposite effect was observed. In two PTENwt neurosphere lines, U87MG PTEN and 189 the quiescent population after GSI and radiation treatment was reduced, while, the G1 population increased. In U87MG and ES, we observed an increase in the quiescent population after GSI plus radiation treatment. Quiescent cells can only enter the cell cycle at G1 (Schafer 1998), therefore we concluded that GSI stimulates glioma stem cells to enter the cell cycle upon radiation in PTENwt neurosphere cultures. However, inhibiting notch through siRNA or GSI, has demonstrated to make stem cells differentiate in *in vivo* murine models when evaluated with markers such as Nestin, Sox2 and Tuj1 (Koch, Lehal et al. 2013). Measuring differentiation is impossible in the *in vitro* neurosphere culturing system. Neurosphere media is specifically defined with minimal growth factors, thus allowing only stem cells, and progenitor cell survival. Glioma cells that do differentiate die, because of the lack of nutrients required for survival. Attempts to measure changes in stem cells through cell surface markers will not depict accurate results because the growth environment doesn't support differentiated cell survival. However, evaluating neurosphere formation after GSI plus radiation, demonstrates that PTENwt glioma cell lines produce more neurospheres than radiation alone. If our GSCs were differentiating upon treatment we would observe a decrease in neurosphere formation. PTEN-null neurosphere lines demonstrate a decrease in neurosphere formation after GSI plus radiation treatment.

PI3K inhibition plus GSI and radiation leads to radioprotection of PTEN-null neurospheres.

To mimic PTEN restoration in PTEN-null neurosphere lines we utilized a PI3K inhibitor. PTEN functions to reverse the action of PI3K (Carnero, Blanco-Aparicio et al. 2008) leading to reduced phosphorylation of AKT. Inhibiting PI3K also reduces phosphorylation of AKT (Fresno Vara, Casado et al. 2004). Interestingly, inhibiting PI3K and then treating with GSI and radiation in U87MG produced the same radioprotective effect seen in U87MG PTEN. This data suggest that FOXO is the key in providing the radioprotection in the absence of notch signaling. By inhibiting PI3K we reduced pAKT. pAKT negatively regulates FOXO expression. Under PI3K inhibition we stabilize FOXO expression, similar to PTENwt neurospheres. As a result of FOXO stabilization we observe a radioprotection after GSI treatment.

FOXO as a therapeutic target in GB

FOXO transcription factors were originally discovered through the cloning chromosomal break points associated with cancer. It was then proposed that FOXO acts as tumor suppressors, and overexpression of FOXOs in adherent grown cells lines caused cell cycle arrest or cell death. Through different posttranslational modification FOXO factors can also regulate detoxification and stress resistance thus protecting tumor cells from various treatment therapies (Brunet, Sweeney et al. 2004). Current literature suggests that

FOXO factors may also play a role in the maintenance of stem cells. The dual roles of FOXOs may dictate the difference between treatment success and failure.

The role of FOXO3 in cancer cell and tumor stem cell survival can be summed up into three main areas, stress protection, stem cell maintenance, and reduction of cell death from the immune system.

Stress Protection

Although FOXOs were first characterized as tumor suppressor proteins, new data also suggests that FOXO transcription factors, specifically FOXO3, supports cancer development by protecting tumor cells against oxidative stress by inducing the enzymes MnSOD and PTEN-induced putative kinase 1 (Pink1) (Kops, Dansen et al. 2002, Lee, Iijima-Ando et al. 2009, Mei, Zhang et al. 2009). Pink1 protects cells from stress induced mitochondrial dysfunction by binding to depolarized mitochondria and inducing autophagy. Deletion of Pink1 sensitizes cells to growth factor withdrawal induced cell death (Mei, Zhang et al. 2009). Furthermore, FOXO3 can induce AKT activity in drug-resistant leukemic cells through induction of PIK3CA (PIK3CA, is the active catalytic subunit of PI3K) (Hui, Francis et al. 2008). The activity of AKT further promotes the expression of anti-apoptotic and growth pathways. Oxidative stress is one means to activate FOXO expression, allowing FOXO translocation it into the nucleus (Kops, Dansen et al. 2002, Calnan and Brunet 2008). Although, FOXO activation induced by oxidative stress can lead to apoptosis (Xie, Hao et al. 2012), FOXO3 signaling in quiescent stem cells acts as a protective mechanism from oxidative stress (Kops, Dansen et al. 2002).

Stem Cell Maintenance

In chronic myeloid leukemia (CML) FOXO3 critically regulates CSC maintenance. CML is characterized by the Bcr-Abl genetic abnormality. Brc-Abl induces the PI3K/Akt signaling pathway, which represses the transcriptional activity of FOXO3 in these cancer cells. However, a major problem with CML treatment is a small population of surviving leukemic initiating cells (LICs), which promote recurrence of CML. These LICs, had stabilized FOXO3 expression, which promoted their maintenance and stress resistance (Naka, Hoshii et al. 2010).

FOXO3 is also an important regulator of stemness in the hematopoietic stem cell pool. Depletion of FOXO3 leads to a reduction colony formation in bone colony formation assays, as well as increased ROS levels. These FOXO deficient cells are defective for maintenance of quiescence (Miyamoto, Araki et al. 2007). In muscle tissues FOXO3 as has been demonstrated to maintain a quiescent population of stem cells. While FOXO3 deficient lines have a reduced stem cell population and a reduction in Notch receptors 1 and 3 (Gopinath, Webb et al. 2014). Lastly, FOXO3 expression has also been demonstrated to be required for the maintenance of neural stem cells in the sub-ventricular zone (Renault, Rafalski et al. 2009).

Reduction of cell death

The environmental niche helps to play a large role in how cancers grow in respond to various environmental perturbations. Evading immune response is one of the hallmarks of cancer (Hanahan and Weinberg 2011). FOXO3 represses immune function and surveillance by inducing apoptosis in T-cells (Pandiyan, Gartner et al. 2004, Dejean, Beisner

et al. 2009) therefore, reducing immune action on tumor tissues. Many cancers are able to evade immune surveillance, and FOXO expression may be responsible, thus promoting CSC survival.

Summary: The model

We've established that after radiation PTEN-null neurospheres are more radioresistant then PTENwt neurospheres through neurosphere survival assays. The increased radioresistance of PTEN-null tumors is supported by literature and the mechanism is through hyperactive pAKT expression (Li, Kim et al. 2009). Treating neurosphere grown cells with combinational treatment of GSI and radiation demonstrated two outcomes. PTEN-null neurospheres were radiosensitized and PTENwt were radioprotected. The radiosensitization of PTEN-null neurospheres and radioprotection of PTENwt neurospheres was observed in neurosphere survival assays as well. Debeb et al. also demonstrated a radioprotective effect in breast cancer stem cells treated with GSI, but no distinction was made between PTEN status and radioprotection (Debeb, Cohen et al. 2012). We evaluated changes in DNA damage as a possible mechanism of changes in radiosensitivity but found that GSI does not affect DNA damage, or repair. Utilizing our syngeneic model (U87MG, U87MG PTENwt) we evaluated differences in Notch receptor expression and Notch downstream targets *Hes1, Hey1* and *HeyL* via qRT-PCR. We evaluated the expression of Notch receptors 1 - 4 and Notch downstream targets as they changed with radiation treatment. Notch receptor 2 increased in both U87MG and U87MG PTEN. Notch receptor 1 and 3 expression is lost in U87MG after radiation, while maintained in U87MG PTENwt. After GSI treatment the down stream targets of Notch,

Hes1, Hey1 and *HeyL*, are reduced in U87MG but not significantly in U87MG PTEN. As a result of PTEN expression FOXOs are positively regulated (Calnan and Brunet 2008). We established through qRT-PCR that specifically FOXO3 expression is upregulated in U87MG PTEN neurospheres. FOXO1 and FOXO4 expression do not differ significantly in our syngeneic U87 model. The enrichment of FOXO3 in stem cells and FOXO3s role in stem cell maintenance is supported in literature (Miyamoto, Araki et al. 2007, Renault, Rafalski et al. 2009, Gopinath, Webb et al. 2014). Increased levels of Notch receptors 1 and 3 observed in U87MG PTEN is consistent with FOXO3 regulation of Notch receptors 1 and 3 in muscle stem cells (Gopinath, Webb et al. 2014). We provide evidence that GSI plus radiation treatment in U87MG PTEN improves survival by demonstrating that we have less apoptotic cells when measured via sub-G1 peak analysis, and by increased neurosphere formation in tertiary sphere formation assay. We rely on established literature that hyperactive AKT leads to senescence upon oxidative stress (Nogueira, Park et al. 2008), to explain why we do not observe an increase in sub-G1 peak in U87MG neurospheres treated with radiation plus GSI. Senescent cells are not detectable in sub-G1 peak analysis. We demonstrated that the quiescent stem cell population changes with GSI treatment and with radiation. Literature supports that; radiation induces stem cell proliferation (Pajonk, Vlashi et al. 2010, Wang, Li et al. 2014). Upon GSI treating U87MG, we observed an increase in the quiescent stem cell population suggesting that fewer quiescent stem cells enter the cell cycle. In U87MG PTENwt we observed a reduction in cells occupying the quiescent state, and an increase in cells occupying G1. Since quiescent cells can only enter the cell cycle through G1 (Schafer 1998) we interpreted this as GSI treatment stimulates PTENwt neurospheres to enter the cell cycle upon subsequent radiation treatment. The increase in

neurospheres in U87MG PTENwt and decrease in neurosphere in U87MG is supported by neurosphere formation assay data. To mimic a PTEN restoration in U87MG we inhibited PI3K activity, and then treated U87MG with GSI plus radiation. We observed a radioprotective effect similar to U87MG PTEN treated with GSI and radiation. The lack of active pAKT in the PI3K inhibited U87MG neurospheres allows for FOXO3 accumulation. Our data provides the bases for further investigation of FOXO3s role in the stem cell maintenance in the absence of Notch signaling in the glioma. We have outlined the proposed model in **Figure 21**.

Figure 21: The Proposed Model

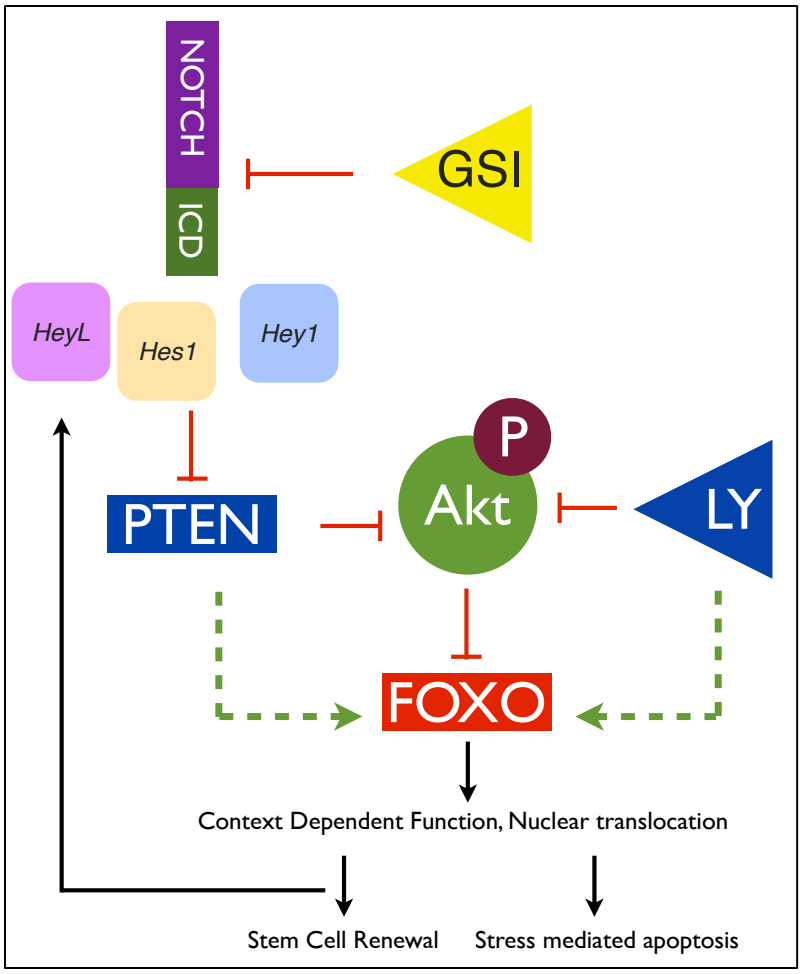

Figure 21: We propose that after IR, the Notch pathway blocks PTEN through *Hes1* expression allowing increased pAKT expression leading to stem cell proliferation. PTEN-null cell lines have a higher number of stem cells entering the cell cycle because they lack the PTEN blockade leading to hyperactive pAKT. Upon GSI treatment the Notch pathway is inhibited. When PTEN is functioning, PTEN expression becomes the dominating presence limiting growth through negative regulation of cell cycle entry from quiescence. This also allows for the accumulation of FOXO factors, in particular FOXO3, which can maintain stemness. Upon Radiation and GSI treatment, PTENwt cell lines rely on FOXO3 expression to maintain the quiescence stem cells. FOXO3 translocates into the nucleus as a result of oxidative stress from IR treatment, thus differentially activating genes for stem cell maintenance and oxidative stress detoxification, as well as increasing Notch receptor expression 1 and 3. In PTEN-null neurospheres, radiation leads to high free radical formation, and no free-radical detoxification. A high level of free radicals with high expression of pAKT leads to cellular senescence, resulting in lower neurosphere formation in PTEN-null neurospheres. The PI3K inhibitor LY phenocopies PTEN functionality, and can rescue PTEN-null neurosphere radiosensitivity once treated with GSI.

Study Limitations

The inability to identify all GSCs thru markers makes studying this isolated population of cells difficult. GSCs are propagated and enriched using *in vitro* neurosphere formation in a defined serum free media supplemented with growth factors. These neurosphere cultures are a heterogeneous population composed of GSCs and early progenitors. Studies using neurosphere cultures may underestimate the response of GSCs compared to non-stem cells. Isolating GSC populations through fluorescence activated cell sorting may be attempted using CD133 or CD44 cell surface markers, but literature as established that these markers do not encompass the entire stem cells population within a glioma.

Secondly, the *in vivo* environmental niche plays another important role in cancer development and response to treatment. The effects seen in *in vitro* models, do not always translate in the *in vivo* setting. *In vivo* mouse models also have specific limitations. Intracranial tumor injections require a specialized head restraint apparatus and injection needle to precisely and slowly inject tumor cells. The additional handling of tumor cells or poor injection techniques leads to decreased cell viability and low tumor initiation at the injection site. A fluorescent or luciferase base reporter system must be used to observe tumor formation in the brain to determine when to start treatment and to evaluate tumor growth after treatment. Additionally, targeting such a small tumor volume for radiotherapy in a mouse model is difficult with current technology. Even with these challenges the studies here should be validated in an *in vivo* setting.

Conclusion

A sustainable cancer cure relies on the elimination and mitigation of all cancer cells. Targeting cancer cells that maintain the entire bulk tumor population is one means to achieve sustained cancer remission. Current treatment methods may have different impacts on the cancer stem cell population, compared to non-cancer stem cells. Furthermore, treatment methods may protect or increase cancer stem cells. Thus it is important to understand CSC response to treatment methods. Glioma stem cells are more radioresistent and chemoresistent than their differentiated counterparts. Currently, methods to identify and target GSCs are lacking. Surgical debulking, radiation and chemotherapy are the standard treatment for glioma therapy. Even with the improvements with radiotherapy and new chemotherapeutics the 5-year survival remains low.

Although utilizing Notch inhibition, as a target for GSCs is promising, we propose that Notch inhibition may improve survival for glioma with intact PTEN function. Genotyping tumors before treatment should be a standard procedure to determine appropriate treatment methods.

Literature Cited

Ables, J. L., J. J. Breunig, A. J. Eisch and P. Rakic (2011). "Not(ch) just development: Notch signalling in the adult brain." Nat Rev Neurosci **12**(5): 269-283.

Ables, J. L., N. A. Decarolis, M. A. Johnson, P. D. Rivera, Z. Gao, D. C. Cooper, F. Radtke, J. Hsieh and A. J. Eisch (2010). "Notch1 is required for maintenance of the reservoir of adult hippocampal stem cells." J Neurosci **30**(31): 10484-10492.

Al-Hajj, M., M. S. Wicha, A. Benito-Hernandez, S. J. Morrison and M. F. Clarke (2003). "Prospective identification of tumorigenic breast cancer cells." Proc Natl Acad Sci U S A **100**(7): 3983-3988.

Allan, A. L., S. A. Vantyghem, A. B. Tuck and A. F. Chambers (2006). "Tumor dormancy and cancer stem cells: implications for the biology and treatment of breast cancer metastasis." Breast Dis **26**: 87-98.

Allenspach, E. J., I. Maillard, J. C. Aster and W. S. Pear (2002). "Notch signaling in cancer." Cancer Biol Ther **1**(5): 466-476.

Alqudah, M. A., S. Agarwal, M. S. Al-Keilani, Z. A. Sibenaller, T. C. Ryken and M. Assem (2013). "NOTCH3 is a prognostic factor that promotes glioma cell proliferation, migration and invasion via activation of CCND1 and EGFR." PLoS One **8**(10): e77299.

Altaner, C. (2008). "Glioblastoma and stem cells." Neoplasma **55**(5): 369-374.

Andersen, P., H. Uosaki, L. T. Shenje and C. Kwon (2012). "Non-canonical Notch signaling: emerging role and mechanism." Trends Cell Biol **22**(5): 257-265.

Ang, H. L. and V. Tergaonkar (2007). "Notch and NFkappaB signaling pathways: Do they collaborate in normal vertebrate brain development and function?" Bioessays **29**(10): 1039-1047.

Asserlechner, M. J., Hagenbuchner, Judith, Fuchs Stefan, Geiger Kathrin, Obexer Petra Ed. (2012). FOXO Transcription Factos as Potential Therapeutic Targets in Neuroblastoma. INTECH. Austria.

Bao, S., Q. Wu, R. E. McLendon, Y. Hao, Q. Shi, A. B. Hjelmeland, M. W. Dewhirst, D. D. Bigner and J. N. Rich (2006). "Glioma stem cells promote radioresistance by preferential activation of the DNA damage response." Nature **444**(7120): 756-760.

Barten, D. M., J. E. Meredith, Jr., R. Zaczek, J. G. Houston and C. F. Albright (2006). "Gamma-secretase inhibitors for Alzheimer's disease: balancing efficacy and toxicity." Drugs R D **7**(2): 87-97.

Beel, A. J. and C. R. Sanders (2008). "Substrate specificity of gamma-secretase and other intramembrane proteases." Cell Mol Life Sci **65**(9): 1311-1334.

Beier, D., S. Rohrl, D. R. Pillai, S. Schwarz, L. A. Kunz-Schughart, P. Leukel, M. Proescholdt, A. Brawanski, U. Bogdahn, A. Trampe-Kieslich, B. Giebel, J. Wischhusen, G. Reifenberger, P. Hau and C. P. Beier (2008). "Temozolomide preferentially depletes cancer stem cells in glioblastoma." Cancer Res **68**(14): 5706-5715.

Biggs, W. H., 3rd, J. Meisenhelder, T. Hunter, W. K. Cavenee and K. C. Arden (1999). "Protein kinase B/Akt-mediated phosphorylation promotes nuclear exclusion of the winged helix transcription factor FKHR1." Proc Natl Acad Sci U S A **96**(13): 7421-7426.

Brescia, P., C. Richichi and G. Pelicci (2012). "Current strategies for identification of glioma stem cells: adequate or unsatisfactory?" J Oncol **2012**: 376894.

Brownawell, A. M., G. J. Kops, I. G. Macara and B. M. Burgering (2001). "Inhibition of nuclear import by protein kinase B (Akt) regulates the subcellular distribution and activity of the forkhead transcription factor AFX." Mol Cell Biol **21**(10): 3534-3546.
Brunet, A., L. B. Sweeney, J. F. Sturgill, K. F. Chua, P. L. Greer, Y. Lin, H. Tran, S. E. Ross, R. Mostoslavsky, H. Y. Cohen, L. S. Hu, H. L. Cheng, M. P. Jedrychowski, S. P. Gygi, D. A. Sinclair, F. W. Alt and M. E. Greenberg (2004). "Stress-dependent regulation of FOXO transcription factors by the SIRT1 deacetylase." Science **303**(5666): 2011-2015.
Buatti, J., T. C. Ryken, M. C. Smith, P. Sneed, J. H. Suh, M. Mehta and J. J. Olson (2008). "Radiation therapy of pathologically confirmed newly diagnosed glioblastoma in adults." J Neurooncol **89**(3): 313-337.
Cahill, D. P., K. K. Levine, R. A. Betensky, P. J. Codd, C. A. Romany, L. B. Reavie, T. T. Batchelor, P. A. Futreal, M. R. Stratton, W. T. Curry, A. J. Iafrate and D. N. Louis (2007). "Loss of the mismatch repair protein MSH6 in human glioblastomas is associated with tumor progression during temozolomide treatment." Clin Cancer Res **13**(7): 2038-2045.
Calnan, D. R. and A. Brunet (2008). "The FoxO code." Oncogene **27**(16): 2276-2288.
Carnero, A., C. Blanco-Aparicio, O. Renner, W. Link and J. F. Leal (2008). "The PTEN/PI3K/AKT signalling pathway in cancer, therapeutic implications." Curr Cancer Drug Targets **8**(3): 187-198.
Chautard, E., Z. G. Ouedraogo, J. Biau and P. Verrelle (2014). "Role of Akt in human malignant glioma: from oncogenesis to tumor aggressiveness." J Neurooncol **117**(2): 205-215.
Chen, J., S. Kesari, C. Rooney, P. R. Strack, J. Chen, H. Shen, L. Wu and J. D. Griffin (2010). "Inhibition of notch signaling blocks growth of glioblastoma cell lines and tumor neurospheres." Genes Cancer **1**(8): 822-835.
Chen, K., Y. H. Huang and J. L. Chen (2013). "Understanding and targeting cancer stem cells: therapeutic implications and challenges." Acta Pharmacol Sin **34**(6): 732-740.
Chen, R., M. C. Nishimura, S. M. Bumbaca, S. Kharbanda, W. F. Forrest, I. M. Kasman, J. M. Greve, R. H. Soriano, L. L. Gilmour, C. S. Rivers, Z. Modrusan, S. Nacu, S. Guerrero, K. A. Edgar, J. J. Wallin, K. Lamszus, M. Westphal, S. Heim, C. D. James, S. R. VandenBerg, J. F. Costello, S. Moorefield, C. J. Cowdrey, M. Prados and H. S. Phillips (2010). "A hierarchy of self-renewing tumor-initiating cell types in glioblastoma." Cancer Cell **17**(4): 362-375.
Clarke, M. F., J. E. Dick, P. B. Dirks, C. J. Eaves, C. H. Jamieson, D. L. Jones, J. Visvader, I. L. Weissman and G. M. Wahl (2006). "Cancer stem cells--perspectives on current status and future directions: AACR Workshop on cancer stem cells." Cancer Res **66**(19): 9339-9344.
Clement, V., P. Sanchez, N. de Tribolet, I. Radovanovic and A. Ruiz i Altaba (2007). "HEDGEHOG-GLI1 signaling regulates human glioma growth, cancer stem cell self-renewal, and tumorigenicity." Curr Biol **17**(2): 165-172.
Collado, M., M. A. Blasco and M. Serrano (2007). "Cellular senescence in cancer and aging." Cell **130**(2): 223-233.
Dang, T. P., A. F. Gazdar, A. K. Virmani, T. Sepetavec, K. R. Hande, J. D. Minna, J. R. Roberts and D. P. Carbone (2000). "Chromosome 19 translocation, overexpression of Notch3, and human lung cancer." J Natl Cancer Inst **92**(16): 1355-1357.
Das, D., F. Lanner, H. Main, E. R. Andersson, O. Bergmann, C. Sahlgren, N. Heldring, O. Hermanson, E. M. Hansson and U. Lendahl (2010). "Notch induces cyclin-D1-dependent proliferation during a specific temporal window of neural differentiation in ES cells." Dev Biol **348**(2): 153-166.

Debeb, B. G., E. N. Cohen, K. Boley, E. M. Freiter, L. Li, F. M. Robertson, J. M. Reuben, M. Cristofanilli, T. A. Buchholz and W. A. Woodward (2012). "Pre-clinical studies of Notch signaling inhibitor RO4929097 in inflammatory breast cancer cells." Breast Cancer Res Treat **134**(2): 495-510.
Dejean, A. S., D. R. Beisner, I. L. Ch'en, Y. M. Kerdiles, A. Babour, K. C. Arden, D. H. Castrillon, R. A. DePinho and S. M. Hedrick (2009). "Transcription factor Foxo3 controls the magnitude of T cell immune responses by modulating the function of dendritic cells." Nat Immunol **10**(5): 504-513.
Eaves, C. J. (2008). "Cancer stem cells: Here, there, everywhere?" Nature **456**(7222): 581-582.
Edbauer, D., E. Winkler, J. T. Regula, B. Pesold, H. Steiner and C. Haass (2003). "Reconstitution of gamma-secretase activity." Nat Cell Biol **5**(5): 486-488.
Ernst, A., S. Hofmann, R. Ahmadi, N. Becker, A. Korshunov, F. Engel, C. Hartmann, J. Felsberg, M. Sabel, H. Peterziel, M. Durchdewald, J. Hess, S. Barbus, B. Campos, A. Starzinski-Powitz, A. Unterberg, G. Reifenberger, P. Lichter, C. Herold-Mende and B. Radlwimmer (2009). "Genomic and expression profiling of glioblastoma stem cell-like spheroid cultures identifies novel tumor-relevant genes associated with survival." Clin Cancer Res **15**(21): 6541-6550.
Esler, W. P., W. T. Kimberly, B. L. Ostaszewski, T. S. Diehl, C. L. Moore, J. Y. Tsai, T. Rahmati, W. Xia, D. J. Selkoe and M. S. Wolfe (2000). "Transition-state analogue inhibitors of gamma-secretase bind directly to presenilin-1." Nat Cell Biol **2**(7): 428-434.
Finkel, T. (2003). "Oxidant signals and oxidative stress." Curr Opin Cell Biol **15**(2): 247-254.
Fiuza, U. M. and A. M. Arias (2007). "Cell and molecular biology of Notch." J Endocrinol **194**(3): 459-474.
Fortini, M. E. (2009). "Notch signaling: the core pathway and its posttranslational regulation." Dev Cell **16**(5): 633-647.
Fraering, P. C., W. Ye, J. M. Strub, G. Dolios, M. J. LaVoie, B. L. Ostaszewski, A. van Dorsselaer, R. Wang, D. J. Selkoe and M. S. Wolfe (2004). "Purification and characterization of the human gamma-secretase complex." Biochemistry **43**(30): 9774-9789.
Frame, F. M. and N. J. Maitland (2011). "Cancer stem cells, models of study and implications of therapy resistance mechanisms." Adv Exp Med Biol **720**: 105-118.
Fresno Vara, J. A., E. Casado, J. de Castro, P. Cejas, C. Belda-Iniesta and M. Gonzalez-Baron (2004). "PI3K/Akt signalling pathway and cancer." Cancer Treat Rev **30**(2): 193-204.
Furuyama, T., T. Nakazawa, I. Nakano and N. Mori (2000). "Identification of the differential distribution patterns of mRNAs and consensus binding sequences for mouse DAF-16 homologues." Biochem J **349**(Pt 2): 629-634.
Ghods, A. J., D. Irvin, G. Liu, X. Yuan, I. R. Abdulkadir, P. Tunici, B. Konda, S. Wachsmann-Hogiu, K. L. Black and J. S. Yu (2007). "Spheres isolated from 9L gliosarcoma rat cell line possess chemoresistant and aggressive cancer stem-like cells." Stem Cells **25**(7): 1645-1653.
Gopinath, S. D., A. E. Webb, A. Brunet and T. A. Rando (2014). "FOXO3 Promotes Quiescence in Adult Muscle Stem Cells during the Process of Self-Renewal." Stem Cell Reports **2**(4): 414-426.
Greer, E. L. and A. Brunet (2005). "FOXO transcription factors at the interface between longevity and tumor suppression." Oncogene **24**(50): 7410-7425.

Groszer, M., R. Erickson, D. D. Scripture-Adams, J. D. Dougherty, J. Le Belle, J. A. Zack, D. H. Geschwind, X. Liu, H. I. Kornblum and H. Wu (2006). "PTEN negatively regulates neural stem cell self-renewal by modulating G0-G1 cell cycle entry." Proc Natl Acad Sci U S A **103**(1): 111-116.
Groszer, M., R. Erickson, D. D. Scripture-Adams, R. Lesche, A. Trumpp, J. A. Zack, H. I. Kornblum, X. Liu and H. Wu (2001). "Negative regulation of neural stem/progenitor cell proliferation by the Pten tumor suppressor gene in vivo." Science **294**(5549): 2186-2189.
Gupta, P. B., C. L. Chaffer and R. A. Weinberg (2009). "Cancer stem cells: mirage or reality?" Nat Med **15**(9): 1010-1012.
Haapasalo, A. and D. M. Kovacs (2011). "The many substrates of presenilin/gamma-secretase." J Alzheimers Dis **25**(1): 3-28.
Hafer, K., K. S. Iwamoto and R. H. Schiestl (2008). "Refinement of the dichlorofluorescein assay for flow cytometric measurement of reactive oxygen species in irradiated and bystander cell populations." Radiat Res **169**(4): 460-468.
Hambardzumyan, D., O. J. Becher, M. K. Rosenblum, P. P. Pandolfi, K. Manova-Todorova and E. C. Holland (2008). "PI3K pathway regulates survival of cancer stem cells residing in the perivascular niche following radiation in medulloblastoma in vivo." Genes Dev **22**(4): 436-448.
Hanahan, D. and R. A. Weinberg (2011). "Hallmarks of cancer: the next generation." Cell **144**(5): 646-674.
Hatton, B. A., E. H. Villavicencio, J. Pritchard, M. LeBlanc, S. Hansen, M. Ulrich, S. Ditzler, B. Pullar, M. R. Stroud and J. M. Olson (2010). "Notch signaling is not essential in sonic hedgehog-activated medulloblastoma." Oncogene **29**(26): 3865-3872.
Hebert, S. S., L. Serneels, T. Dejaegere, K. Horre, M. Dabrowski, V. Baert, W. Annaert, D. Hartmann and B. De Strooper (2004). "Coordinated and widespread expression of gamma-secretase in vivo: evidence for size and molecular heterogeneity." Neurobiol Dis **17**(2): 260-272.
Hill, R. and H. Wu (2009). "PTEN, stem cells, and cancer stem cells." J Biol Chem **284**(18): 11755-11759.
Hitoshi, S., T. Alexson, V. Tropepe, D. Donoviel, A. J. Elia, J. S. Nye, R. A. Conlon, T. W. Mak, A. Bernstein and D. van der Kooy (2002). "Notch pathway molecules are essential for the maintenance, but not the generation, of mammalian neural stem cells." Genes Dev **16**(7): 846-858.
Holdhoff, M., X. Ye, J. O. Blakeley, L. Blair, P. C. Burger, S. A. Grossman and L. A. Diaz, Jr. (2012). "Use of personalized molecular biomarkers in the clinical care of adults with glioblastomas." J Neurooncol **110**(2): 279-285.
Hosaka, T., W. H. Biggs, 3rd, D. Tieu, A. D. Boyer, N. M. Varki, W. K. Cavenee and K. C. Arden (2004). "Disruption of forkhead transcription factor (FOXO) family members in mice reveals their functional diversification." Proc Natl Acad Sci U S A **101**(9): 2975-2980.
Hui, R. C., R. E. Francis, S. K. Guest, J. R. Costa, A. R. Gomes, S. S. Myatt, J. J. Brosens and E. W. Lam (2008). "Doxorubicin activates FOXO3a to induce the expression of multidrug resistance gene ABCB1 (MDR1) in K562 leukemic cells." Mol Cancer Ther **7**(3): 670-678.
Hunter, C., R. Smith, D. P. Cahill, P. Stephens, C. Stevens, J. Teague, C. Greenman, S. Edkins, G. Bignell, H. Davies, S. O'Meara, A. Parker, T. Avis, S. Barthorpe, L. Brackenbury, G. Buck, A. Butler, J. Clements, J. Cole, E. Dicks, S. Forbes, M. Gorton, K. Gray, K. Halliday, R. Harrison, K. Hills, J. Hinton, A. Jenkinson, D. Jones, V. Kosmidou, R. Laman, R. Lugg, A. Menzies, J. Perry,

R. Petty, K. Raine, D. Richardson, R. Shepherd, A. Small, H. Solomon, C. Tofts, J. Varian, S. West, S. Widaa, A. Yates, D. F. Easton, G. Riggins, J. E. Roy, K. K. Levine, W. Mueller, T. T. Batchelor, D. N. Louis, M. R. Stratton, P. A. Futreal and R. Wooster (2006). "A hypermutation phenotype and somatic MSH6 mutations in recurrent human malignant gliomas after alkylator chemotherapy." Cancer Res **66**(8): 3987-3991.
Iso, T., L. Kedes and Y. Hamamori (2003). "HES and HERP families: multiple effectors of the Notch signaling pathway." J Cell Physiol **194**(3): 237-255.
Jacobs, F. M., L. P. van der Heide, P. J. Wijchers, J. P. Burbach, M. F. Hoekman and M. P. Smidt (2003). "FoxO6, a novel member of the FoxO class of transcription factors with distinct shuttling dynamics." J Biol Chem **278**(38): 35959-35967.
Jacobsen, T. L., K. Brennan, A. M. Arias and M. A. Muskavitch (1998). "Cis-interactions between Delta and Notch modulate neurogenic signalling in Drosophila." Development **125**(22): 4531-4540.
Jeon, H. M., X. Jin, J. S. Lee, S. Y. Oh, Y. W. Sohn, H. J. Park, K. M. Joo, W. Y. Park, D. H. Nam, R. A. DePinho, L. Chin and H. Kim (2008). "Inhibitor of differentiation 4 drives brain tumor-initiating cell genesis through cyclin E and notch signaling." Genes Dev **22**(15): 2028-2033.
Jiang, L., J. Wu, Q. Chen, X. Hu, W. Li and G. Hu (2011). "Notch1 expression is upregulated in glioma and is associated with tumor progression." J Clin Neurosci **18**(3): 387-390.
Johnson, M. A., J. L. Ables and A. J. Eisch (2009). "Cell-intrinsic signals that regulate adult neurogenesis in vivo: insights from inducible approaches." BMB Rep **42**(5): 245-259.
Kanamori, M., T. Kawaguchi, J. M. Nigro, B. G. Feuerstein, M. S. Berger, L. Miele and R. O. Pieper (2007). "Contribution of Notch signaling activation to human glioblastoma multiforme." J Neurosurg **106**(3): 417-427.
Kang, M. K. and S. K. Kang (2007). "Tumorigenesis of chemotherapeutic drug-resistant cancer stem-like cells in brain glioma." Stem Cells Dev **16**(5): 837-847.
Kelly, P. N., A. Dakic, J. M. Adams, S. L. Nutt and A. Strasser (2007). "Tumor growth need not be driven by rare cancer stem cells." Science **317**(5836): 337.
Kennedy, J. A., F. Barabe, A. G. Poeppl, J. C. Wang and J. E. Dick (2007). "Comment on "Tumor growth need not be driven by rare cancer stem cells"." Science **318**(5857): 1722; author reply 1722.
Kimberly, W. T., M. J. LaVoie, B. L. Ostaszewski, W. Ye, M. S. Wolfe and D. J. Selkoe (2003). "Gamma-secretase is a membrane protein complex comprised of presenilin, nicastrin, Aph-1, and Pen-2." Proc Natl Acad Sci U S A **100**(11): 6382-6387.
Kitamura, T., Y. I. Kitamura, Y. Funahashi, C. J. Shawber, D. H. Castrillon, R. Kollipara, R. A. DePinho, J. Kitajewski and D. Accili (2007). "A Foxo/Notch pathway controls myogenic differentiation and fiber type specification." J Clin Invest **117**(9): 2477-2485.
Koch, U., R. Lehal and F. Radtke (2013). "Stem cells living with a Notch." Development **140**(4): 689-704.
Kops, G. J., T. B. Dansen, P. E. Polderman, I. Saarloos, K. W. Wirtz, P. J. Coffer, T. T. Huang, J. L. Bos, R. H. Medema and B. M. Burgering (2002). "Forkhead transcription factor FOXO3a protects quiescent cells from oxidative stress." Nature **419**(6904): 316-321.
Lagadec, C. and F. Pajonk (2012). "Catch-22: does breast cancer radiotherapy have negative impacts too?" Future Oncol **8**(6): 643-645.
Laudon, H., E. M. Hansson, K. Melen, A. Bergman, M. R. Farmery, B. Winblad, U. Lendahl, G. von Heijne and J. Naslund (2005). "A nine-transmembrane domain topology for presenilin 1." J Biol Chem **280**(42): 35352-35360.

Lee, J., S. Kotliarova, Y. Kotliarov, A. Li, Q. Su, N. M. Donin, S. Pastorino, B. W. Purow, N. Christopher, W. Zhang, J. K. Park and H. A. Fine (2006). "Tumor stem cells derived from glioblastomas cultured in bFGF and EGF more closely mirror the phenotype and genotype of primary tumors than do serum-cultured cell lines." Cancer Cell **9**(5): 391-403.
Lee, J. J., B. C. Kim, M. J. Park, Y. S. Lee, Y. N. Kim, B. L. Lee and J. S. Lee (2011). "PTEN status switches cell fate between premature senescence and apoptosis in glioma exposed to ionizing radiation." Cell Death Differ **18**(4): 666-677.
Lee, K. S., K. Iijima-Ando, K. Iijima, W. J. Lee, J. H. Lee, K. Yu and D. S. Lee (2009). "JNK/FOXO-mediated neuronal expression of fly homologue of peroxiredoxin II reduces oxidative stress and extends life span." J Biol Chem **284**(43): 29454-29461.
Li, H. F., J. S. Kim and T. Waldman (2009). "Radiation-induced Akt activation modulates radioresistance in human glioblastoma cells." Radiat Oncol **4**: 43.
Li, Y. M., M. Xu, M. T. Lai, Q. Huang, J. L. Castro, J. DiMuzio-Mower, T. Harrison, C. Lellis, A. Nadin, J. G. Neduvelil, R. B. Register, M. K. Sardana, M. S. Shearman, A. L. Smith, X. P. Shi, K. C. Yin, J. A. Shafer and S. J. Gardell (2000). "Photoactivated gamma-secretase inhibitors directed to the active site covalently label presenilin 1." Nature **405**(6787): 689-694.
Lin, J., X. M. Zhang, J. C. Yang, Y. B. Ye and S. Q. Luo (2010). "gamma-secretase inhibitor-I enhances radiosensitivity of glioblastoma cell lines by depleting CD133+ tumor cells." Arch Med Res **41**(7): 519-529.
Liu, G., X. Yuan, Z. Zeng, P. Tunici, H. Ng, I. R. Abdulkadir, L. Lu, D. Irvin, K. L. Black and J. S. Yu (2006). "Analysis of gene expression and chemoresistance of CD133+ cancer stem cells in glioblastoma." Mol Cancer **5**: 67.
Lottaz, C., D. Beier, K. Meyer, P. Kumar, A. Hermann, J. Schwarz, M. Junker, P. J. Oefner, U. Bogdahn, J. Wischhusen, R. Spang, A. Storch and C. P. Beier (2010). "Transcriptional profiles of CD133+ and CD133- glioblastoma-derived cancer stem cell lines suggest different cells of origin." Cancer Res **70**(5): 2030-2040.
Luo, H., Y. Yang, J. Duan, P. Wu, Q. Jiang and C. Xu (2013). "PTEN-regulated AKT/FoxO3a/Bim signaling contributes to reactive oxygen species-mediated apoptosis in selenite-treated colorectal cancer cells." Cell Death Dis **4**: e481.
Luo, W. J., H. Wang, H. Li, B. S. Kim, S. Shah, H. J. Lee, G. Thinakaran, T. W. Kim, G. Yu and H. Xu (2003). "PEN-2 and APH-1 coordinately regulate proteolytic processing of presenilin 1." J Biol Chem **278**(10): 7850-7854.
Majdan, M., C. Lachance, A. Gloster, R. Aloyz, C. Zeindler, S. Bamji, A. Bhakar, D. Belliveau, J. Fawcett, F. D. Miller and P. A. Barker (1997). "Transgenic mice expressing the intracellular domain of the p75 neurotrophin receptor undergo neuronal apoptosis." J Neurosci **17**(18): 6988-6998.
Martinez, S. C., C. Cras-Meneur, E. Bernal-Mizrachi and M. A. Permutt (2006). "Glucose regulates Foxo1 through insulin receptor signaling in the pancreatic islet beta-cell." Diabetes **55**(6): 1581-1591.
Mei, Y., Y. Zhang, K. Yamamoto, W. Xie, T. W. Mak and H. You (2009). "FOXO3a-dependent regulation of Pink1 (Park6) mediates survival signaling in response to cytokine deprivation." Proc Natl Acad Sci U S A **106**(13): 5153-5158.
Mellor, H. R., D. J. Ferguson and R. Callaghan (2005). "A model of quiescent tumour microregions for evaluating multicellular resistance to chemotherapeutic drugs." Br J Cancer **93**(3): 302-309.

Mihaliak, A. M., C. A. Gilbert, L. Li, M. C. Daou, R. P. Moser, A. Reeves, B. H. Cochran and A. H. Ross (2010). "Clinically relevant doses of chemotherapy agents reversibly block formation of glioblastoma neurospheres." Cancer Lett **296**(2): 168-177.
Miletti-Gonzalez, K. E., K. Murphy, M. N. Kumaran, A. K. Ravindranath, R. P. Wernyj, S. Kaur, G. D. Miles, E. Lim, R. Chan, M. Chekmareva, D. S. Heller, D. Foran, W. Chen, M. Reiss, E. V. Bandera, K. Scotto and L. Rodriguez-Rodriguez (2012). "Identification of function for CD44 intracytoplasmic domain (CD44-ICD): modulation of matrix metalloproteinase 9 (MMP-9) transcription via novel promoter response element." J Biol Chem **287**(23): 18995-19007.
Miyamoto, K., K. Y. Araki, K. Naka, F. Arai, K. Takubo, S. Yamazaki, S. Matsuoka, T. Miyamoto, K. Ito, M. Ohmura, C. Chen, K. Hosokawa, H. Nakauchi, K. Nakayama, K. I. Nakayama, M. Harada, N. Motoyama, T. Suda and A. Hirao (2007). "Foxo3a is essential for maintenance of the hematopoietic stem cell pool." Cell Stem Cell **1**(1): 101-112.
Naka, K., T. Hoshii, T. Muraguchi, Y. Tadokoro, T. Ooshio, Y. Kondo, S. Nakao, N. Motoyama and A. Hirao (2010). "TGF-beta-FOXO signalling maintains leukaemia-initiating cells in chronic myeloid leukaemia." Nature **463**(7281): 676-680.
Niimi, H., K. Pardali, M. Vanlandewijck, C. H. Heldin and A. Moustakas (2007). "Notch signaling is necessary for epithelial growth arrest by TGF-beta." J Cell Biol **176**(5): 695-707.
Niimura, M., N. Isoo, N. Takasugi, M. Tsuruoka, K. Ui-Tei, K. Saigo, Y. Morohashi, T. Tomita and T. Iwatsubo (2005). "Aph-1 contributes to the stabilization and trafficking of the gamma-secretase complex through mechanisms involving intermolecular and intramolecular interactions." J Biol Chem **280**(13): 12967-12975.
Nogueira, V., Y. Park, C. C. Chen, P. Z. Xu, M. L. Chen, I. Tonic, T. Unterman and N. Hay (2008). "Akt determines replicative senescence and oxidative or oncogenic premature senescence and sensitizes cells to oxidative apoptosis." Cancer Cell **14**(6): 458-470.
Obsil, T. and V. Obsilova (2011). "Structural basis for DNA recognition by FOXO proteins." Biochim Biophys Acta **1813**(11): 1946-1953.
Pajonk, F., E. Vlashi and W. H. McBride (2010). "Radiation resistance of cancer stem cells: the 4 R's of radiobiology revisited." Stem Cells **28**(4): 639-648.
Palomero, T., W. K. Lim, D. T. Odom, M. L. Sulis, P. J. Real, A. Margolin, K. C. Barnes, J. O'Neil, D. Neuberg, A. P. Weng, J. C. Aster, F. Sigaux, J. Soulier, A. T. Look, R. A. Young, A. Califano and A. A. Ferrando (2006). "NOTCH1 directly regulates c-MYC and activates a feed-forward-loop transcriptional network promoting leukemic cell growth." Proc Natl Acad Sci U S A **103**(48): 18261-18266.
Pandiyan, P., D. Gartner, O. Soezeri, A. Radbruch, K. Schulze-Osthoff and M. C. Brunner-Weinzierl (2004). "CD152 (CTLA-4) determines the unequal resistance of Th1 and Th2 cells against activation-induced cell death by a mechanism requiring PI3 kinase function." J Exp Med **199**(6): 831-842.
Pannuti, A., K. Foreman, P. Rizzo, C. Osipo, T. Golde, B. Osborne and L. Miele (2010). "Targeting Notch to target cancer stem cells." Clin Cancer Res **16**(12): 3141-3152.
Podlesniy, P., A. Kichev, C. Pedraza, J. Saurat, M. Encinas, B. Perez, I. Ferrer and C. Espinet (2006). "Pro-NGF from Alzheimer's disease and normal human brain displays distinctive abilities to induce processing and nuclear translocation of intracellular domain of p75NTR and apoptosis." Am J Pathol **169**(1): 119-131.
Polavarapu, R., J. An, C. Zhang and M. Yepes (2008). "Regulated intramembrane proteolysis of the low-density lipoprotein receptor-related protein mediates ischemic cell death." Am J Pathol **172**(5): 1355-1362.

Pollard, S. M., K. Yoshikawa, I. D. Clarke, D. Danovi, S. Stricker, R. Russell, J. Bayani, R. Head, M. Lee, M. Bernstein, J. A. Squire, A. Smith and P. Dirks (2009). "Glioma stem cell lines expanded in adherent culture have tumor-specific phenotypes and are suitable for chemical and genetic screens." Cell Stem Cell **4**(6): 568-580.
Radtke, F. and K. Raj (2003). "The role of Notch in tumorigenesis: oncogene or tumour suppressor?" Nat Rev Cancer **3**(10): 756-767.
Rahman, M., L. Deleyrolle, V. Vedam-Mai, H. Azari, M. Abd-El-Barr and B. A. Reynolds (2011). "The cancer stem cell hypothesis: failures and pitfalls." Neurosurgery **68**(2): 531-545; discussion 545.
Ramaswamy, S., N. Nakamura, I. Sansal, L. Bergeron and W. R. Sellers (2002). "A novel mechanism of gene regulation and tumor suppression by the transcription factor FKHR." Cancer Cell **2**(1): 81-91.
Reedijk, M. (2012). "Notch signaling and breast cancer." Adv Exp Med Biol **727**: 241-257.
Renault, V. M., V. A. Rafalski, A. A. Morgan, D. A. Salih, J. O. Brett, A. E. Webb, S. A. Villeda, P. U. Thekkat, C. Guillerey, N. C. Denko, T. D. Palmer, A. J. Butte and A. Brunet (2009). "FoxO3 regulates neural stem cell homeostasis." Cell Stem Cell **5**(5): 527-539.
Rich, J. N. (2007). "Cancer stem cells in radiation resistance." Cancer Res **67**(19): 8980-8984.
Rizzo, P., C. Osipo, K. Foreman, T. Golde, B. Osborne and L. Miele (2008). "Rational targeting of Notch signaling in cancer." Oncogene **27**(38): 5124-5131.
Ro, S. H., D. Liu, H. Yeo and J. H. Paik (2013). "FoxOs in neural stem cell fate decision." Arch Biochem Biophys **534**(1-2): 55-63.
Sahlberg, S. H., D. Spiegelberg, B. Glimelius, B. Stenerlow and M. Nestor (2014). "Evaluation of cancer stem cell markers CD133, CD44, CD24: association with AKT isoforms and radiation resistance in colon cancer cells." PLoS One **9**(4): e94621.
Saito, N., J. Fu, S. Zheng, J. Yao, S. Wang, D. D. Liu, Y. Yuan, E. P. Sulman, F. F. Lang, H. Colman, R. G. Verhaak, W. K. Yung and D. Koul (2014). "A high Notch pathway activation predicts response to gamma secretase inhibitors in proneural subtype of glioma tumor-initiating cells." Stem Cells **32**(1): 301-312.
Sakamoto, K., K. Iwasaki, H. Sugiyama and Y. Tsuji (2009). "Role of the tumor suppressor PTEN in antioxidant responsive element-mediated transcription and associated histone modifications." Mol Biol Cell **20**(6): 1606-1617.
Sakariassen, P. O., H. Immervoll and M. Chekenya (2007). "Cancer stem cells as mediators of treatment resistance in brain tumors: status and controversies." Neoplasia **9**(11): 882-892.
Salmaggi, A., A. Boiardi, M. Gelati, A. Russo, C. Calatozzolo, E. Ciusani, F. L. Sciacca, A. Ottolina, E. A. Parati, C. La Porta, G. Alessandri, C. Marras, D. Croci and M. De Rossi (2006). "Glioblastoma-derived tumorospheres identify a population of tumor stem-like cells with angiogenic potential and enhanced multidrug resistance phenotype." Glia **54**(8): 850-860.
Sang, L., H. A. Coller and J. M. Roberts (2008). "Control of the reversibility of cellular quiescence by the transcriptional repressor HES1." Science **321**(5892): 1095-1100.
Sardi, S. P., J. Murtie, S. Koirala, B. A. Patten and G. Corfas (2006). "Presenilin-dependent ErbB4 nuclear signaling regulates the timing of astrogenesis in the developing brain." Cell **127**(1): 185-197.
Schafer, K. A. (1998). "The cell cycle: a review." Vet Pathol **35**(6): 461-478.

Scopelliti, A., P. Cammareri, V. Catalano, V. Saladino, M. Todaro and G. Stassi (2009). "Therapeutic implications of Cancer Initiating Cells." Expert Opin Biol Ther **9**(8): 1005-1016.
Serneels, L., T. Dejaegere, K. Craessaerts, K. Horre, E. Jorissen, T. Tousseyn, S. Hebert, M. Coolen, G. Martens, A. Zwijsen, W. Annaert, D. Hartmann and B. De Strooper (2005). "Differential contribution of the three Aph1 genes to gamma-secretase activity in vivo." Proc Natl Acad Sci U S A **102**(5): 1719-1724.
Shafee, N., C. R. Smith, S. Wei, Y. Kim, G. B. Mills, G. N. Hortobagyi, E. J. Stanbridge and E. Y. Lee (2008). "Cancer stem cells contribute to cisplatin resistance in Brca1/p53-mediated mouse mammary tumors." Cancer Res **68**(9): 3243-3250.
Shah, S., S. F. Lee, K. Tabuchi, Y. H. Hao, C. Yu, Q. LaPlant, H. Ball, C. E. Dann, 3rd, T. Sudhof and G. Yu (2005). "Nicastrin functions as a gamma-secretase-substrate receptor." Cell **122**(3): 435-447.
Shih, A. H. and E. C. Holland (2006). "Notch signaling enhances nestin expression in gliomas." Neoplasia **8**(12): 1072-1082.
Srinivasan, R., C. E. Gillett, D. M. Barnes and W. J. Gullick (2000). "Nuclear expression of the c-erbB-4/HER-4 growth factor receptor in invasive breast cancers." Cancer Res **60**(6): 1483-1487.
Stockhausen, M. T., K. Kristoffersen and H. S. Poulsen (2010). "The functional role of Notch signaling in human gliomas." Neuro Oncol **12**(2): 199-211.
Strozyk, E. and D. Kulms (2013). "The role of AKT/mTOR pathway in stress response to UV-irradiation: implication in skin carcinogenesis by regulation of apoptosis, autophagy and senescence." Int J Mol Sci **14**(8): 15260-15285.
Stupp, R., W. P. Mason, M. J. van den Bent, M. Weller, B. Fisher, M. J. Taphoorn, K. Belanger, A. A. Brandes, C. Marosi, U. Bogdahn, J. Curschmann, R. C. Janzer, S. K. Ludwin, T. Gorlia, A. Allgeier, D. Lacombe, J. G. Cairncross, E. Eisenhauer, R. O. Mirimanoff, R. European Organisation for, T. Treatment of Cancer Brain, G. Radiotherapy and G. National Cancer Institute of Canada Clinical Trials (2005). "Radiotherapy plus concomitant and adjuvant temozolomide for glioblastoma." N Engl J Med **352**(10): 987-996.
Stupp, R., J. C. Tonn, M. Brada, G. Pentheroudakis and E. G. W. Group (2010). "High-grade malignant glioma: ESMO Clinical Practice Guidelines for diagnosis, treatment and follow-up." Ann Oncol **21 Suppl 5**: v190-193.
Sunters, A., S. Fernandez de Mattos, M. Stahl, J. J. Brosens, G. Zoumpoulidou, C. A. Saunders, P. J. Coffer, R. H. Medema, R. C. Coombes and E. W. Lam (2003). "FoxO3a transcriptional regulation of Bim controls apoptosis in paclitaxel-treated breast cancer cell lines." J Biol Chem **278**(50): 49795-49805.
Takeuchi, H., Y. Kondo, K. Fujiwara, T. Kanzawa, H. Aoki, G. B. Mills and S. Kondo (2005). "Synergistic augmentation of rapamycin-induced autophagy in malignant glioma cells by phosphatidylinositol 3-kinase/protein kinase B inhibitors." Cancer Res **65**(8): 3336-3346.
Thinakaran, G., D. R. Borchelt, M. K. Lee, H. H. Slunt, L. Spitzer, G. Kim, T. Ratovitsky, F. Davenport, C. Nordstedt, M. Seeger, J. Hardy, A. I. Levey, S. E. Gandy, N. A. Jenkins, N. G. Copeland, D. L. Price and S. S. Sisodia (1996). "Endoproteolysis of presenilin 1 and accumulation of processed derivatives in vivo." Neuron **17**(1): 181-190.
Tsai, W. B., Y. M. Chung, Y. Takahashi, Z. Xu and M. C. Hu (2008). "Functional interaction between FOXO3a and ATM regulates DNA damage response." Nat Cell Biol **10**(4): 460-467.

Tun, T., Y. Hamaguchi, N. Matsunami, T. Furukawa, T. Honjo and M. Kawaichi (1994). "Recognition sequence of a highly conserved DNA binding protein RBP-J kappa." Nucleic Acids Res **22**(6): 965-971.
Ulasov, I. V., S. Nandi, M. Dey, A. M. Sonabend and M. S. Lesniak (2011). "Inhibition of Sonic hedgehog and Notch pathways enhances sensitivity of CD133(+) glioma stem cells to temozolomide therapy." Mol Med **17**(1-2): 103-112.
Vakifahmetoglu, H., M. Olsson and B. Zhivotovsky (2008). "Death through a tragedy: mitotic catastrophe." Cell Death Differ **15**(7): 1153-1162.
Venere, M., H. A. Fine, P. B. Dirks and J. N. Rich (2011). "Cancer stem cells in gliomas: identifying and understanding the apex cell in cancer's hierarchy." Glia **59**(8): 1148-1154.
Vivanco, I. and C. L. Sawyers (2002). "The phosphatidylinositol 3-Kinase AKT pathway in human cancer." Nat Rev Cancer **2**(7): 489-501.
Wang, J., T. P. Wakeman, J. D. Lathia, A. B. Hjelmeland, X. F. Wang, R. R. White, J. N. Rich and B. A. Sullenger (2010). "Notch promotes radioresistance of glioma stem cells." Stem Cells **28**(1): 17-28.
Wang, S. I., J. Puc, J. Li, J. N. Bruce, P. Cairns, D. Sidransky and R. Parsons (1997). "Somatic mutations of PTEN in glioblastoma multiforme." Cancer Res **57**(19): 4183-4186.
Wang, Y., W. Li, S. S. Patel, J. Cong, N. Zhang, F. Sabbatino, X. Liu, Y. Qi, P. Huang, H. Lee, A. Taghian, J. J. Li, A. B. DeLeo, S. Ferrone, M. W. Epperly, C. R. Ferrone, A. Ly, E. F. Brachtel and X. Wang (2014). "Blocking the formation of radiation-induced breast cancer stem cells." Oncotarget **5**(11): 3743-3755.
Webb, A. E., E. A. Pollina, T. Vierbuchen, N. Urban, D. Ucar, D. S. Leeman, B. Martynoga, M. Sewak, T. A. Rando, F. Guillemot, M. Wernig and A. Brunet (2013). "FOXO3 shares common targets with ASCL1 genome-wide and inhibits ASCL1-dependent neurogenesis." Cell Rep **4**(3): 477-491.
Westhoff, B., I. N. Colaluca, G. D'Ario, M. Donzelli, D. Tosoni, S. Volorio, G. Pelosi, L. Spaggiari, G. Mazzarol, G. Viale, S. Pece and P. P. Di Fiore (2009). "Alterations of the Notch pathway in lung cancer." Proc Natl Acad Sci U S A **106**(52): 22293-22298.
Woolard, K. and H. A. Fine (2009). "Glioma stem cells: better flat than round." Cell Stem Cell **4**(6): 466-467.
Xie, Q., Y. Hao, L. Tao, S. Peng, C. Rao, H. Chen, H. You, M. Q. Dong and Z. Yuan (2012). "Lysine methylation of FOXO3 regulates oxidative stress-induced neuronal cell death." EMBO Rep **13**(4): 371-377.
Xuan, Z. and M. Q. Zhang (2005). "From worm to human: bioinformatics approaches to identify FOXO target genes." Mech Ageing Dev **126**(1): 209-215.
Yan, K., Q. Wu, D. H. Yan, C. H. Lee, N. Rahim, I. Tritschler, J. DeVecchio, M. F. Kalady, A. B. Hjelmeland and J. N. Rich (2014). "Glioma cancer stem cells secrete Gremlin1 to promote their maintenance within the tumor hierarchy." Genes Dev **28**(10): 1085-1100.
Yip, S., J. Miao, D. P. Cahill, A. J. Iafrate, K. Aldape, C. L. Nutt and D. N. Louis (2009). "MSH6 mutations arise in glioblastomas during temozolomide therapy and mediate temozolomide resistance." Clin Cancer Res **15**(14): 4622-4629.
Zagouras, P., S. Stifani, C. M. Blaumueller, M. L. Carcangiu and S. Artavanis-Tsakonas (1995). "Alterations in Notch signaling in neoplastic lesions of the human cervix." Proc Natl Acad Sci U S A **92**(14): 6414-6418.
Zhang, X. P., G. Zheng, L. Zou, H. L. Liu, L. H. Hou, P. Zhou, D. D. Yin, Q. J. Zheng, L. Liang, S. Z. Zhang, L. Feng, L. B. Yao, A. G. Yang, H. Han and J. Y. Chen (2008). "Notch activation

promotes cell proliferation and the formation of neural stem cell-like colonies in human glioma cells." Mol Cell Biochem **307**(1-2): 101-108.